Analysis of second messengers in peripheral and central circadian pacemakers

Dissertation

zur Erlangung des akademischen Grades eines
Doktors der Naturwissenschaften (Dr. rer. nat.)

vorgelegt von

Thomas Schendzielorz

Universität Kassel – Fachbereich 10
Mathematik und Naturwissenschaften
Institut für Biologie – Abteilung Tierphysiologie

Kassel, 04. August 2014

Vom Fachbereich 10 / Mathematik und Naturwissenschaften der Universität Kassel als Dissertation am 06.10.2014 angenommen.

Prüfungskommission

1. Gutachterin:	Prof. Dr. Monika Stengl
2. Gutachterin:	Dr. Christine Nowack
Prüferin:	Prof. Dr. Mireille Schäfer
Prüfer:	Prof. Dr. Raffael Schaffrath (i.v. Prof. Dr. Markus Maniak)

Tag der mündlichen Prüfung: 14.10.2014

So eine Arbeit wird eigentlich nie fertig,
man muss sie für fertig erklären,
wenn man nach der Zeit und den Umständen
das Möglichste getan hat.

Johann Wolfgang von Goethe
(Deutscher Dichter, 1749 - 1832)

Eidesstattliche Erklärung

Hiermit versichere ich, dass ich die vorliegende Dissertation selbstständig, ohne unerlaubte Hilfe Dritter angefertigt und andere als die in der Dissertation angegebenen Hilfsmittel nicht benutzt habe. Alle Stellen, die wörtlich oder sinngemäß aus veröffentlichten oder unveröffentlichten Schriften entnommen sind, habe ich als solche kenntlich gemacht. Dritte waren an der inhaltlich-materiellen Erstellung der Dissertation nicht beteiligt; insbesondere habe ich hierfür nicht die Hilfe eines Promotionsberaters in Anspruch genommen. Kein Teil dieser Arbeit ist in einem anderen Promotions- oder Habilitationsverfahren verwendet worden.

Kassel, 04.08.2014

Thomas Schendzielorz

Index

Contribution statements

My contributions for each chapter will be stated clearly according to the "Allgemeine Bestimmungen für Promotionen an der Universität Kassel (AB-PromO) vom 13. Juni 2012". Parts of this thesis have already been published and exact wording is highlighted in **grey** in this doctoral thesis:

Schendzielorz T, Peters W, Boekhoff I, and Stengl M (2012) Time of day changes in cyclic nucleotides are modified via octopamine and pheromone in antennae of the Madeira cockroach. Journal of Biological Rhythms 27:388-397.

Schendzielorz J, Schendzielorz T, Arendt A, and Stengl M (2014) Bimodal oscillations of cyclic nucleotide concentrations in the circadian system of the Madeira cockroach Rhyparobia maderae. Journal of Biological Rhythms accepted (07.07.2014).

Chapter 3.1 Behavioural analysis of *Rhyparobia maderae* and *Manduca sexta*

- Development, implementation, and analysis of *R. maderae* behaviour with the Noldus tracking assay.
- Investigation and analysis of *R. maderae* calling behaviour was performed together with trainees.
- Investigation and analysis of *M. sexta* flight- and feeding behaviour was performed together with Dipl. Biol. Katja Schirmer.
- Preparation of figures and tables.

Chapter 3.2 Quantification of second messenger in the antennae of female *R. maderae* and male *M. sexta*

- Development and implementation of an enzyme-linked immunosorbent assay (ELISA) for cyclic nucleotide quantification was performed together with Dr. Julia Schendzielorz.
- Development, implementation, and analysis of second messenger quantification in *R. maderae* and *M. sexta* antennae were performed together with Dr. Wladimir Peters (minor part), Dipl. Biol. Katja Schirmer (minor part), and Bsc. Nano. Sc. Mark Benfer (minor part).
- Statistical analysis, preparation of figures and tables.

Chapter 3.3 Zeitgeber time (ZT)-dependent effect of octopamine (OA)

- Development, implementation, and analysis of OA quantification in *M. sexta* antennae.
- Development, implementation, and analysis of ZT-dependent OA effects in *R. maderae* and *M. sexta* antennae were performed together with Dr. Wladimir Peters (minor part).
- Development, implementation, and analysis of half maximal effective dose (EC_{50}) of OA in *M. sexta* antennae.
- Development, implementation, and analysis of reaction speed of OA in *M. sexta* antennae.
- Statistical analysis, preparation of figures and tables.

Chapter 3.4 ZT-dependent effects of calcium concentrations

- Development, implementation, and analysis of calcium-dependent effects in *R. maderae* and *M. sexta* antennae.
- Statistical analysis, preparation of figures and tables.

Chapter 3.5 Cyclic nucleotide effects in the circadian pacemaker of *R. maderae*

- Development and implementation of all experiments were performed in equal parts with Dipl. Biol. Andreas Arendt and Dr. Julia Schendzielorz.
- Statistical analysis.
- Preparation of all figures together with Dr. Julia Schendzielorz.

Zusammenfassung

Sowohl die tägliche Drehung der Erde um ihre Achse als auch ihre Umlaufbahn um die Sonne bestimmt den Tagesablauf aller auf ihr existierenden Lebensformen. Diese Rhythmen führten zur Entwicklung von inneren Uhren mit einer Periodendauer von etwa 24 Stunden, um sich an die verändernden Umweltbedingungen anzupassen. Das erste Tier, in dem solch eine Uhr im Zentralnervensystem identifiziert und lokalisiert werden konnte, war die Madeira-Schabe, *Rhyparobia maderae*. Der strukturelle Aufbau dieses circadianen Schrittmachers, der akzessorischen Medulla (AMe), ähnelt sehr stark dem Aufbau des Hauptschrittmachers der Säugetiere, dem suprachiasmatischen Nukleus. Darüber hinaus ist die Schabe ein besonders robustes und langlebiges Insekt, was zu ihrer Etablierung als circadianen Modellorganismus geführt hat. Neben dem Hauptschrittmacher im Zentralnervensystem existieren noch zahlreiche weitere Taktgeber in peripheren Nervensystemen. Zusammen steuern sie zahlreiche Effektoren wie die Physiologie sowie das Verhalten. Es konnte gezeigt werden, dass nicht nur das Lauf-, sondern auch das Fress- und Paarungsverhalten bei Schaben circadian reguliert wird. Obwohl die molekularen Mechanismen, welche diesem circadian olfaktorischen Verhalten zugrunde liegen, weitestgehend unbekannt sind, ist bekannt, dass sekundäre Botenstoffe eine Schlüsselrolle bei der Modulation der olfaktorischen Wahrnehmung, aber auch bei der primären olfaktorischen Antwort eine entscheidende Rolle spielen. Diese sollten im Rahmen dieser Doktorarbeit näher untersucht werden.

<u>Kapitel 3.1</u> Analyse des Verhaltens von *R. maderae* und *Manduca sexta*

Zunächst wurde das Verhalten von *R. maderae,* aber auch das des Tabakschwärmers *M. sexta* unter Laborbedingungen untersucht, unter denen auch die späteren biochemischen Experimente durchgeführt wurden. Mittels eines Videoanalysesystems wurde das Lauf-, Fress-, Paarungsverhalten männlicher sowie weiblicher Madeira-Schaben untersucht. Es konnte gezeigt werden, dass isolierte männliche sowie weibliche Madeira-Schaben zwei Aktivitätspeaks im Tagesverlauf aufweisen. Der erste Peak tritt zu Beginn/Mitte der Nacht auf, der zweite gegen Ende der Nacht. Darüber hinaus konnte eine sehr gute Korrelation zwischen der Aktivität weiblicher Schaben und deren Aufenthalt in einer Futterzone beo-

bachtet werden. Hingegen wurde der maximale Aufenthalt in der Pheromonzone gegen Ende des Tages und zu Beginn der Nacht erfasst. Zur selben Zeit wurde das maximale Rufverhalten männlicher Schaben in Laborkolonien beobachtet. Diese Resultate zeigen, dass Pheromonabgabe und -detektion bei *R. maderae* synchronisiert stattfindet. Im Anschluss scheint die weibliche Schabe auf Nahrungssuche zu gehen.

Ebenso wurde das Verhalten männlicher Tabakschwärmer in Abwesenheit von weiblichen Tieren in einem Flugraum untersucht. Hierbei konnte aufgrund des dreidimensionalen Bewegungsmusters des Schwärmers keine Videoanalyse durchgeführt werden, sodass das Flug- und Fressverhalten manuell erfasst wurde. Männliche Tabakschwärmer zeigten während der gesamten Nacht ein gesteigertes Flugverhalten. Zudem wurden Tiere zu Beginn und zum Ende des Flugverhaltens bei der Nahrungsaufnahme beobachtet. Diese Ergebnisse stehen in Korrelation zu bereits publizierten Daten hinsichtlich der Aktivität des Tabakschwärmers.

<u>Kapitel 3.2</u> Quantifizierung von sekundären Botenstoffen in der Antenne von *R. maderae* und *M. sexta*

In früheren Studien konnte gezeigt werden, dass die Perfusion von cAMP in die Antenne von *M. sexta* zu einer tageszeitabhängigen Sensitisierung der olfaktorischen Wahrnehmung auf das artspezifische Pheromon Bombykal führt. Hingegen resultierten cGMP-Perfusionen in einer tageszeitabhängigen Adaptation der olfaktorischen Antwort. Daher wurde angenommen, dass eine antennale Oszillation zyklischer Nukleotide für die tageszeitabhängigen Effekte ursächlich sein könnte. Darüber hinaus wurde hypothesiert, dass die intrazelluläre Kalziumkonzentration einer tageszeitabhängigen Schwankung unterliegen könnte, was weitere Signalmoleküle in ihrer Aktivität beeinflusst, wie etwa Phospholipasen. Diese spielen eine zentrale Rolle bei der primären olfaktorischen Signaltransduktionskaskade. Daher wurden im Rahmen der Doktorarbeit die Konzentrationen antennaler zyklischer Nukleotide und IP_3 mittels enzymgekoppelter antikörperbasierter Nachweisverfahren (ELISA) im Tagesverlauf untersucht.

Sowohl bei der weiblichen Madeira-Schabe als auch beim männlichen Tabakschwärmer, welche beide die Empfänger des artspezifischen Sexuallockstoffs sind, konnten tageszeitabhängige Oszillationen von antennalen cAMP- und IP_3-Konzentrationen nachgewiesen werden. Während die höchste cAMP-Konzentration zur Paarungszeit beo-

bachtet wurde, schienen die detektierten IP_3-Peaks mit der generellen Aktivität der Versuchstiere oder deren Fressverhalten zu korrelieren. Darüber hinaus konnte bei der weiblichen Madeira-Schabe gezeigt werden, dass die cAMP- und cGMP-Level antizyklisch oszillieren. Dieser Effekt wurde jedoch nicht bei den Tabakschwärmern beobachtet. Hier verblieben die cGMP-Level auf einem konstant niedrigen Niveau. Da die Tabakschwärmer, im Gegensatz zur Madeira-Schabe, isoliert von Kopulationspartnern gehalten wurden, könnte die Abwesenheit von Sexuallockstoffen ursächlich für den beobachteten Unterschied sein. Darüber hinaus blieben die cAMP- und IP_3-Oszillationen bei *R. maderae* auch unter konstanten Umweltbedingungen bestehen, sodass anzunehmen ist, dass diese sekundären Botenstoffe unter der Kontrolle des circadianen Uhrwerks stehen. Dieser Effekt wurde jedoch nicht beim Tabakschwärmer beobachtet. Hier verblieben alle untersuchten sekundären Botenstoffe auf einem gleichbleibenden Niveau. Daher ist anzunehmen, dass sie entweder nicht vom circadianen System gesteuert werden oder sehr schnell desynchronisieren.

<u>Kapitel 3.3</u> Effekte des biogenen Amins Octopamin (OA) auf die antennale IP_3- und cAMP-Konzentration

Das biogene Amin OA ist in zahlreichen physiologischen Vorgängen, aber auch im Verhalten von Insekten als Neuromodulator, Neurohormon sowie als Neurotransmitter involviert. Perfusionen von OA in die Antenne der amerikanischen Küchenschabe *Periplaneta americana* als auch in die von *M. sexta* resultierten in einer sensitisierten Pheromonwahrnehmung. Dieser Effekt war beim Tabakschwärmer wesentlich effektiver zur Ruhezeit der Tiere, sodass angenommen wurde, dass tageszeitabhängige Oszillationen von OA in der Hämolymphe die Ursache hierfür sein könnten. Darüber hinaus konnten die von OA induzierten Effekte zum Teil auch bei cAMP-Perfusionen beobachtet werden. Daher wurde angenommen, dass OA über einen G-Protein-gekoppelten Rezeptor Adenylycyclasen aktiviert.

Aus diesem Grund wurde zunächst beim Tabakschwärmer überprüft, ob die antennale OA-Konzentration im Tagesverlauf variiert und welche sekundären Botenstoffe in antennalen Lysaten durch OA beeinflusst werden können. Es konnte gezeigt werden, dass die antennale OA-Konzentration den Verlauf der antennalen cAMP-, aber nicht den der IP_3-Konzentrationen sehr gut widerspiegelt. Zudem steigerte OA in antennalen

Lysaten den cAMP- und IP_3-Level zur Ruhezeit des Tabakschwärmers. Zur Aktivitätsphase konnte jedoch nur noch die cAMP-, allerdings nicht die IP_3-Konzentartion durch OA gesteigert werden, sodass scheinbar unterschiedliche Mechanismen die cAMP- und IP_3-Level beeinflussen. Darüber hinaus wurde der antennale OA-Rezeptor näher charakterisiert. Die kinetische Analyse zeigte, dass OA innerhalb von 50 ms einen signifikanten cAMP-Anstieg bewirkt. Darüber hinaus wurde die mittlere effektive Konzentration (EC_{50}) des antennalen OA-Rezeptors untersucht. Der EC_{50} Wert betrug 708 nM OA zur Ruhezeit und 234 nM zur Aktivitätszeit des Tabakschwärmers. Diese Daten sind im Einklang mit früheren Publikationen bei Invertebraten, in denen gezeigt wurde, dass OA über einen α-adrenergen OA Rezeptor, mit einem EC_{50} Wert von 10^{-8}-10^{-5} M, die IP_3- und cAMP-Spiegel hochregulieren kann.

Auch bei *R. maderae* wurde untersucht, ob antennale Lysate durch OA in ihrer cAMP- aber auch IP_3-Synthese stimuliert werden können. Hier wurde allerdings nur der cAMP-, nicht jedoch der IP_3-Level beeinflusst, sodass die Anwesenheit eines β-adrenergen OA Rezeptor wahrscheinlich ist, welcher nur Adenylylcyclasen aktiviert.

<u>Kapitel 3.4</u> Kalzium-bedingte Effekte auf die antennale cAMP-, cGMP- und IP_3-Konzentration

Physiologische Daten legen nahe, dass die intrazellulären Kalziumkonzentrationen von olfaktorischen Rezeptorneuronen (ORNs) in *M. sexta* im Tagesverlauf oszillieren. Kalzium moduliert zahlreiche Enzyme wie etwa Adenylylcyclasen, Guanylylcyclasen, aber auch Phopholipasen und könnte so den internen Zustand von ORNs über die Interaktion mit verschiedenen Signaltransduktionskaskaden orchestrieren. Im Rahmen dieser Arbeit konnten tageszeitabhängige Kalziumeffekte auf die antennalen cAMP-, cGMP- und IP_3-Level nachgewiesen werden, welche diese Hypothese stützen. Sowohl in *M. sexta* als auch in *R. maderae* reduzierte 60 nM freies Kalzium die cAMP-Synthese signifikant zur Aktivitätsphase, jedoch nicht zur Ruhephase. Sowohl niedrigere als auch höhere Kalziumkonzentrationen (untersucht: 0 nM-1 µM freies Kalzium) beeinflussten die cAMP-Konzentration nicht. Ein ähnlicher Effekt konnte auch beim antennalen IP_3-Level in *M. sexta* zur Aktivitätsphase beobachtet werden. Hier erhöhte 140 nM freies Kalzium die IP_3-Konzentration signifikant. Hingegen konnte eine signifikante kalziumabhängige Modulati-

on der cGMP-Konzentration nur zur Ruhephase des Tabakschwärmers beobachtet werden, zu der 60 nM freies Kalzium die Guanylylcyclasenaktivität erhöhte.

Daher wird angenommen, dass die intrazelluläre Kalziumkonzentration ein entscheidender Faktor bei der Regulation der olfaktorischen Sensitivität ist. Ob die Kalziumkonzentration von dem circadianen System gesteuert wird, wie es bei circadianen Schrittmacherneuronen des suprachiasmatischen Nukleus der Fall ist, müssen weitere Untersuchungen zeigen.

<u>Kapitel 3.5</u> Analyse zyklischer Nukleotide im Hauptschrittmacher von *R. maderae*

Das Neuropeptid *Pigment-dispersing factor* (PDF) ist der wichtigste Kopplungsfaktor des circadianen Systems in Insekten, vergleichbar mit dem vasoaktiven intestinalen Polypeptid (VIP), dem funktionellen Ortholog des circadianen Systems der Säugetiere. In der Fruchtfliege *Drosophila melanogster* aktiviert das Neuropeptid PDF einen G-proteingekoppelten Rezeptor, welcher zu cAMP-Erhöhungen führt. Überdies steuert PDF die circadiane Bewegungsaktivität in der Abenddämmerung und im Morgengrauen. Daher wurde zunächst untersucht, ob PDF die cAMP-Level in der AMe der Madeira-Schabe erhöhen kann. Des Weiteren wurde untersucht, ob cAMP- und PDF-Injektionen zu unterschiedlichen circadianen Tageszeiten die circadiane lokomotorische Aktivität der Schabe in ähnlicher Weise beeinflusst. Darüber hinaus wurde nach circadianen Oszillationen von cAMP, und seinem funktionellen Gegenspieler, cGMP, in der AMe sowie dem optischen Lobus, einer wichtigen Eingangs- und Ausgangsregion des circadianen Schrittmachers, gesucht.

Es konnte gezeigt werden, dass PDF die cAMP-, aber nicht die cGMP-Konzentration erhöht. Darüber hinaus wurden tageszeitabhängige Oszillationen von cAMP- und cGMP-Konzentrationen in der AMe beobachtet. Beide sekundären Botenstoffe wiesen signifikant gesteigerte Konzentrationen zur Abenddämmerung und im Morgengrauen auf. Obwohl diese Oszillationen am ersten Tag unter konstanten Umweltbedingungen (DD1) verschwanden, konnten sie am zweiten Tag unter konstanten Umweltbedingungen (DD2) im cAMP-Level wieder nachgewiesen werden. Im Gegensatz zur AMe oszillierten die cAMP-Konzentrationen im optischen Lobus nicht unter Licht-Dunkel-Bedingungen. Allerdings oszillierten sie in DD2 in Phase mit den cAMP-Konzentrationen der AMe. Darüber hinaus wurde mittels Verhaltens- und Injektionsexperimenten herausgefunden, dass cAMP- und PDF-Injektionen die Phasenlage der circadian Lokomotion sehr

ähnlich beeinflussen. Beide verzögerten diese, wenn sie gegen Ende des subjektiven Tages injiziert wurden, und beschleunigten sie, sobald sie gegen Ende der subjektiven Nacht injiziert wurden. cGMP-Injektionen resultierten in Phasenverzögerungen zu Beginn der subjektiven Nacht. Daher wird hypothesiert, dass PDF-Freisetzung gegen Ende des subjektiven Tages und zu Beginn der subjektiven Nacht den Hauptschrittmacher, aber auch das visuelle System mittels cAMP-Erhöhungen beeinflusst.

Summary

Previous electrophysiological, biochemical, and immunocytochemical experiments indicated an involvement of cAMP, cGMP, and IP_3 in olfactory signal transduction cascade of the hawk moth *Manduca sexta*. While cGMP adapted pheromone detection daytime-dependently, cAMP sensitized it partly mimicking octopamine (OA) effects. Consequently, daytime-dependent second messenger oscillations generated by intracellular calcium- and hemolymph OA concentration were assumed to adjust the pheromone detection threshold. Thus, with enzyme-linked immunosorbent assays it was searched in antennae of *M. sexta* and *Rhyparobia maderae* for daytime-dependent rhythms in the concentrations of OA, cAMP, cGMP, and IP_3.

Indeed, daytime-dependent changes in the concentration of OA, cAMP, and IP_3, but not of cGMP were detected in the hawk moth antennae. While cAMP- and OA oscillations closely resembled each other with maxima at the animals mating phase, IP_3 concentrations correlated with the animals' flight- and/or feeding activity. Also in the antennae of the Madeira cockroach second messenger concentrations correlated with behavioural rhythms. Moreover, cAMP- and IP_3 oscillations were demonstrated to be controlled by the circadian clock since they persisted under constant conditions (DD). Additionally, cAMP- and partially IP_3 concentrations were increased by OA. Contrarily, calcium affected all investigated second messengers in the hawk moth, but only cAMP levels in the Madeira cockroach. Thus, both cellular calcium- and antennal OA concentrations seemed to be critical factors for adjusting ORNs sensitivity.

Since cyclic nucleotide oscillations were demonstrated in putative peripheral circadian pacemakers, it was also investigated whether cAMP- and cGMP oscillations occur in the central circadian pacemaker of the Madeira cockroach and whether the neuropeptide pigment-dispersing factor (PDF), the most important coupling factor of the circadian system in insects, could drive these rhythms. In fact, PDF increased cAMP concentrations. Furthermore, bimodal cAMP oscillations were observed under light-dark conditions and persisted under DD. Thus, PDF release at dusk and dawn is assumed to synchronize the circadian clock cAMP-dependently.

Introduction

Both, the daily rotation of the earth around its axis and its elliptical orbit around the sun determine the temporal order of all existing terrestrial life forms. Next to the 24 h circadian rhythm of the daily light-dark (LD) cycle, the length of night and day, humidity, and temperature vary consistently during the course of a year resulting in circannual rhythms. These geophysical rhythms of different periods favoured the development of internal clocks. The most prominent internal clock is the circadian (lat. *circa* = approximately, lat. *dies* = day) clock with an endogenous period length (Tau = τ) of approximately 24 h under constant conditions.

1.1 General properties of circadian clocks

Circadian clocks maintain their endogenous τ under constant conditions. They are temperature compensated and keep a constant τ within a certain physiological temperature range. Furthermore, their periods are genetically determined and species-specific

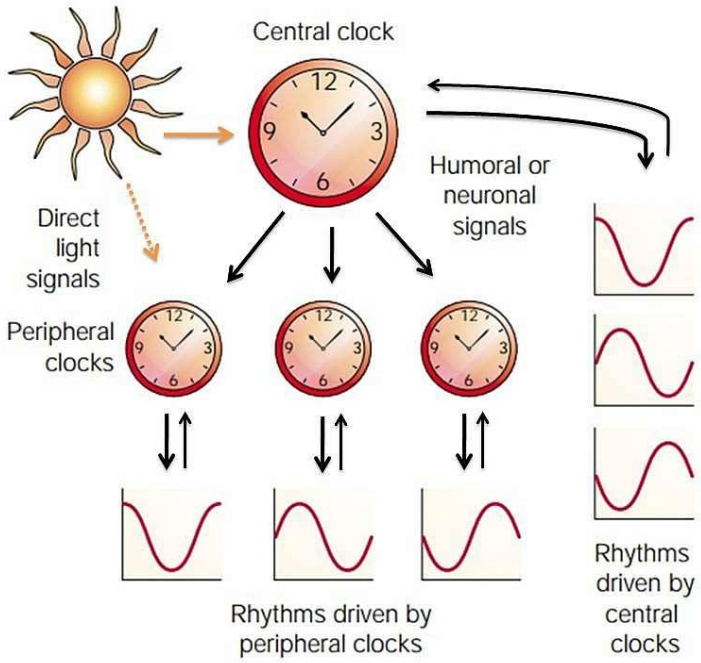

Figure 1. Schematic drawing of the circadian system consisting of a central clock and numerous peripheral circadian clocks. In addition to the central clock controlling numerous effectors, peripheral clocks drive tissue-specific rhythms. Both clocks can be synchronized by light and gets feedback input by effectors. Additionally, the peripheral clocks receive direct input by the central pacemaker (modified after Cermakian and Sassone-Corsi, 2000).

(Dunlap, 1999; Cermakian and Sassone-Corsi, 2000; Saunders, 2002; Tomioka and Abdelsalam, 2004; Golombek and Rosenstein, 2010). The circadian clocks control the temporal order of physiological processes (such as hormone release) and of behaviour (such as locomotor activity rhythms) via gating of clock outputs or via phase-control of downstream oscillators (**Fig. 1**; Corbet, 1960; Pittendrigh, 1960; Aschoff, 1969; Block and Page, 1978; Cermakian and Sassone-Corsi, 2000). Zeitgebers such as the daily LD cycle entrain the circadian clock to exactly 24 h via light-dependent phase shifts (**Fig. 1**; Aschoff, 1954). Light as well as other input signals into the circadian clockwork either accelerate (phase advance = +Δϕ = delta phi in circadian time [CT] hours) or decelerate its phase (phase delay = -Δϕ in CT hours) resulting in a stimulus-specific phase response curve (PRC; **Fig. 2**). For example, light pulses always slow down the circadian pacemaker at the beginning of the subjective night and advance it at the middle/end of the subjective night, resulting in a biphasic PRC. Contrarily, other inputs such a injections of neuropeptides can also result in monophasic PRCs either all-delay, or all-advance PRCs. Circadian rhythm researchers distinguish different time axes such as the time of day, the Zeitgeber time (ZT), and the CT. The time of day is measured with man-made clocks. The ZT of a 12:12 LD cycle starts with lights on at ZT 0 (beginning of day). The light cycle extends from ZT 0 to ZT 12 (the end of day = beginning of night) the dark cycle lasts from ZT

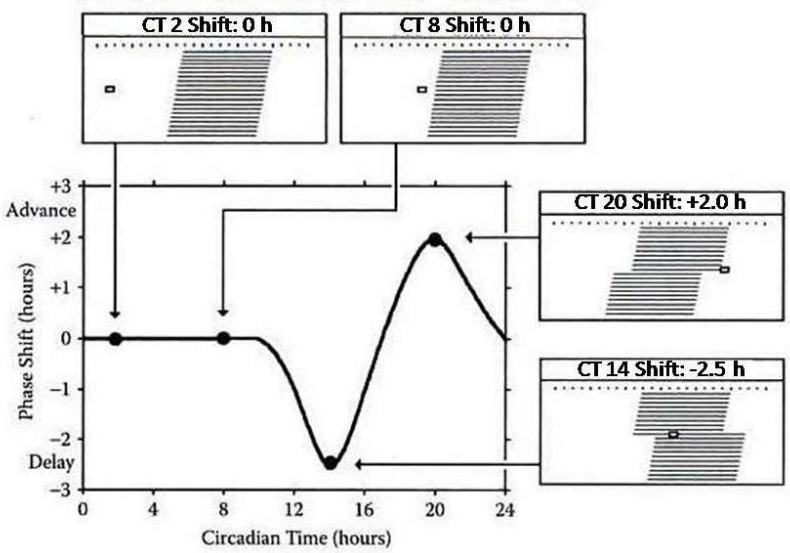

Figure 2. Generating a phase response curve (PRC) using fictitious running trails of a night active animal with an endogenous period length <24 h. Light pulses are induced at various circadian times (CTs; rectangle in actograms). Next, calculated phase shifts are plotted as function of CT. PRC demonstrates no effects of light pulses at the subjective day, while they induced a phase delay of 2.5 h at the beginning and a phase advance at the end of subjective night (Refinetti, 2010).

12 to ZT 24 (end of night=beginning of day). The CT is measured under constant conditions (DD) such as constant darkness and is divided into the subjective day from CT 0 to CT 12 and the subjective night from CT 12 to CT 24. The circadian day has the length of the animals' τ, with τ/24 h as the length of one circadian hour. When animals locomotor activity rhythms are measured under constant conditions the beginning of locomotor activity of a night-active animal is defined as CT 12, while the beginning of locomotor activity of a day-active animal is defined as CT 0.

1.2 Molecular mechanisms in *Drosophila melanogaster*

The fruit fly *D. melanogaster* is the best studied model organism for functional analysis of molecular mechanisms in circadian pacemaker neurons. The first clock gene *period* (*per*) was identified in the fruit fly in 1971, since eclosion rhythms of population and locomotor rhythms of individual flies were demonstrated to be disrupted in three *per* mutants (Konopka and Benzer, 1971). However, further clock genes like *timeless* (*tim*), *clock* (*clk*), and cycle (*cyc*) were identified about 20 years later (Sehgal et al., 1994; Allada et al., 1998; Rutila et al., 1998). These clock genes form the basis for a molecular feedback loop, the *per*/*tim* feedback loop (**Fig. 3**). First, during midday the transcription factors CLOCK (CLK) and CYCLE (CYC) dimerize and bind to an E-Box motive (CACGTG), which induces the transcription of *per* and *tim* resulting in increased PERIOD (PER) and TIMELESS (TIM)

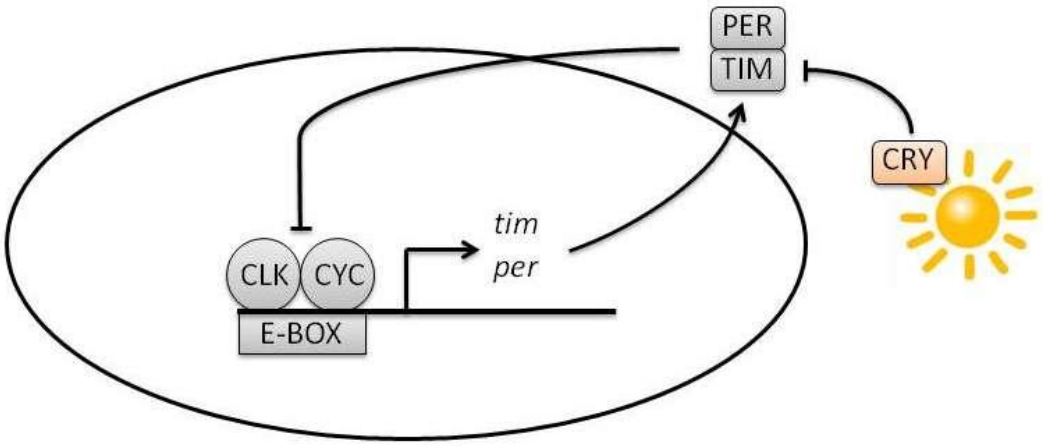

Figure 3. *Drosophila melanogaster* feedback loop. CLOCK (CLK) and CYCLE (CYC) activate E-Box motive of *period* (*per*) and *timeless* (*tim*) promoter. PERIOD (PER) and TIMELESS (TIM) accumulate in cytosol, enter the nucleus and inactivate their own transcription. In addition, CRYPTOCHROME 1 (CRY 1) is activated by blue light and destabilize TIM, which is sufficient for PER stability. Modified and strongly simplified after Tomioka and Matsumoto (2010).

concentrations. At the late night, these circadian clock proteins enter the nucleus as homo- and/or as heterodimers, interact with CLK, and inactivate the E-Box motive. Thus, PER/TIM inhibit their own transcription in a negative feedback loop and are degraded until the E-Box can be activated again by CLK/CYC (Hardin, 2005). In addition, the negative feedback loop is modulated by the blue light sensor CRYPTOCHROME 1 (CRY 1; Stanewsky et al.,1998; Isikawa et al., 1999). Light activates CRY 1, which binds and, thereby, degrades TIM, which is sufficient for PER stability, resulting in a delayed feedback (Hardin, 2005).

1.3 The circadian system of *D. melanogaster*

Through the identification of clock genes, an assignment of clock neurons was possible in the fruit fly brain. With immunocyctochemistry against clock proteins approximately 150 clock neurons per hemisphere could be identified and were assigned to seven subgroups (Kaneko and Hall, 2000; Helfrich-Förster, 2003, 2006). Four of them are located laterally, the small- and large ventro-lateral- (sLN_vs, lLN_vs), the dorso-lateral- (LN_ds), and the posterior-lateral neurons (LPNs). In addition, three other cell groups were identified in the dorsal protocerebrum (DN_{1-3}; **Fig. 4**). Next to clock proteins, pacemaker neurons contain a variety of different neuropeptides (Peschel and Helfrich-Forster, 2011), such as pigment-dispersing factor (PDF). While only ten percent of the clock neurons express PDF,

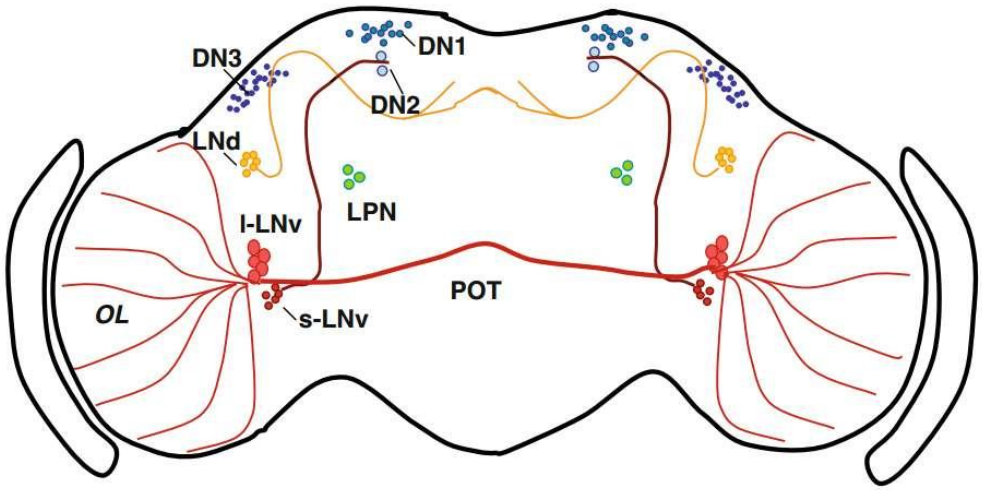

Figure 4. Scheme of *Drosophila melanogaster* cells expressing PERIOD. Dorso-lateral neurons (LNd), dorsal neurons 1-3 (DN1-3), large ventro-lateral neurons (l-LNv), optic lobe (OL), posterior lateral neurons (LPN), posterior optic tract (POT), small ventro-lateral neurons (s-LNv). The s-LNvs and l-LNvs express the neuropeptide pigment-dispersing factor. l-LNvs send their axons to the ipsi- and contralateral OL, sLNvs poject to the dorso-medial region of the protocerebrum (Tomioka and Matsumoto, 2010).

such as sLN_vs and lLN_vs, over 60 percent of them express its receptor (PDFR), such as lLN_vs, LN_ds and the $DN_{1-3}s$ (Helfrich-Forster, 1995; Hyun et al., 2005; Lear et al., 2005; Mertens et al., 2005). Interestingly, the brain structure mutant fly *disconnected* (*disco*) which lack LNs, was demonstrated to be arrhythmic (Dushay et al., 1989; Helfrich-Forster, 1998). Also mutant flies lacking PDF or its receptor became arrhythmic in DD (Renn et al., 1999; Lear et al., 2005; Mertens et al., 2005). Furthermore, PDF was shown to adjusts cycling amplitude, period, and phase of *Drosophilas'* clockwork (Yoshii et al., 2009). Thus, PDF containing cells are pacemaker neurons controlling circadian locomotor activity (Helfrich-Förster, 1996).

1.4 The circadian system of *Rhyparobia maderae*

The cockroach *R. maderae* was the first animal where a circadian pacemaker controlling circadian locomotor activity was localized. Microlesions located the circadian clock to a general area of the ventral medulla in the cockroaches' optic lobe (Nishiitsutsuji-Uwo and Pittendrigh, 1968; Roberts, 1974; Sokolove, 1975). However, the cellular nature of the circadian clock remained elusive. Later, with immunocytochemistry against the crustacean β-pigment-dispersing hormone (PDH = insect pigment dispersing factor, PDF) neurons were detected (Homberg et al., 1991) which fulfilled all morphological criteria previously suggested for circadian pacemaker neurons (**Fig. 5**; Page, 1982). Thus, Homberg et al., (1991) was the first who suggested that PDF-immunoreactive (-ir) neurons are circadian pacemaker neurons in insects. Lesion- and transplantation experiments combined with behavioural assays tested this hypothesis in the cockroach *R. maderae* and identified the accessory medulla (AMe) with associated PDF-ir neurons as the circadian pacemaker system (Stengl and Homberg, 1994; Reischig and Stengl 2003). A total of four PDF-ir cell groups in the optic lobes were observed in the Madeira cockroach. Two of them were found in the distal- (dPDFLa) and ventral lamina (vPDFLa) with processes into the lamina, accessory laminae, medulla, and the first optic chiasm. The other two neuron groups were located posteriorly (pPDFMe) and anteriorly (aPDFMe) to the medulla. These neurons branched in the AMe, ipsilateral medulla and lamina, midbrain, and also in the contralateral AMe, medulla, and lamina, projecting via anterior and posterior

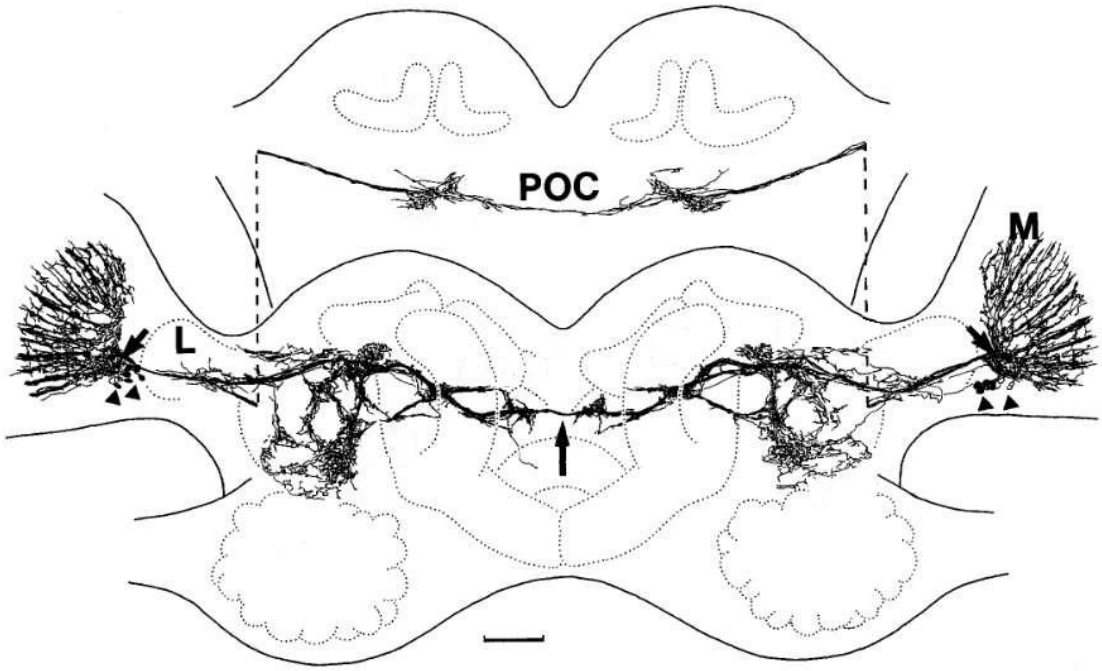

Figure 5. Frontal reconstruction of the branching pattern of pigment-dispersing factor (PDF) immunoreactivity in the Madeira cockroach. Arrowheads point to the PDF-immunreactive medulla neurons which arborize in the accessory medulla (short arrow) and have branchings to the contralateral optic lobe via the anterior (long arrow) and posterior optic commissures (POC). Lamina (L), medulla (M), scale bar: 200 µm (modified after Stengl and Homberg, 2004).

optic commissures (Reischig and Stengl, 2002; Reischig et al., 2004; Wei et al., 2010; Soehler et al., 2011; Wei and Stengl, 2011). Thus, the morphological data as well as electrophysiological experiments (Loesel and Homberg, 2001) in the Madeira cockroach suggested that PDF-ir neurons are involved in transmitting ipsi- and contralateral light and phase information to the AMe and that they couple both accessory medullae (AMae). This assumption was strengthened by further lesion- and AMe transplantation experiments as well as injections of PDF which phase shifted the circadian locomotor activity (Stengl and Homberg, 1994; Petri and Stengl, 1997; Reischig and Stengl, 2003a). Moreover, further neuropeptides and neurotransmitter are involved in the circadian sys-

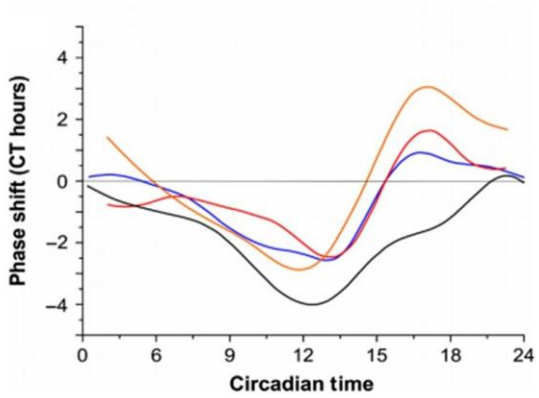

Figure 6. Splined phase response curves (Schulze et al., 2013). Comparison of light pulses (orange; Page and Barrett, 1989) and of injections of *Rhyparobia*-MIP-1 (black; Schulze et al., 2013), orcokinin (blue; Hofer and Homberg, 2006), and γ-aminobutyric acid (red; Petri et al., 2002) .

tem (**Fig. 6**). In addition, with immunocyctochemistry and matrix-assisted laser desorption/ionization-time of flight mass spectrometry numerous neuropeptides and -transmitters in approximately 250 cells associated with the AMe were identified (Reischig and Stengl, 1996, 2003b; Soehler et al., 2008; Schulze et al., 2012; Schulze et al., 2013; Schendzielorz and Stengl, 2014). In injection experiments, several neuropeptides and -transmitters generated either biphasic PRCs (**Fig. 6**), such as γ-aminobutyric acid (GABA) and orcokinins (ORCs), or monophasic all delay PRCs such as serotonin, PDF, *Rhyparobia*-myoinhibitory peptide (MIP)-1, allatotropin (AT), and acetylcholine (ACh), with maximum phase shifts at the beginning of the subjective night. So far, only *Rhyparobia*-MIP-2 induced an all advance PRC with its maximum phase shift at the end of subjective night (Page, 1987; Petri et al., 2002; Hofer and Homberg, 2006; Schendzielorz, 2013; Schulze et al., 2013; Schendzielorz and Stengl, 2014).

1.5 Light entrainment

In the fruit fly *D. melanogaster* several photoreceptors are involved in transmitting light information to the circadian pacemaker center. The blue light receptor CRY 1 (Myers et al., 1996; Stanewsky et al., 1998; Ishikawa et al., 1999), the Hofbauer-Buchner eyelets (Helfrich-Forster et al., 2002), ocelli, and compound eyes (Hofbauer and Buchner, 1989; Rieger et al., 2003) are all relaying light information to the circadian clock. In contrast, in the hemimetabolous cockroaches only the compound eye was shown to entrain the circadian system (Roberts, 1965). However, the cellular nature of the light entrainment pathways to the AMe are not known. Immunocytochemical experiments demonstrated that the AMe is not directly innervated by histaminergic photoreceptor cells. Thus, indirect photic pathways to the AMe from the lamina, where photoreceptors R1-R6 terminate and from a layer in the medulla, where photopreceptors R7 and R8 arborize were assumed (Shaw, 1981; Loesel and Homberg, 1999). A candidate for the ipsilateral light entrainment pathway is the GABAergic distal tract which connects the distal medulla and probably the lamina with the AMe (Reischig and Stengl, 1996). Furthermore, several light-responsive median neurons appear to connect the AMe with ipsilateral optic lobe neuropils (Loesel and Homberg, 2001). In addition, contralateral light input could reach the AMe via ORC-ir neurons which appear to connect contralateral optic lobe neuropils to the

AMe (Reischig and Stengl, 1996; Loesel and Homberg, 2001). This assumption is supported by GABA- and ORC injection experiments (**Fig. 6**), since both induced biphase light-like PRCs (Petri et al., 2002; Hofer and Homberg, 2006; Schulze et al., 2013). However, injections of further neuroactive substances such as *Rhyparobia*-AT, -MIP-1, -MIP-2, and ACh only resemble light-induced delay or advance parts. Therefore, they are assumed to be involved in transmitting delay or advance information (Schendzielorz, 2013; Schulze et al., 2013; Schendzielorz and Stengl, 2014).

1.6 Peripheral circadian pacemaker

Next to the central clock that organizes behavioural rhythms, autonomous clocks in sensory neurons as well as different effector organs exist (**Fig. 1**). They express circadian clock genes, are directly entrained by light, and/or coupled among each other via mostly unknown coupling factors to serve synchronized sensory input or respective vegetative outputs (Giebultowicz, 2001; Tomioka et al., 2012). In the Madeira cockroach, individual olfactory receptor neurons (ORNs) are peripheral circadian pacemaker neurons since they sustain rhythmic responsiveness to odours after removal of the "central clocks" located in the optic lobes (Saifullah and Page, 2009). Moreover, rhythmical clock genes expression could be detected in antenna of moths (Merlin et al., 2007; Schuckel et al., 2007). Thus, also ORNs of the hawk moth *M. sexta* are assumed to be peripheral circadian pacemaker neurons (Schuckel et al., 2007).

1.7 Olfaction

The olfactory sense is very prominent in the animal kingdom and is essential for foraging, search for partners, egg deposition, and recognition of predators. Olfactory organs are the antennae and the pedipalps on the head of insects. They contains numerous sensory hairs which are innervated by two or more ORNs. The ORNs express sensory neurons which belong either to the gene family of the IRs (glutamate-like receptors) or to the olfactory receptors (ORs) and can be distinguished in generalists, specialised generalists, and specialists. While generalists can be activated by a wide range of molecules and specialized generalists by substance classes, specialists, such as pheromone-sensitive ORNs

respond only to one species-specific pheromone component (Boeckh et al., 1965; Gesteland, 1971).

1.7.1 Mating behaviour of *M. sexta*

Female hawk moths attract their specific males with pulsatile release of a characteristic pheromone blend from a gland in the ninth abdominal segment (Karlson and Butenandt, 1959; Karlson and Lüscher, 1959). The pheromone blend of the hawk moth was identified with mass- as well as proton magnetic resonance spectrometric analysis. It consists of eleven components at defined ratios (**Fig. 7 B**): (Z)-9-hexadecenal, (Z)-11-hexadecenal, (*E*)-11-hexadecenal, hexadecanal, (*E*,Z)-10,12-hexadecadienal, (*E*,*E*)-10,12-hexadecadienal, (*E*,*E*,Z)-10,12,14-hexadecatrienal, (*E*,*E*,*E*,)-10,12,14-hexadecatrienal, (Z)-11-octadecenal, (Z)-13-octadecenal, octadecanal, and (Z,Z)-11,13-octadecadienal (Tumlinson et al., 1989). (*E*,Z)-10,12-hexadecadienal (bombykal [BAL]) was identified as the main component (26 %). Furthermore, a synthetic blend of all components was tested in wind tunnel experiments and confirmed their behavioural relevance (**Fig. 7 A**). It triggered the specific sequence of mating behaviour in male hawk moths: arousal, upwind flight, approach, hover, hit, and bend abdomen (Tumlinson et al., 1989). Surprisingly, a two component mixture containing BAL and *(E*,*E*,Z)-10,12,14-hexadecatrienal at a specific ratio was enough to trigger arousal and mating flight in males. Thus, some of the components were assumed to be by-products.

Mating behaviour of male and female hawk moths is under circadian control. At night, female hawk moths start calling behaviour: they evert their pheromone gland and emit pheromone in a pulsatile fashion. This behaviour is controlled by an endogenous circadian clock (**Fig. 8**), since calling is rhythmic in DD with a circadian period of 25.4 h (Itagaki and Conner, 1988). Moreover, both females' pheromone release and males' search behaviour are synchronized (**Fig. 9**). Virgin females express two flight peaks at the beginning and end of night at ZT 0 and 16 (ZT 0 = light on, ZT 16 = light off), whereas calling behaviour was observed during the night (**Fig. 9 A**). Virgin males flight activity in the absence of females began at lights-off at ZT 16 and spanned the entire period of females calling behaviour (**Fig. 9 B**). Combining both sexes, maximal mating was observed at the beginning of females' calling behaviour at ZT 17 (Sasaki and Riddiford, 1984).

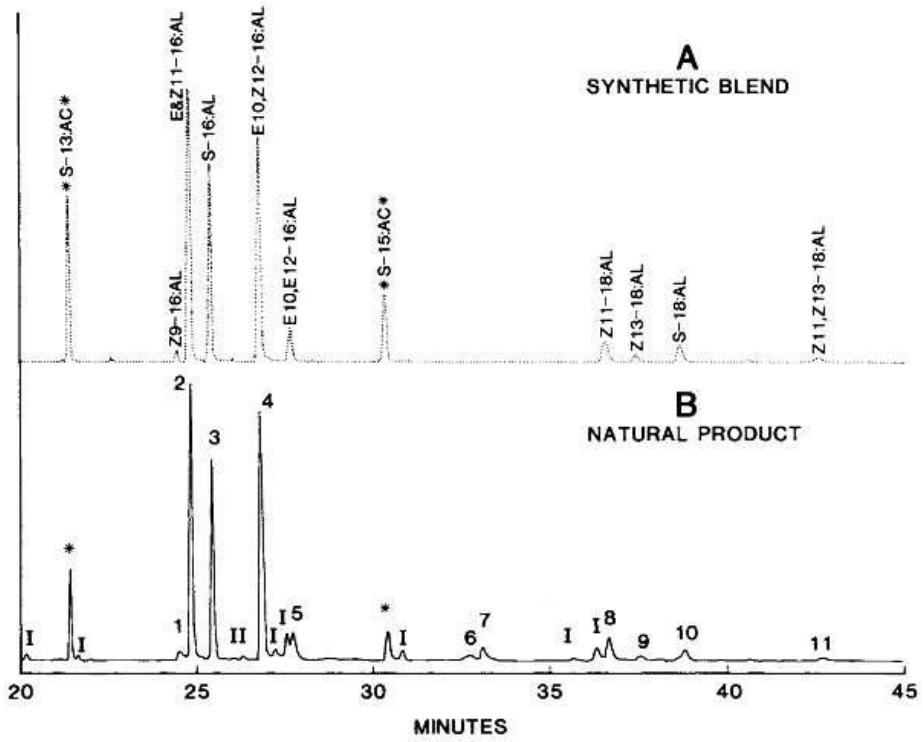

Figure 7. Gas-liquid chromatography of synthetic blend (A) and five female gland equivalents rinsed in hexane of *Manduca sexta*. Internal standards are indicated by asterisks. Solvent impurities (I), (Z)-9-hexadecenal (Z9-16:AL; 1), (Z)-11-hexadecenal and (*E*)-11-hexadecenal (E&Z11-16:AL; 2), (S)-16-hexadecenal (S-16:AL; 3), (*E*,Z)-10,12-hexadecadienal (E10,Z12-16:AL; 4), (*E*,*E*)-10,12-hexadecadienal (E10,E12-16:AL; 5), (Z)-11-Octadecenal (Z11-18:AL; 8), (Z)-13-octadecenal (Z13-18:AL; 9), (S)-18-octadecenal (S-18:AL; 10), (Z,Z)-11,13 octadecadienal (Z11,Z13-18:AL; 11) (Tumlinson et al., 1989).

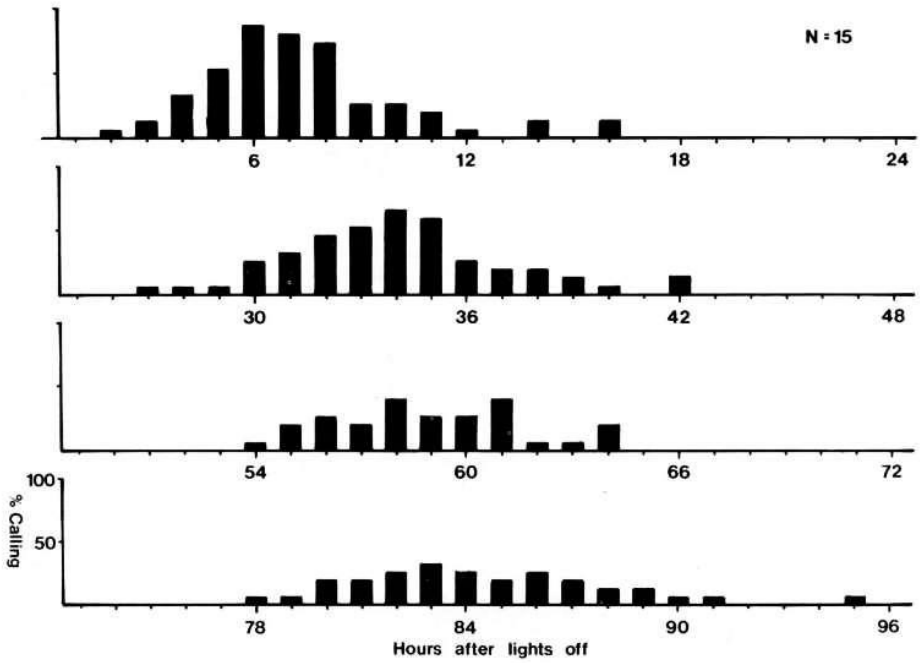

Figure 8. Rhythmic calling behaviour of female *Manduca sexta* under constant conditions (DD). Illustration demonstrates the first four days under DD indicated by hours after lights off. Period length = 25.4 h (Itagaki and Conner, 1988).

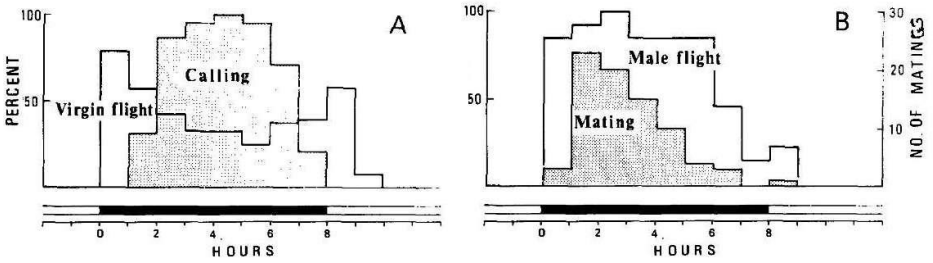

Figure 9. Timing of virgin female- (A; n=24) and male (B; n=21) flight activity (open bars). Stripped bars indicate calling of virgin females beginning at Zeitgeber time (ZT) 17 (**A**; n=21) and maximum mating activity of virgin animals at ZT 17 (**B**; n=78) observed in laboratory colonies (modified after Sasaki and Riddiford, 1984).

1.7.2 Mating behaviour of *R. maderae*

The cockroach *R. maderae* belongs to the subfamily of Oxyhaloniae and lives in large associations without stable hierarchies or territorial behaviour. However, aggressive and competitive behaviour can occur when fighting for rare resources (Bell et al., 1979). In this subfamily males attract females with pheromone which is synthesized in the sternal glands on anterior and posterior sternites and consists of hydroxy-3-butan-2-one, (2R,3R)-butanediol, senecioic acid, and (E)-2-octenoic acid (**Fig. 10**). A mixture of hydroxy-3-butan-2-one and senecio acid was sufficient to attract females in Y-maze olfactometer experiments (Farine et al., 2007). When a female is attracted and in direct proximity, the

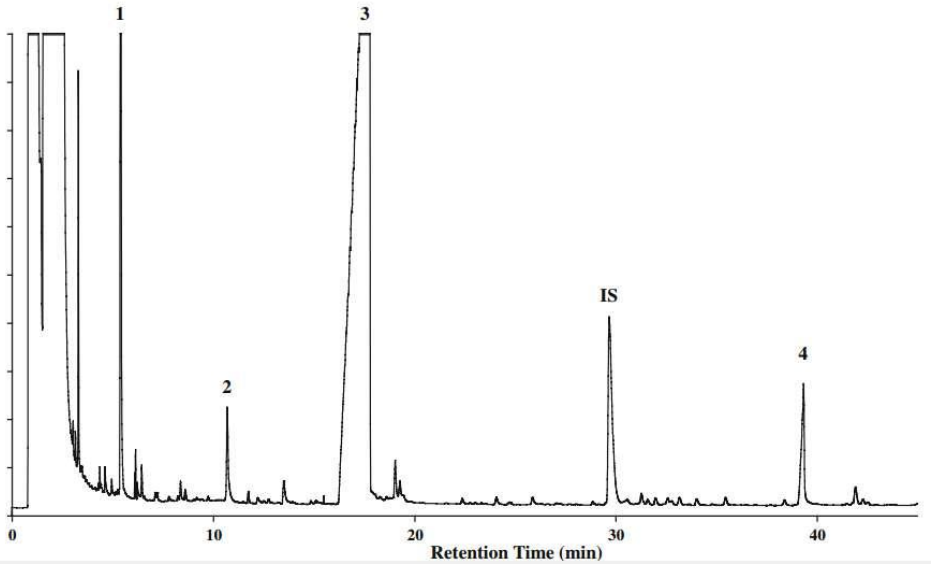

Figure 10. Gas chromatographic analysis of *Rhyparobia maderae* pheromone. In total, four components were identified in sternal glands: hydroxy-3-butan-2-one (1), (2R,3R)-butanediol (2), senecioic acid (3), (E)-2-octenoic acid (4), internal standard (IS; Farine et al., 2007).

male begins to touch the female with his antenna and raises his wings. Finally, the female mounts the abdomen of the male and tests his aphrodisiac from his tergites. The aphrodisiac resembles the male-specific pheromone. Thereafter, the female decides whether it will copulate or not (Sreng, 1993). Cockroaches' mating activity is maximal at the end of the day at ZT 8-10 and the beginning of the night at ZT 12-14 (**Fig. 11**). It can be initiated by both, males and females and it remains rhythmic in DD (Rymer et al., 2007).

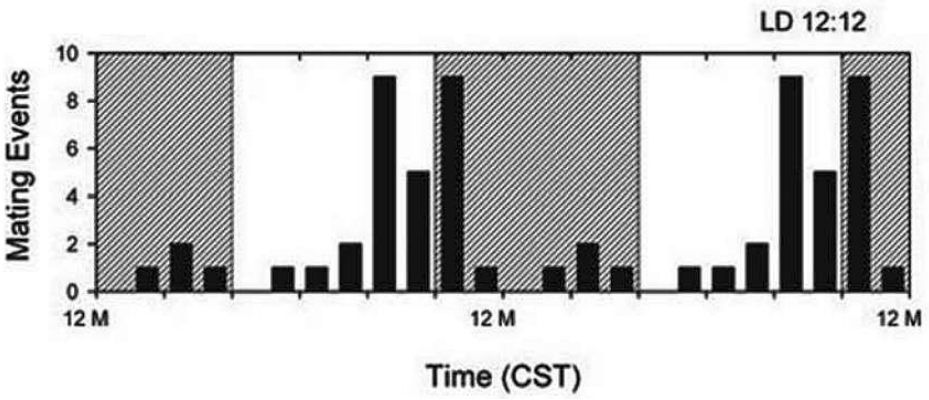

Figure 11. Diurnal mating rhythms of *Rhyparobia maderae*. The number of observed mating events is demonstrated on y-axis, the time of day on x-axis (double plot). Hatched bars illustrate scotophase, white bars photophase (Rymer et al., 2007).

Cockroaches' mating behaviour is gated by a circadian clock located in the optic lobes, since abolishing of both optic tracts disrupted mating rhythms (Rymer et al., 2007). Since male and female mating behaviour is initiated, synchronized, and maintained by pheromones, it is not surprising that pheromone-sensitive ORNs express circadian rhythms in pheromone-sensitivity as shown in antennal electroantennogram (EAG) recordings (Rymer et al., 2007; Saifullah and Page, 2009). Unexpectedly, the maximum in the ethyl acetate-dependent EAG amplitude was detected at the animals' resting time (**Fig. 12**).

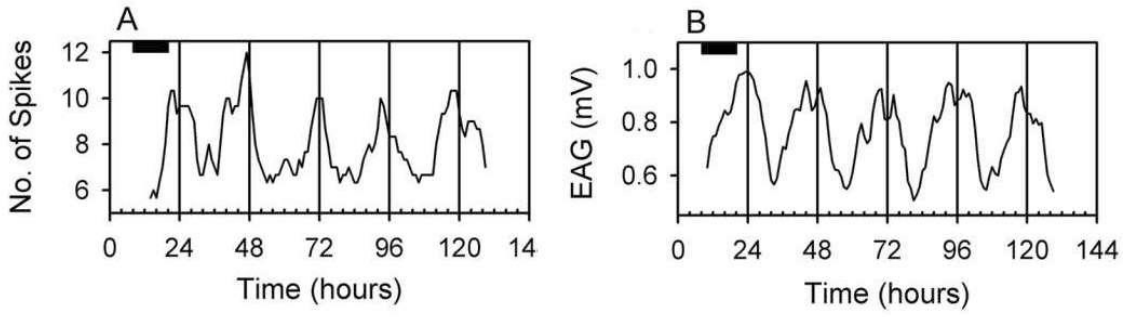

Figure 12. Circadian oscillations in number of spikes (A) and electroantennogram (EAG) amplitude (B) in response to ethyl acetate pulses. Recording was performed under constant conditions prior 12:12 light-dark (LD) changes. Last dark phase of LD condition is illustrated with black bar (modified after Saifullah and Page, 2009).

1.7.3 Structure of the hawk moth antenna

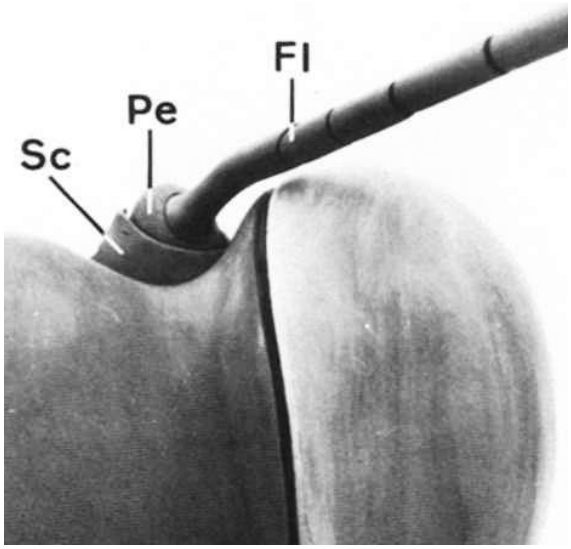

Figure 13. Model of the head of *Aglais urticae* (Lepidoptera; modified after Niehaus and Gewecke, 1978). Scape (Sc), pedicel (Pe), flagellum (Fl).

The antenna, the main olfactory organ of insects, consist of the scape, pedicel, and flagellum (**Fig. 13**). In hawk moths, it is surrounded by a 25 µm thick epidermis and has a total length of 2 cm. The flagellum is much larger as compared to the first two segments, the scape and pedicel, and consists of 80 annuli. A large trachea and a large blood vessel run from the brain up to the tip of the antenna, basally on the scale-side of the antenna. Along the top of the trachea the antennal nerve projects to the antennal lobe of the brain. The antennal nerve consists of two bundles which contain the axons of the sensory neurons which innervate sensilla on the two faces of the sensilla-side of the antenna (**Fig. 14**; Sanes and Hildebrand, 1976). Most prominent on the sexually dimorphic, keyhole-shaped male antenna is the V-shaped phalanx of long, pheromone-sensitive trichoid sensilla. In contrast, these long trichoid sensilla are missing on the smaller, round female antenna (Lee and Strausfeld, 1990). Altogether, nine types of sensilla were identified on the male antenna with 2,222 of them on one annulus (**Tab. 1**). Most of them are trichoid sensilla type one and two. Type one is 70-600 µm long and is innervated by two sensory cells, whereas type two is only 30-70 µm long and includes up to three sensory cells. Moreover, numerous pores are located

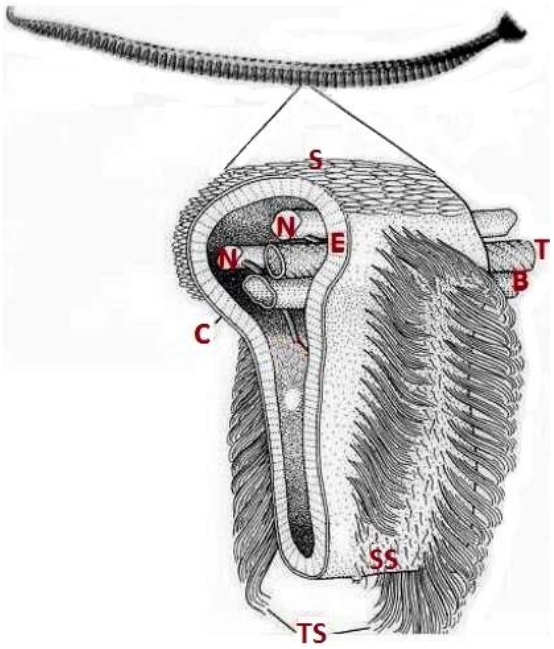

Figure 14. Cross-section of *Manduca sexta* annulus. Blood vessel (B), cuticle (C), epidermis (E), nerve bundle (N), scale site (S), short sensilla (SS), trichoid sensilla (TS), trachea (T; modified after Sanes and Hildebrand, 1976).

on them, required for penetration of odour molecules (Lee and Strausfeld, 1990; Kalinova et al., 2001). In the hawk moth one of the two ORNs of the long trichoid sensilla always detects BAL, while the second most often is tuned to either of the two trienals, (*E*,*E*,Z)-10,12,14-hexadecatrienal and (*E*,*E*,*E*,)-10,12,14-hexadecatrienal (Kalinova et al., 2001).

Table 1. Total number of sensilla on one annulus and their function in *Manduca sexta* (modified after Lee and Strausfeld, 1990).

Sensilla types	Function	Counted sensilla	Calculated neurons	Neurons per antenna*
Trichodea I	Olfaction	834	1,664	133,120
Trichodea II	Olfaction	736	1,921	153,680
Basiconica I	Olfaction	166	390	31,200
Basiconica II	Olfaction	372	833	66,640
Chaetica I	Chemoreception, mechanoreception	8	40	3,200
Chaetica II	Mechanoreception	9	9	720
Coeloconica I	Olfaction, thermoreception	22	110	8,800
Coeloconica II	Thermoreception, hygroreception	3	9	720
Styliform complex	Thermoreception hygroreception	6	18	1,440
Not-identified		66	168	13,440
Total		**2,222**	**5,162**	**412,960**

* Calculation based on 80 annuli.

1.7.4 The antenna of the Madeira cockroach

The antennal flagellum of *R. maderae* consists of 130 annuli and is twice as long as the antennal flagellum of the hawk moth. The total number of sensilla per antenna was calculated to be 33,000 containing 93,790 neuronal cells (**Tab. 2**; Schafer, 1971). Also in this cockroach, the largest number of sensilla are responsible for odour perception, as 22,500 sensillae trichodea and 4,000 sensillae basiconicae were calculated. However, shaft length of trichodea A and B is only up to 8 µm long. Additionally, 5,400 sensilla chaetica type I were counted, which are assumed to be mechanosensors (Schafer, 1971). Thus, their number on the cockroach antenna is much higher than on hawk moth antennae,

possibly because cockroaches live together in large colonies, as compared to the solitary hawk moths (Huber et al., 1990).

Table 2. Calculated total number of antennal sensory neurons in *Rhyparobia maderae* (modified after Schafer, 1971).

Sensilla types	Function	Neurons per antenna
Trichodea A	Olfaction	45,200
Trichodea B	Olfaction	200
Basiconica	Olfaction	21,000
Scolopidia	Olfaction	40
Chaetica A	Chemo-, mechanoreception	110
Chaetica B	Mechanoreception	27,000
Coeloconica	Olfactory, thermoreception	100
Campaniformia	Thermo- and hygroreception	140
Johnston's organ	Thermo- and hygroreception	unknown
Total		**93,790**

1.7.5 Perireceptor events in insect sensilla

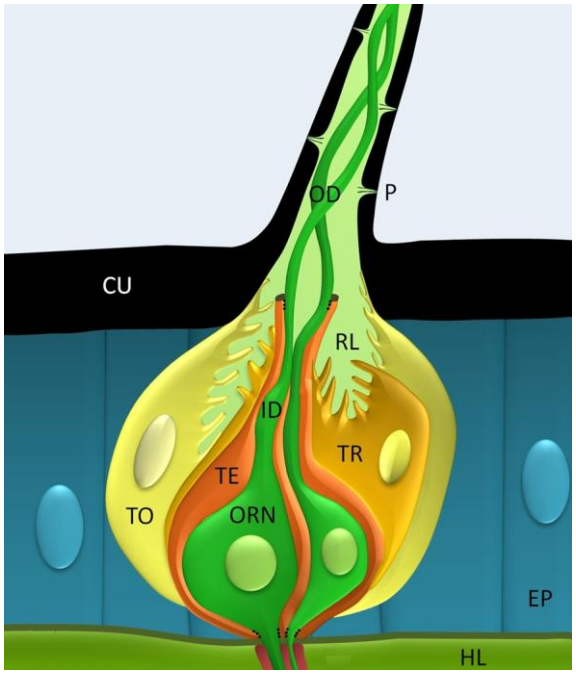

Figure 15. Trichoid sensillum of *Manduca sexta* consisting of two olfactory receptor neurons (ORNs). Cuticle (CU), epithelial cells (EC), hemolymph (HL), inner- and outer dendrite (ID,OD), pores (P), thecogen- (TE), tormogen- (TO), and trichogen- (TR) cells, receptor lymph (RL; modified after Stengl, 2010).

After passing the pores of the trichoid sensilla the hydrophobic pheromones are carried via pheromone-binding proteins (PBPs) through the receptor lymph to reach pheromone receptors on the outer dendrite (Pelosi et al., 2006; Kaissling, 2013). The PBPs are synthesized and secreted into the receptor lymph by accessory cells. These tormogen- and trichogen cells (Steinbrecht and Gnatzy, 1984; Steinbrecht, 1998) also form the cuticular shaft of the sensillum and the receptor lymph cavity around the inner dendrite and soma (**Fig. 15**; Sanes and Hildebrand, 1976). The accessory cells´ membranes

contain vATPases which generate a transepithelial potential via potassium release (200 mM, up to 40 mV potential, hyperpolarizing the ORN) into the receptor lymph (Thurm and Wessel, 1979). The ORNs are separated into three different compartments via septate junctions and enveloping non-neuronal cells. A thecogen cell surrounds the inner dendrite segment as well as the soma of the ORN, isolating its membranes from the receptor lymph via septate junctions. The axons of the ORNs are enveloped by glia cells, shielding them from the hemolymph. Thus, only the outer dendrite is exposed to the high potassium concentration of the receptor lymph (Keil, 1989).

1.8 Olfactory signal transduction

Binding of an odorant to its receptor activates a signal transduction cascade resulting in conversion of the chemical- into an electrical signal. Although, signal transduction cascades in insects are the focus of intensive research, the mechanisms are still not completely understood. Currently, three different hypotheses of insect odour transduction are discussed. Next to pheromone induced activation of metabotropic mechanisms via of G-proteins (Stengl, 2010), activation of a sole ionotropic pathway (Sato et al., 2008) or an integrative pathway (Wicher et al., 2008) is proposed . In *D. melanogaster* ligand-binding ORs are 7-transmembrane receptors with intracellular N-terminal. They multimerize with

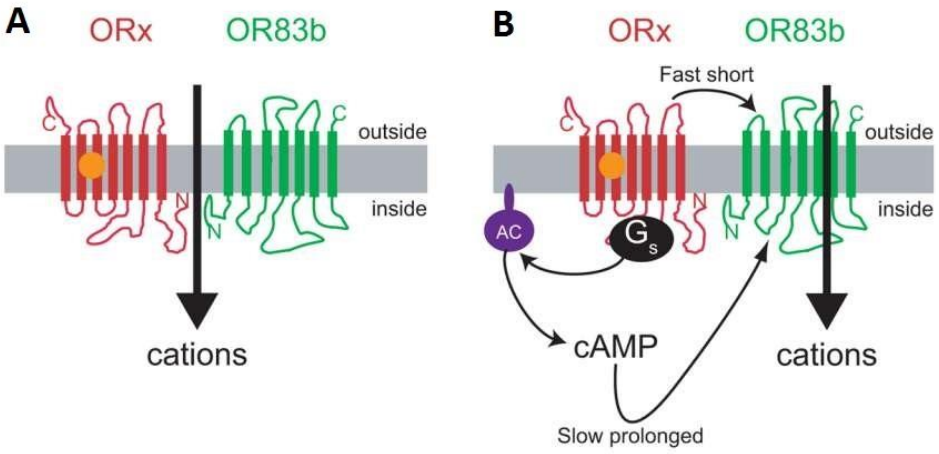

Figure 16. Proposed models for signal transduction cascades in insects. Ligand-gated nonselective cation channel activated by odours without G-protein involvement (**A**). Both, a fast ionotropic- and a slow, prolonged metabotropic response to odours (**B**). Moreover, the location of the cation differs in both models (modified after Nakagawa and Vosshall, 2009). Adenylyl cyclase (AC), olfactory receptor coreceptor in *Drosophila melanogaster* (OR83b), variable olfactory receptor (ORx).

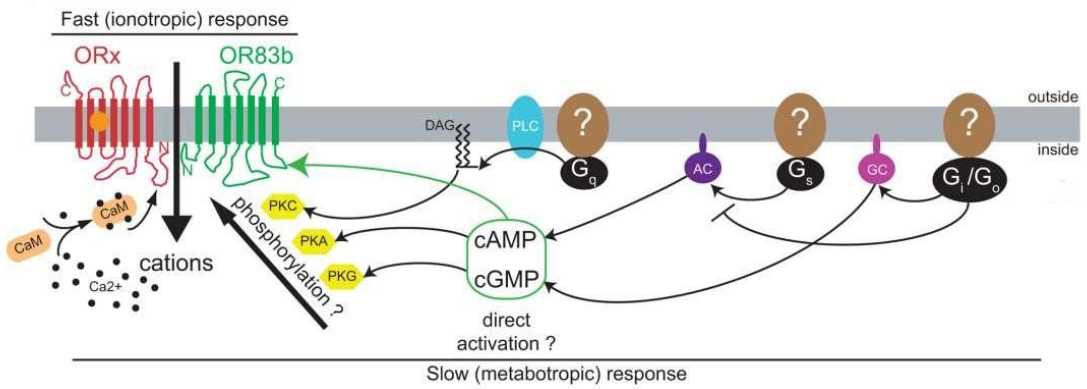

Figure 17. Integrative model of insect olfactory signal transduction proposed by Nakagawa and Vosshall, 2009. Adenylyl cyclase (AC), calmodulin (CaM), diacyl gycerol (DAG), guanylyl cyclase (GC), variable olfactory receptor (ORx), olfactory receptor coreceptor (OR83b), phospholipase C (PLC), protein kinase A (PKA), protein kinase C (PKC), protein kinase G (PKG).

a conserved cation channel called OR-coreceptor (ORCO; **Fig. 16).** Orco is essential for localization and maintainment of ORs in the dendritic membranes (Larsson et al., 2004; Benton et al., 2006; Sato et al., 2008). Coexpressing *Drosophila* OR22a and ORCO in human embryonic kidney cells resulted in a slow prolonged cAMP increase, which boosted open probability of OR/ORCO multimeric ion channels (**Fig. 16 B;** Wicher et al., 2008). Additionally, disruption of G_q signalling in *Drosophila* reduced mutants response to odours (Kain et al., 2008) as was also observed upon protein kinase C (PKC) inhibition. Interestingly, five PKC phosphorylation sites were identified in ORCO (Sargsyan et al., 2011). The phosphorylation of ORCO was necessary for its activation via cAMP (Sargsyan et al., 2011). In addition, phosphorylation of ORCO by protein kinase A (PKA) and protein kinase G (PKG) as well as direct modulation by cAMP and cGMP is proposed in a integrative model by Nakagawa and Vosshall (2009; **Fig. 17**). Contrarily to studies in the fruit fly, in the hawk moth no evidence for ionotropic ORCO-based signal transduction cascades were found (Nolte et al., 2013). As in the fruit fly also in hawk moths ORCO form a leaky cation channel, which determines spontaneous activity of ORNs (Wicher et al., 2008; Sargsyan et al., 2011; Nolte et al., 2013; Stengl and Funk, 2013). In the hawk moth ORCO is suggested to be a pacemaker channel controlling intracellular Ca^{2+} concentration, thus affecting kinetics and threshold of pheromone detection (**Fig. 18**; Stengl and Funk, 2013). Patch clamp experiments from primary cultures of ORNs suggested that pheromone transduction involves G_q-protein activation (Stengl, 2010; Nolte et al., 2013; Stengl and Funk, 2013). Thus, pheromones stimulate enzymatic degradation of phosphatidylinositol

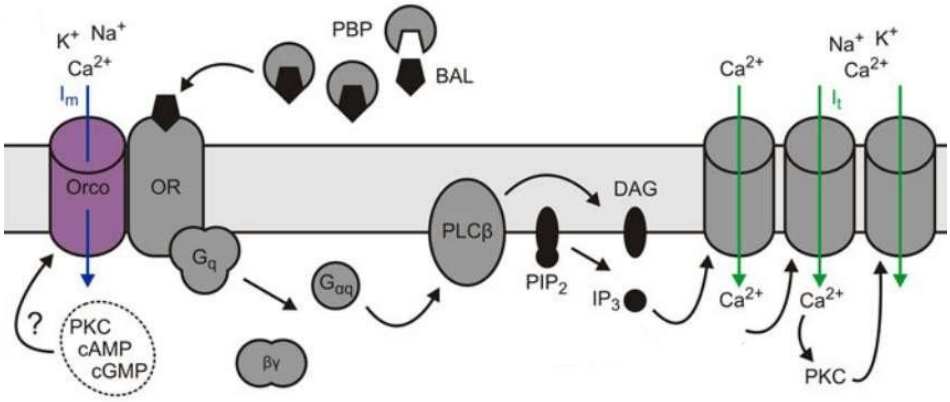

Figure 18. Proposed metabotropic cascade in *Manduca sexta*. Pheromone binding protein (PBP) transmit bombykal (BAL, hawk moth pheromone) from sensillar pore to olfactory receptor (OR). Olfactory receptor coreceptor (ORCO) affects kinetic and threshold of pheromone detection. Binding of pheromone to its receptor induces G_q-protein activation resulting in transient increased IP_3 levels. IP_3-dependent Ca^{2+} channels are opened rapidly, followed by Ca^{2+}- dependent cation channels. Consequently, elevation in protein kinase C (PKC) activity leads to further cation influx (modified after Stengl and Funk, 2013).

bisphosphate (PIP_2) into equimolar amounts of diacylglycerol (DAG) and inositol trisphosphate (IP_3) by phospholipase Cβ (PLCβ; **Fig. 18**). This is also assumed for cockroaches, since transient increases in IP_3 could be measured after pheromone stimulation in antennal homogenates of cockroaches and moths in less than 100 ms (Boekhoff et al., 1990a; Boekhoff et al., 1990b; Boekhoff et al., 1993). Moreover, elevation of guanosin triphosphate (GTP) concentration boosted this effect, indicative for G-protein activation (Boekhoff et al., 1990a). Termination of IP_3 signalling occurred via protein kinase C (PKC), since PKC inhibitors abolished transient IP_3 peaks, most probably via PLCβ inactivation (Boekhoff and Breer, 1992). Patch clamp experiments of primary ORNs from *M. sexta* supported involvement of IP_3 signalling (Stengl, 1993). Stimulation with BAL, the main pheromone component of the hawk moth, induced opening of three different channel types. First, an apparently directly or indirectly IP_3-depended Ca^{2+} channel opened and closed within less than 50 milliseconds, followed by Ca^{2+}-dependent cation channels which closed Ca^{2+}-dependently within seconds and finally, PKC-dependent cation influx occurred which was stable over several minutes. Since the last channels opened very slowly and in response to high BAL concentrations, they seemed to be involved in adaptation processes (Stengl, 1993, 1994; Krannich, 2008). Moreover, cAMP- and cGMP-activated nonselective cation currents were identified which seemed to be involved in olfactory sensitization and adaptation mechanisms, since they affect intracellular Ca^{2+} concentration (Krannich and Stengl, 2008).

1.8.1 Function of second messengers in olfaction

Since its discovery in the early 1960's as an effector of epinephrine and glucagon, cAMP became one of the best studied second messenger (Sutherland and Rall, 1960; Sutherland et al., 1967; Robinson et al., 1968). Ligand-receptor binding mediates extracellular signals into cells via activation of G-proteins. Next to direct activation of receptor adenylyl cyclases (rAC) by $G_{\alpha s}$-proteins, also inhibitory $G_{\alpha i}$-proteins as well as more complex non direct mechanisms are known (**Fig. 19**; Taylor, 1990; Sunahara et al., 1996). So far, ten isoforms of human adenylyl cyclases (ACs) have been described, whereby AC 1-9 are rACs. They contain of -NH_2 and -COOH termini, twelve transmembrane domains and two

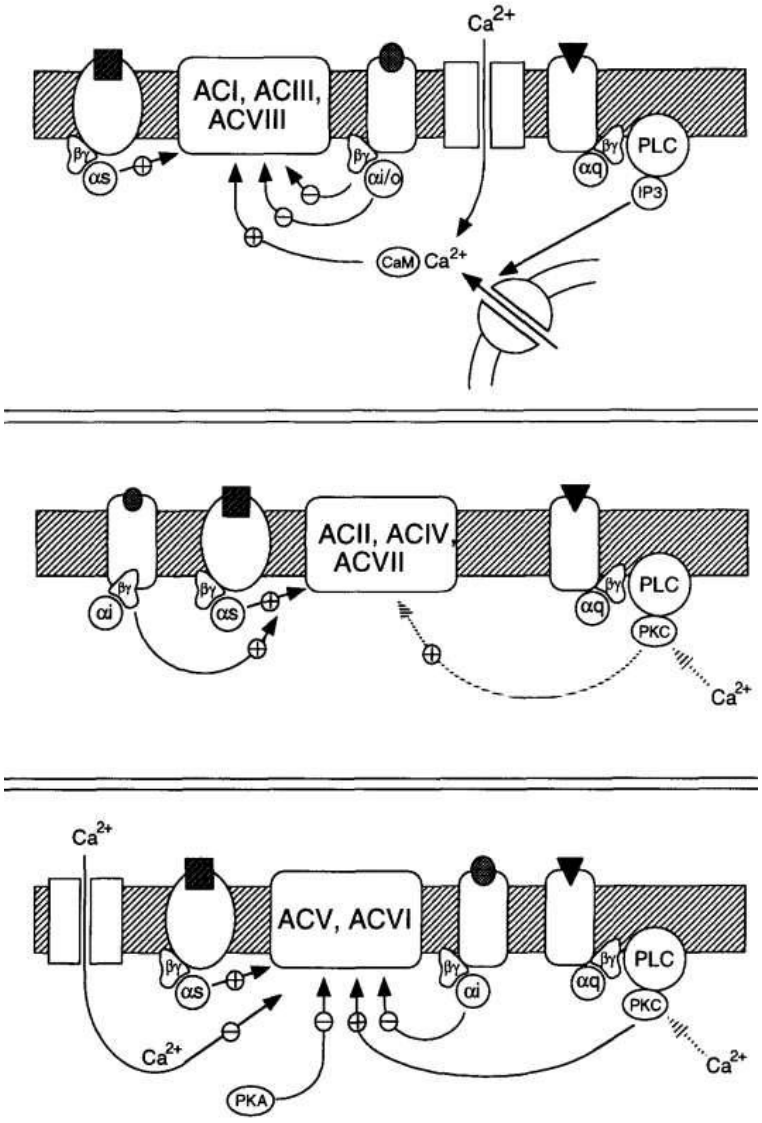

Figure 19. Regulation patterns of adenylyl cyclase (AC) 1-8. All ACs are activated by $G_{\alpha s}$-protein. Additionally, some ACs are modulated by $G_{\beta\gamma}$- as well as $G_{\alpha i}$-proteins, Ca^{2+}, Ca^{2+}/calmodulin (CaM), protein kinase A (PKA) and protein kinase C (PKC; Sunahara et al. , 1996).

cytosolic ATP binding structures (**Fig. 20**; Willoughby and Cooper, 2007). Contrarily, AC 10 is a soluble AC (sAC) which is not responsive to G-proteins but is assumed to be a sensor for bicarbonate mediating change in pH and/or membrane potential (Chen et al., 2000; Cooper, 2003). All of them catalyze ATP to cAMP, leading to increased local concentration of cAMP which affects numerous cellular targets such as PKA, exchange proteins activated by cAMP (EPAC) or cyclic-nucleotide-gated ion channels (Hanoune and Defer, 2001). Due to their high turnover number ranging up to 100 sec^{-1}, AC activation is a very potent cellular amplification mechanism (Tang and Hurley, 1998). All rAC isozymes can be activated by the diterpen forskolin (FSK) which is produced by the Indian Coleus plant, *coleus forskohlii.* Thus, forskolin became an extremely valuable and widely reagent used as a tool for examining AC activity in intact and broken cell preparations (Seamon and Daly, 1981; Daly, 1984; Insel and Ostrom, 2003). Moreover, the biogenic amine octopamine (OA), closely related to the human norepinephrine, is a potent activator of ACs in insects (Nathanson and Greengard, 1973; Roeder, 1999) which binds to α- and β-adrenergic like OA receptors (Farooqui, 2007). Degradation of cAMP to AMP is catalyzed by phosphodiesterases (PDEs; Beavo, 1995). Until now, eleven PDE isozymes are known. While three of them are cAMP specific with Michaelis-Menten constant ranging from 0.06 to 4 µmol/L (K_m, substrate concentration at half-maximal enzyme activity), five of them degrade cAMP and cGMP with similar K_m. They can be modulated in their activity by numerous molecules/ions involved in signal transduction cascades, as protein kinases, Ca^{2+}, Ca^{2+}/calmodulin (CaM) or cyclic nucleotides themselves. Moreover, PDE 5, 6, and 9 are cGMP-specific (Conti, 2000; Essayan, 2001; Lugnier, 2006). Also this cyclic nucleotide is

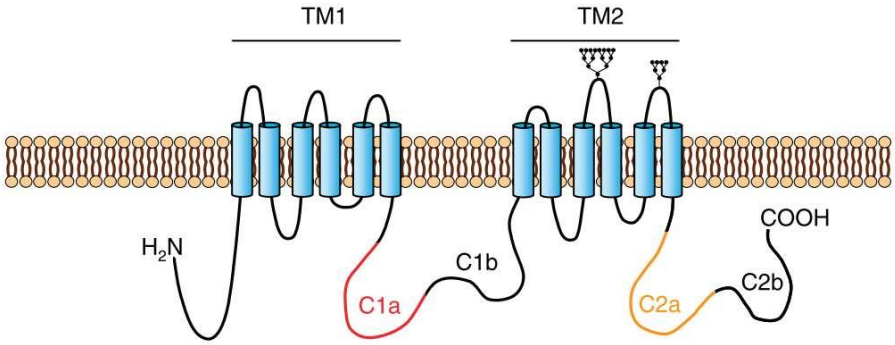

Figure 20. Structure of receptor adenylyl cyclase containing -NH_2 and -COOH termini, two transmembrane- (TM1, TM2) and cytosolic domains (C1, C2). C1a (red) and C2a (orange) are highly conserved, catalytic ATP binding domains (Willoughby and Cooper, 2007).

involved in a variety of physiological responses such as vision and olfaction (Fitzpatrick et al., 2006). cGMP is synthesized by guanylyl cyclases (GCs), described for the first time in the 1970's, which can be subdivided into soluble- (sGCs) and receptor guanylyl cyclases (rGCs; Kimura and Murad, 1974; Chrisman et al., 1975). sGCs consist of a guanylyl cyclase- and heme Fe^{2+} domain catalytically activated by nitric oxide (NO) binding (**Fig. 21**). Contrarily, rGCs are composed of an intracellular-, a transmembrane- and an extracellular ligand binding domain activated e.g. by peptides (**Fig. 21**; Kuhn, 2003). Local increase in cellular cGMP concentration can affect ion channels, PKG or cyclic nucleotide levels itself due to effects on PDEs (Lucas et al., 2000).

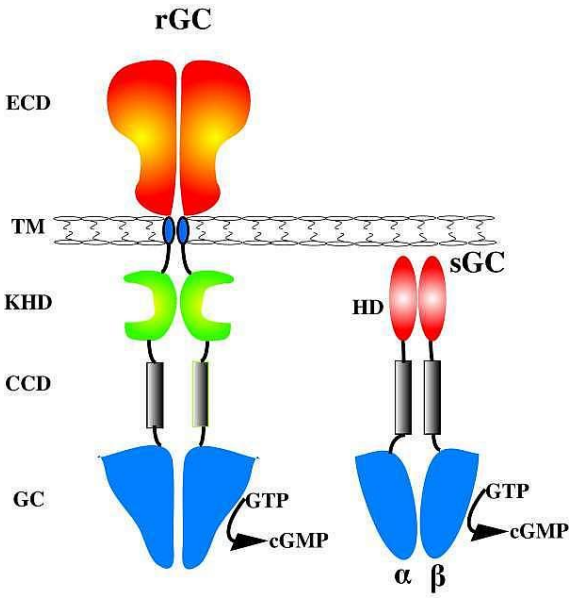

Figure 21. Structure of guanylyl cyclases. Both receptor guanylyl cyclase (rGC) and soluble guanylyl cyclases (sGC) contain guanylyl cyclase domain (GC) and contain coiled-coil domain (CC). Furthermore, sGCs have heme domain (HD), whereas rGCs have kinase homology domaine (KHD), transmembrane segment (TM) as well as extracellular domain (ECD; Fitzpatrick et al., 2006).

Recent studies focused on the role of both cyclic nucleotides in the olfactory signal transduction cascade of *M. sexta*. In tip recording experiments perfusion of cAMP into pheromone-sensitive trichoid sensilla sensitized ORNs by increasing sensillar potential amplitude (SPA) effective at the animals resting phase, but not at the animals activity phase (Flecke et al., 2010). Since OA perfusions also increased SPA and additionally action potential frequency (APF) at the same time, it was hypothesized that OA increased cAMP levels via G-proteins (Flecke and Stengl, 2009). Thereby, the effect on the APF could be mediated by another second messenger or by different cell targets of OA. Contrarily, cGMP perfusion reduced APF of ORNs (Flecke et al., 2006). Thus, cGMP is assumed to be involved in olfactory adaptation processes. This is further supported by biochemical experiments in *Antheraea polyphemus* and in *Bombyx mori.* Here, long lasting, adapting pheromone stimulation could be demonstrated to increase antennal cGMP concentration (Ziegelberger et al., 1990). Additionally, histochemical amide adenine dinucleotide phosphate diaphorase (NADPH diaphorase) staining was demonstrated in the hawk moth an-

tenna indicative for NO synthase (Stengl and Zintl, 1996). Moreover, adaptive, long-lasting pheromone stimulation increased NAPDH diaphorase activity in trichoid sensilla (Stengl and Zintl, 1996) suggesting the presence of sGCs. cGMP immunocyctochemistry confirmed this assumption since more somata were stained on the sensillar side of the antenna after NO and/or adapting pheromone stimuli than in control experiments (Stengl et al., 2001). This is in accordance with DNA sequencing and expression experiments performed by Nighorn and colleagues (1998, 1999). They found GC isoforms similar to mammalian sGCs called MsGCalpha1 and MsGCbeta1 function as NO-sensitive heterodimer as well as a novel isoform (MsGCbeta3) which is weakly stimulated by NO and act as monomer in cells from the kidney of the African Green Monkey (COS-7; Nighorn et al., 1998; Nighorn et al. 1999). Also a rGC (MsGC-II) which was inhibited by Ca^{2+} was detected (Morton and Nighorn, 2003). MsGC-I represents a new GC configuration since it shares strong similarities to mammalian rGCs, but lacks on extracellular-, transmembrane- and kinase homology domain and forms active homodimers in cytosol of COS-7 cells.

1.9 Aims of this study

Previous electrophysiological, biochemical, and immunocytochemical studies demonstrated an involvement of the second messenger cAMP, cGMP, and IP_3 in processes of olfactory signal transduction. An oscillation of second messengers was assumed as a basis for daily rhythms in olfactory behaviour. Thus, it was focused in particular on the following issues employing biochemical and behavioural methods:

- Do second messengers oscillate daytime-dependently in the antennae of holometabolous hawk moth or hemimetabolous cockroach and do they persist under constant conditions?
- Are there correlations between second messenger concentrations and behavioural rhythms depending on olfaction?
- Can these second messengers be influenced by calcium or octopamine?
- Do second messengers oscillate in the central circadian pacemaker of the Madeira cockroach?
- Could PDF influence these oscillations?
- Do second messenger injections phase shift the central clock of the Madeira cockroach?

Materials and methods

2.1 Keeping conditions

Madeira Cockroaches were kept in laboratory colonies located in 60 x 40 x 40 cm boxes including cardboard as hiding-places. They were reared under a 12:12 h LD photoperiod, at 50 % relative humidity, 25 °C room temperature (RT). They were fed with dried dog food, vegetables, and water *ad libitum*. ZT 0-12 is the light phase, while ZT 12-24 is the dark phase. Hawk moths were kept under 17:7 h long-day conditions including one hour dusk and dawn (light phase = 500 lux; dusk and dawn = 50 lux), at 40 % to 60 % relative humidity and approximately 27 °C RT. They were raised from eggs and larvae were fed with an artificial diet (modified after Bell and Joachim, 1976). To avoid olfactory adaptation (Ziegelberger et al., 1990; Boekhoff et al., 1993; Stengl et al., 2001) a few days before eclosion male pupae were cleaned from pheromone with alcohol and isolated in a flight cage (19 m^3) without females. Adults were fed with Colibri-nectar (*Nektar-plus*) which was presented in cups wrapped in artificial, scented-flowers measuring 6.5 cm in diameter (Goyret and Raguso, 2006). The paper-flowers were scented with synthetic odour of *Datura wrightii* (modified after Riffel et al. 2009). Life expectancy of adult male hawk moths was up to two weeks.

2.2 Behavioural experiments

2.2.1 Behavioural analysis of isolated cockroaches with a tracking system

Adult cockroaches were taken from laboratory colonies and isolated in white boxes (35 x 27 x 17 cm, Slugis, Ikea, Leiden, Netherlands; **Fig. 22**) for one week. The animals were able to move freely. Petroleum jelly on the wall of the boxes prevented the cockroaches' escape. Three cell culture dishes (35 x 10 mm, Cellstar, Greiner Bio-one, Kremsmünster, Austria) were placed in the boxes and provided water and glucose/casein (2:1) *ad libitum*, as well as 1 g of the male pheromone senecio acid in a closed dish with perforated lid (**Fig. 22**). LD photoperiod and temperature corresponded to conditions of laboratory colonies the animals were taken from. To detect movements at night, animals were recorded in

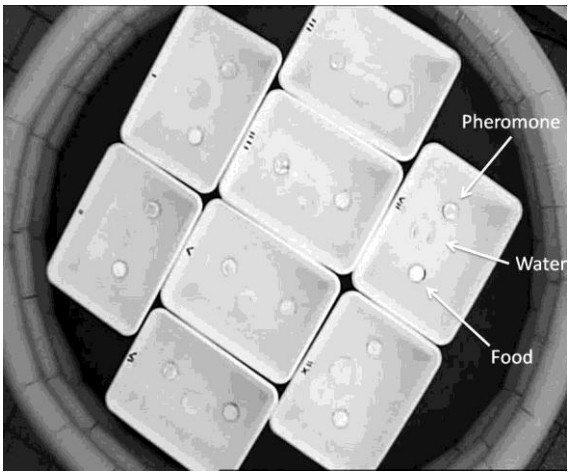

Figure 22. Structure of arena for *Rhyparobia maderae*. Female cockroaches were kept in white boxes including dishes with pheromone, water and food. Males were kept in boxes without pheromone dish. Petroleum jelly on the wall of the boxes as well as water with surfactant surround boxes prevented cockroaches' escape.

red light (<1 lux). Activity was detected by a highly sensitive closed circuit television (CCTV) colour camera (WV-CP500/G, Panasonic, Osaka, Japan) for one week with automatically regulated aperture. Saturation of the video was set to minimum values, resulting in a black and white video. Therefore, the difference between day and night video was strongly reduced and day and night data could be tracked in one step. The movie was analysed with following settings in Ethovision XT 7 software. For trial control settings standard settings were employed. The following settings were employed for cockroach tracking: video sample rate=6.33 samples per second; detection method=static subtraction; if the cockroach was darker than background, dark contrast=44 to 155; subject size=40 to 400; contour erosion=1; dilation=1 (dilate first). Track smoothing profile=14 samples before and after every sample point. Data profile: Time bin duration=6 minutes. Analysis profile: distance moved and residence per zone were calculated. Both variables were averaged for eight animals per seven days. Additionally, data were smoothed with 2nd order polynomials (Prism 5.0, GraphPad Software, La Jolly, USA).

2.2.2 Behavioural analysis of cockroaches in colonies

Overall movement of cockroaches in colonies could not be recorded reliably with the tracking system due to the large number of crossing animals and hiding-places, which induced detection failures. Thus, pheromone guided behaviour was analyzed via direct observations. The number of males which expressed calling behaviour (raising of wings up) per box were counted every hour for 15 minutes over a period of 24 h in LD. Counts were normalized by dividing number of calling males per hour by total number of calling males per day (100 %). Additionally, adaptation (sensory desensitization) experiments were performed by comparing two sets of data to determine the effect of excess male pheromones. The first set contained an equal ratio of males to females in colonies, the

second contained a large excess of male cockroaches to expose females to adapting concentrations of male pheromones.

2.2.3 Behavioural analysis of isolated hawk moths

Flight and feeding activity of isolated adult male hawk moths were detected by visual observation in flight rooms. The number of flight and feeding events was counted every hour for 15 minutes over a period of 24 h in LD. Due to varying numbers of moths per room, a normalization was performed by dividing number of events per 15 minutes by total number of events per day (100 %). Hovering before a plant and one ejection and following rejection of the proboscis was defined as one “feeding event”; one flight-start until landing was defined as one “flight event”.

2.3 Biochemical experiments

2.3.1 Collection of antennal samples

Ten female Madeira cockroaches were taken out of laboratory colonies and temporarily stored in vessels until they calmed down to avoid stress-induced cAMP increases (Peters, 2010). For DD experiments animals were taken out of laboratory colonies at the end of night and temporally stored in vessels in DD. Then, they were shock-frozen in liquid nitrogen by rapid emptying the vessel into a dewar (Typ 29B, 4 l, Carl Roth, Karlsruhe, Germany). In contrast, antennae of male *M. sexta* were collected from three animals per sample by collecting animals carefully by hand and throwing them quickly into liquid nitrogen (within three seconds). In general, frozen antennae were ground in a mortar, transferred into cups, and mixed with homogenization buffer (HB; 20 cockroach antennae/400 µl; 6 hawk moth antennae/650µl). The HB contained 0.05% sodium cholat, 200 mM sodium chloride (NaCl), 2 mM magnesium chloride ($MgCl_2$), 10 mM ethylene glycol-bis(2-aminoethylether)-N,N,N’,N’-tetraacetic acid, 50 mM 3-(N-morpholino)propanesulfonic acid (MOPS), and 1 mM DL-1,4-dithiothreitol (DTT) at pH 7.4. After mixing three times for 10 seconds samples were centrifuged at 900 g for 5 minutes at 4 °C and supernatant was used for incubation.

2.3.2 Collection of AMe and optic lobe tissue

For sample collection cockroaches were taken out of laboratory colonies at either ZT 6, 12, 18, or 24 or isolated at the end of the night in vessels for 6, 12, 18, 24, 30, 36, 42, or 48 hours under DD (DD-preparations with ZT 24 = CT 0). For ZT-preparations, they were stored temporarily together in vessels to reduce stress and allow the cockroaches to calm down. For dissecting, cockroaches were cold-anesthetized, decapitated, and the head capsule was opened. All preparations were performed in insect saline with the following composition: 128 mM NaCl, 2.7 mM potassium chloride; 2 mM calcium chloride ($CaCl_2$); 1.2 mM sodium bicarbonate; pH 7.25. Trachea and fat body were put aside to expose the optic lobes. Using an ultrafine scissor, the AMe was separated from the optic lobes and both were subsequently put in separate iced cups filled with 900 µl HB. Samples contained either 20 AMae or 6 optic lobes per 900 µl HB. All DD-preparations were performed under constant dim red light conditions. After that, samples were crushed in an ice-cooled ultrasonic bath (Transonic 310, Elma, Germany) for 25 minutes. After mixing three times for 10 seconds samples were centrifuged at 900 g for 5 minutes at 4 °C and supernatant was used for incubation.

2.3.3 Incubation and quantification of second messengers

For incubation 50 µl of the homogenate of interest was transferred into 200 µl incubation buffer (IB) at 37 °C. Protein determination with 5 µl homogenate in duplicate was performed with Bradford assays (Bradford, 1976). The IB contained 0.05 % sodium cholate, 200 mM NaCl, 5 mM MgCl2, 1 mM 1,2-bis(o-aminophenoxy)ethane-N,N,N',N'-tetraacetic acid, 50 mM MOPS, 1mM DTT, 1mM adenosine triphosphate, 4 µM guanosine triphosphate, and 220 µM $CaCl_2$ at pH 7.4 (modified after Vogl et al., 2000). Additionally, IB contained 1 mM 3-isobutyl-1-methylxanthine (IBMX) in cAMP and cGMP experiments to prevent degradation of cyclic nucleotides. Moreover, further additives like octopamine (OA), epinastine (EPI), FSK, an phospholipase (PLC) -activator (m-3M3FBS), *Rhyparobia*-PDF, as well as $CaCl_2$ were added to test their effects on second messenger concentration. The incubation lasted 10 minutes and was stopped by adding 100 µl of 7 % perchloric acid solution. This step was followed by mixing the contents and centrifuging at 900 g for 15 minutes at 4 °C. All proteins were denatured by perchloric acid. To neutralise the liquid

phase 200 µl of each incubation solution was mixed three times for 10 seconds with 50 µl 10 nM ethylenediaminetetraacetic acid solution and 250 µl chloroform/trioctylamine solution (1:1), then centrifuged at 500 g for 5 minutes at 4 °C. For cAMP, cGMP, and IP_3 quantifications 50 µl supernatant was taken in triplicate. Commercial immunoassays kits for determining second messenger concentrations were applied as described in corresponding user manual (TRK500, TRK432, GE Healthcare, Chalfonst St. Giles, Great Britain; 581001, 581021, Cayman, Michigan, USA; CSB-E12636h, Cusabio, Wuhan, P.R. China). Finally, the amount per well was multiplied by the dilution factor and normalized by calculating a quotient of second messenger concentration by corresponding protein concentration.

2.3.4 Manufacturing of competitive ELISAs

Microtitre plates (Maxisorp, Nunc, Roskilde, Denmark) were coated with 125 µl 15 µg/ml goat-anti rabbit IgG (Dianova, Hamburg, Germany), dissolved in phosphate buffer (PBS; 100 mM sodium phosphate dibasic dehydrate, 20 mM sodium phosphate monobasic monohydrate; pH 7.4) at 4 °C overnight on a shaker covered with adhesive foil. After washing the wells one time with 250 µl washing buffer (WB; 0.05 % Tween® 20 in PBS), non-specific binding (NSB) was prevented by adding 250 µl blocking buffer (BB; 1 % bovines serum albumin in WB) for one hour at RT. Then, the wells were rinsed three times with WB. Both, rabbit-anti cAMP and rabbit-anti cGMP antibodies (Genscript, Piscataway, USA) were diluted at 1:26,666 in BB. Standards of cAMP ranged from 12.5 pmol/50 µl to 390 fmol/50 µl and of cGMP from 1000 fmol/50 µl to 31.25 fmol/50 µl and were dissolved in PBS. cAMP- and cGMP conjugated to horseradish peroxidase (HRP, Genscript, Piscataway, USA) were used at a concentration of 1:6,666 in BB. NSB, maximum binding (B0) of tracer, standards and samples were measured as described in **Tab. 3**.

Table 3. Schematic drawing of ELISA layout.

	PBS	BB	Sample or standard	HRP-conjugate	Antibody
NSB	50 µl	50 µl		50 µl	
BO	50 µl			50 µl	50 µl
Standard or sample			50 µl	50 µl	50 µl

Blocking buffer (BB), maximum binding of tracer (B0), non-specific binding (NSB), phosphate buffer system (PBS).

Incubation was carried out on a shaker covered with adhesive foil over night at 4 °C. Finally, wells were washed three times with WB and 25 µl of development solution 1 (100 mM citric buffer at pH 5, 0.02 Vol.-% hydrogen peroxide, 0.3 Vol.-% phosphoric acid) and 50 µl of development solution 2 ($_{dd}H_2O$, 0.1 Vol.-% phosphoric acid, 0.7 Vol.-% of DMSO containing 420mM 3,3‘,5,5‘-Tetramethylbenzidin) were successively added with a repetitive pipette (HandyStep, Brand, Wertheim, Germany) into the wells. After 10 to 30 minutes incubation time at RT, reaction was stopped by adding 50 µl 1 M sulphuric acid. Photometric quantification was performed at 450 nm on a wellplate reader (POLARstar, BMG Labtech, Ortenberg, Germany, Bos et al., 1981). For calculation of cyclic nucleotide amount per well, four parametric logistic fit was performed through standards (**Fig. 23**). The goodness of fit was never above 0.95.

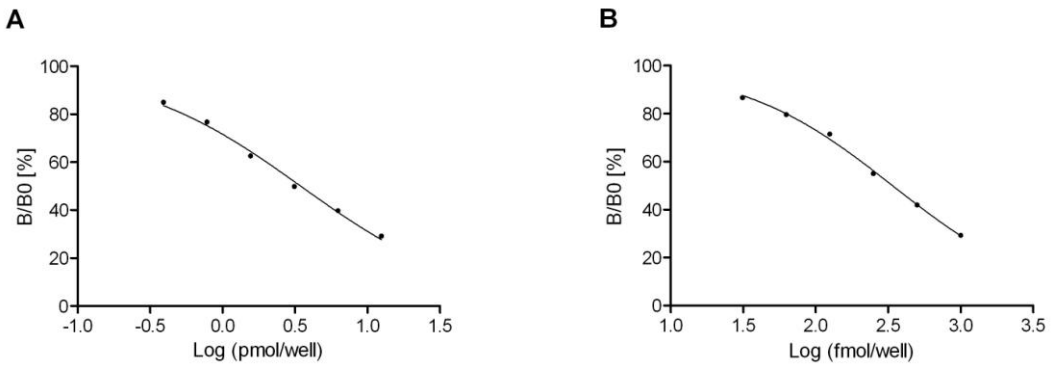

Figure 23. Four parametric logistic fit of cAMP- (A) and cGMP ELISA (B) based on six standards (cGMP: 31.25 - 1000 fmol/well; cAMP: 0.39 - 12.50 pmol/well). The goodness of fit was above 0.99.

2.3.5 Quantification of OA

For sample collections three male hawk moths each were taken out of the flight room at ZT 1, 9, 16, 18, 20, and 23. Then, the animals were quickly shock-frozen in liquid nitrogen, their antennae were ground in a mortar and transferred into cups. To disrupt enzymatic reactions nitrogen cooled samples were mixed with 100 µl 7 % perchloric acid followed by 250 µl 10 mM ethylenediaminetetraacetic acid (EDTA) solution. Then, the mixture was centrifuged at 900 g for 15 minutes at 4 °C. For neutralization 275 µl supernatant was mixed in 400 µl 10 mM EDTA as well as 400 µl chloroform/trioctylamine solution (1:1) and centrifuged at 500 g for 5 minutes at 4 °C. OA quantification was performed in triplicate with a commercially available OA kit (MBS726911, Mybiosource, San Diego, USA).

2.3.6 Rapid kinetic-assays

To determine whether OA-signalling takes place in the millisecond range rather than in the range of seconds to minutes, assays for rapid kinetic measurements were developed. In a self-made setup computer-controlled pressure injection mixed respective incubation buffers with antennal homogenates. The reaction was stopped with injection of 7 % perchloric acid solution after defined delays in the ms range. Pressure injection of reagents was controlled via magnetic valves. Neutralization, normalization, and second messenger quantification was performed as described previously (Schendzielorz et al., 2012).

2.3.7 Data analysis

Before data were evaluated statistically, the distributions were analysed by Shapiro Wilk tests. Since data did not display normal distributions nonparametric tests were applied. Depending on the experimental structure the Kruskal-Wallis test for unpaired- or Friedman test for paired samples followed by Dunn's multiple comparison post hoc test as well as Mann-Whitney U-test was employed. Arithmetic means and standard errors of data were calculated and are stated in the text and figures.

2.4 Injection experiments

2.4.1 Behavioural assay

Analysis was performed in constant darkness at constant temperature (25 °C) in a running-wheel assay. Experimental animals were fed with sesame sticks and water ad libitum. The free-running period (tau = τ) before and after injection as well as phase shifts (delta phi = Δϕ) after injections were calculated as described in Schulze et al. (2013). Briefly, τ was determined by applying Chi-Square periodgram analysis using ActogramJ (Schmid et al., 2011). With a linear regression through the corresponding activity onset, defined as CT12 and used as phase reference point, the circadian time of each animal was determined before injection. To evaluate Δϕ, τ was determined the same way after the injection whereas Δϕ corresponds to the difference of linear regression before and after the experiments at the day of injection.

2.4.2 Injections

Under constant dim red light conditions at different CTs the cockroaches were removed from the running-wheels, anesthetized with CO_2 and fixed in a metal holder. Injections (2 µl) were performed into the hemolymph of the head capsule by using a repetitive pipette (HandyStep, Brand, Wertheim, Germany; Schulze et al., 2013). The phase response curves (PRCs) were prepared with 2 x 10^{-10} mol membrane permeable cyclic nucleotides (Sigma, Germany) or with 2 x 10^{-12} mol Rhyparobia-PDF (NSELINSLLGLPKVLNDAa, Hamasaka et al., 2005, Iris Biotech), whereas for the dose-dependency curves and calculation of the half maximal effective dose (EC_{50}) 2 x 10^{-7} mol, 2 x 10^{-10} mol, 2 x 10^{-13} mol, and 2 x 10^{-16} mol 8-br-cAMP or 8-br-cGMP were applied. Cyclic nucleotide analoga and Rhyparobia-PDF were dissolved in insect saline. Control injections contained only insect saline.

2.4.3 Data analysis

Phase shifts caused by cyclic nucleotide analoga-, *Rhyparobia*-PDF-, and control injections were statistically evaluated in three hour time bins at CT 1.5, 4.5, 7.5, 10.5, 13.5, 16.5, 19.5, and 22.5 using the Kruskal-Wallis test followed by Dunn's post hoc test to examine whether there are CT-dependent effects. Moreover, injections of cyclic nucleotide analoga and *Rhyparobia*-PDF were compared with control injections at each CT with Kruskal-Wallis followed by Dunn's post hoc test to detect drug-dependent effects. These tests were also used for the analysis of dose-dependency. The determined phase shifts in hours circadian time (h_{CT}) and period length in hours were presented as mean in the text and as mean±standard error in graphs and tables. Graphical illustration was performed using OriginLab 8 (Northhampton, Massachusetts, USA) and CorelDRAW Graphics Suite X5.

Results

3.1 Behavioural analysis of *R. maderae* and *M. sexta*

3.1.1 Locomotor behaviour of isolated male and female cockroaches

Locomotor behaviour of single, isolated male (n=12) and female (n=12) cockroaches in a 12:12 LD photoperiod was investigated. Both genders were inactive during the day and expressed two activity peaks, one at the beginning/middle of the night (females: ZT 17.2, 12.96±2.89 cm/bin; males: ZT 15.1, 24.35±5.75 cm/bin; **Fig. 24**) and another at the end of the night/beginning of the day (females: ZT 23.8, 13.40±2.05 cm/bin; males: ZT 23.3, 22.58±4.35 cm/bin; **Fig. 24**). Moreover, males demonstrated increased locomotion activity as compared to female cockroaches (females: 12.89±2.22 m; males: 23.71±5.42 m; **Fig. 24**).

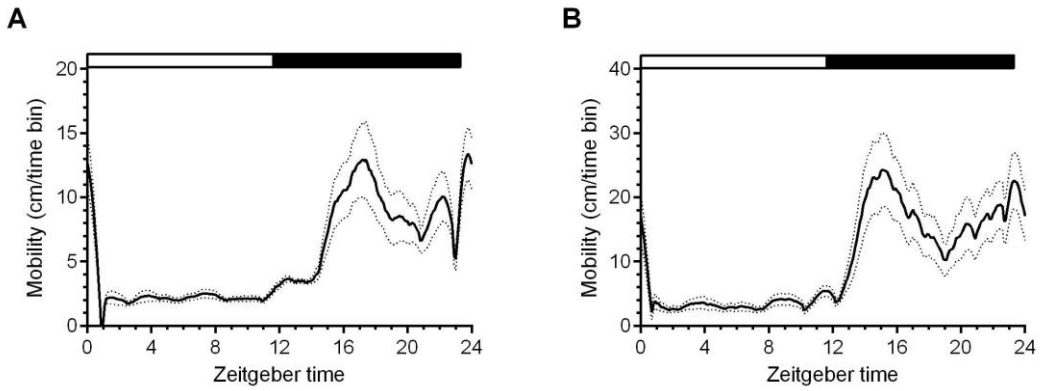

Figure 24. Isolated male and female *Rhyparobia maderae* express two activity peaks at night. Locomotor pattern of single, isolated female (**A**; n=12) and male (**B**; n=12) cockroaches. Polynomial fit of averaged locomotion distance per six minute time bin (solid lines) including standard error (dotted lines). Analysis was performed with distance moved function of Ethovision XT 7.0 for six minutes each. Bar indicates light conditions.

3.1.2 Residence in zones

Behaviour of naive female cockroaches (n=8) was analysed to investigate the preference for either food, water, or the main pheromone component senecio acid (Farine et al., 2007). Increased residence in the food zone was observed at ZT 17.6 (5.59±4.10 sec/bin). Moreover, a second peak was observed at ZT 21.9 (6.43±4.66 sec/bin), which declined progressively until ZT 2.2 (**Fig. 25 A**). Altogether, females spend 6.34±1.22 minutes in the

food zone per day, while spending 30.59±23.66 seconds time in the water zone (**Fig. 25 A,B**). Most time of their day the female cockroaches remained in the senecio acid zone (9.02±1.37 h) with a maximum at ZT 14.4 (201.80±22.37 sec/bin; **Fig. 25 C**).

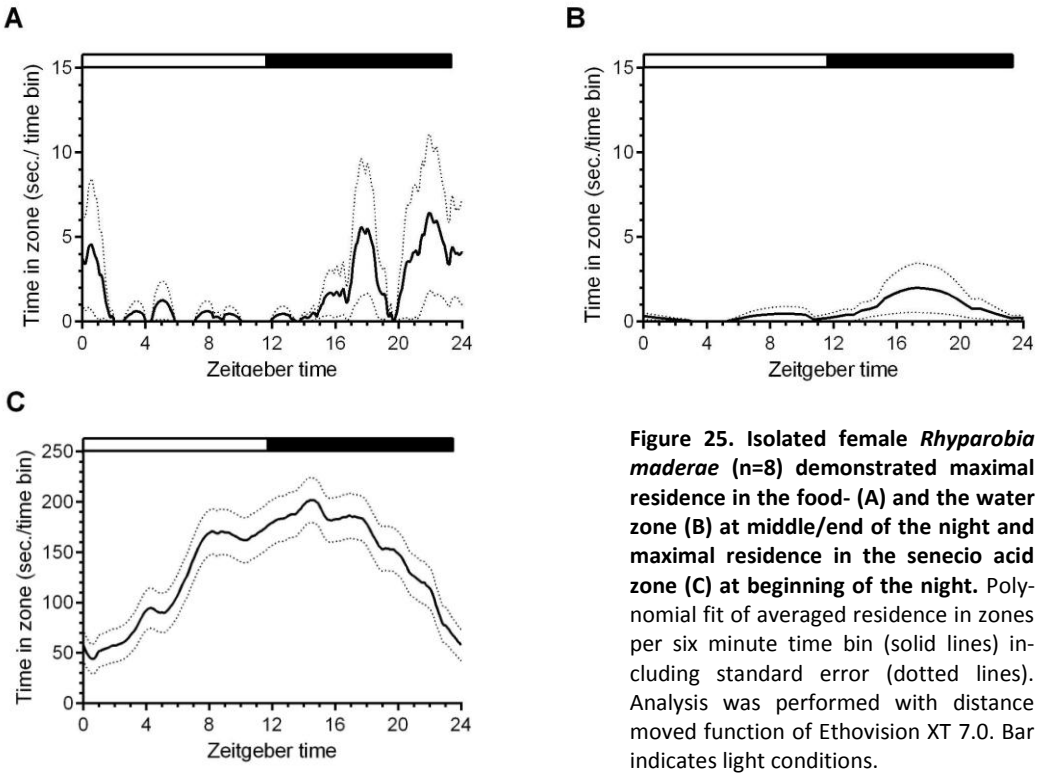

Figure 25. Isolated female *Rhyparobia maderae* (n=8) demonstrated maximal residence in the food- (A) and the water zone (B) at middle/end of the night and maximal residence in the senecio acid zone (C) at beginning of the night. Polynomial fit of averaged residence in zones per six minute time bin (solid lines) including standard error (dotted lines). Analysis was performed with distance moved function of Ethovision XT 7.0. Bar indicates light conditions.

3.1.3 Calling behaviour

Male *R. maderae* were observed directly in laboratory colonies (n=8). Calling behaviour was mostly exhibited at the end of the day and the beginning of the night when colonies had about equal ratios of males to females (**Fig. 26 A**). Two main peaks could be observed at ZT 10 (8.15±1.91 %) and at ZT 14 (9.54±1.23%). Minimum calling activity was observed at the middle of the day (ZT 5, 1.09±0.65 %) and the end of the night (ZT 23, 0.74±0.28 %). A third, smaller calling peak occurred at ZT 2 (4.38±1.59 %). Reducing the number of females in colonies changed male calling behaviour (n=3; **Fig. 26 B**). They started calling at the end of the night at ZT 24 (5.07±0.75 %) and maintained calling throughout the day until the middle of the night. Previously observed calling peaks (**Fig. 26 A**) got lost.

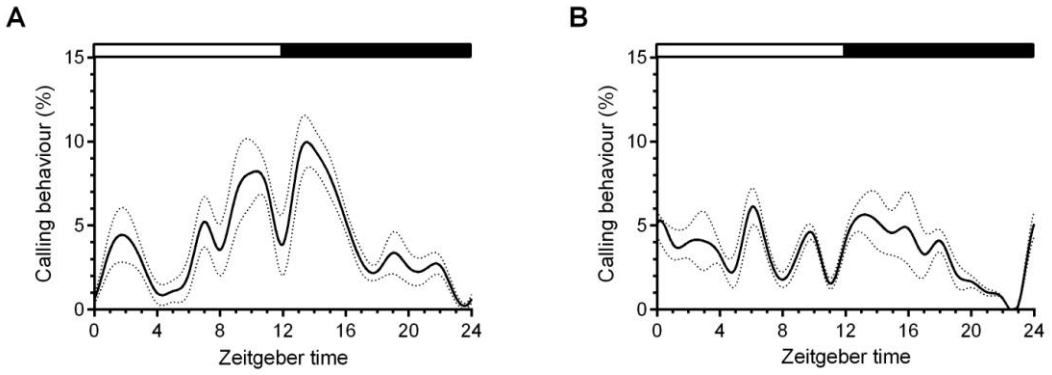

Figure 26. Massive reduction of female *Rhyparobia maderae* in colonies abolished previous observed male calling peaks. Normalized calling behaviour (total calling per day = 100 %) of male cockroaches in laboratory colonies is presented as polynomial fit of mean (solid line) including standard error (dotted lines). Animals were kept either under conditions of an equal ratio of males to females (**A;** n=8) or under a large surplus of males (**B**; n=3). Bar indicates light conditions.

3.1.4 Locomotion and feeding behaviour of naive male hawk moths

Isolated *M. sexta* males were observed in the flight room (n=5; **Fig. 27**). They were active between dusk (ZT 16, 2.54±1.31 %) and dawn (ZT 0, 7.03±2.88 %), 89.27±18.4 % of total activity per day was observed during the night and almost none during the day. Moreover, they showed two activity peaks, first at ZT 18 (16.68±3.50 %) and second, at ZT 23 (13.51±2.30 %). In contrast to flight activity, feeding activity was observed more rarely per day. The highest percentage of feeding events was detected at dusk (ZT 16, 15.00±15.00 %) and dawn (ZT 0, 26.43±12.04 %). Altogether, 41.42±27.04 % of total feeding events were observed at twilight and 50.00±31.41 % at night.

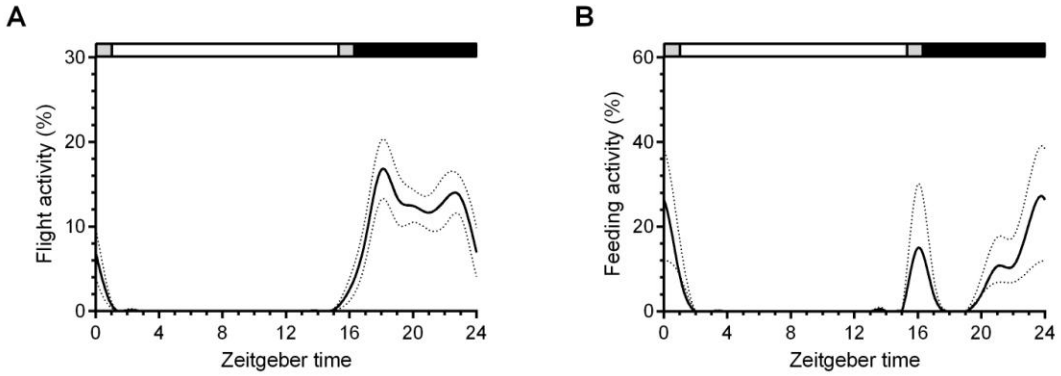

Figure 27. Isolated *Manduca sexta* males demonstrated maximal flight activity during the night (A) and maximal feeding activity at dusk and dawn (B). Normalized flight- (**A**) and feeding activity (**B**) of isolated, male hawk moths (total events per day=100%; n=5). Polynomial fit of mean (solid line) including standard error (dotted lines). Bar indicates light conditions.

3.2 Quantification of second messengers in the antennae of female *R. maderae* and male *M. sexta*

Electrophysiological, biochemical, and immunocytochemical experiments indicated an involvement of cAMP, cGMP, and IP_3 in olfactory signal transduction cascade (Ziegelberger et al., 1990; Stengl, 1993, 1994; Flecke et al., 2006; Dolzer et al., 2008; Krannich, 2008; Flecke et al., 2010). Since in tip recording experiments perfusion of cAMP and cGMP into pheromone-sensitive trichoid sensilla affected the olfactory sensitivity to pheromone differentially at the animals rest- and activity phase (Flecke et al., 2006; Flecke et al., 2010), it was investigated, whether daily rhythms in second messenger concentration occur and whether these rhythms correlate with rhythms in olfactory behaviour.

3.2.1 Oscillation of antennal cAMP, cGMP, and IP_3 levels in LD cycles in *R. maderae* females

Female cockroach antennae expressed significant ZT-dependent changes in second messenger concentrations (Kruskal-Wallis test, $p<0.01$; **Fig. 28 A-C**; **Tab. 4**). The lowest cAMP baseline levels were detected at ZT 2 (n=27) and 5 (n=34). They increased up to a maximum level at ZT 10 (n=35) and stayed elevated until ZT 20 (n=12), though the level slightly declined at ZT 14 (n=12). Thus, a significant difference occurred between ZT 10 and ZT 2 as well as ZT 10 and ZT 5 (Dunn's multiple comparison post hoc test, $p<0.01$). In contrast to cAMP levels, cGMP baseline levels were significant increased during night (ZT 14, n=11; ZT 20, n=9) and at the beginning of the day (ZT 2, n=11), while they were lowest during at ZT 5 (n=31) and 10 (n=34; Dunn's multiple comparison post hoc test, $p<0.05$; **Fig. 28 B**). Additionally, antennal IP_3 content was measured at three ZT times. Similar to cAMP oscillation, the lowest IP_3 contents were measured at the beginning and in the middle of the day (ZT 2, n=4; ZT 6, n=8) and the highest at the end of the day (ZT 10, n=15), resulting in a significant difference between ZT 6 and ZT 10 (Dunn's multiple comparison post hoc test, $p<0.01$; **Fig. 28 C**).

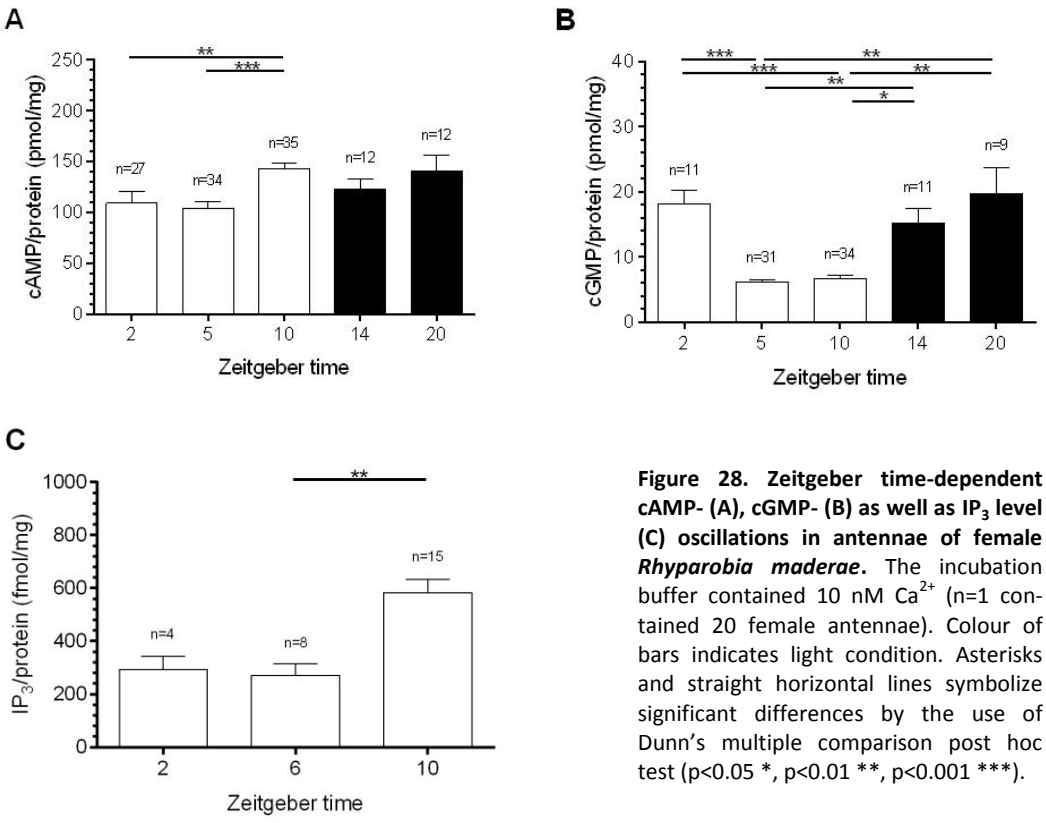

Figure 28. Zeitgeber time-dependent cAMP- (A), cGMP- (B) as well as IP_3 level (C) oscillations in antennae of female *Rhyparobia maderae*. The incubation buffer contained 10 nM Ca^{2+} (n=1 contained 20 female antennae). Colour of bars indicates light condition. Asterisks and straight horizontal lines symbolize significant differences by the use of Dunn's multiple comparison post hoc test ($p<0.05$ *, $p<0.01$ **, $p<0.001$ ***).

Table 4. Quantification of second messengers (mean±SE) in *Rhyparobia maderae* antennae at Zeitgeber time (ZT) 2, 5/6, 10, 14, and 20.

	cAMP (pmol/mg)	n	cGMP (pmol/mg)	n	IP3 (fmol/mg)	n
ZT 2	109.4±11.6	27	18.2±2.0	11	293.8±49.3	4
ZT 5/6	104.1±6.4	34	6.2±0.4	31	270.9±42.6	8
ZT 10	143.0±5.5	35	6.7±0.6	34	582.9±49.7	15
ZT 14	123.4±10.1	12	15.2±2.3	11	---	
ZT 20	141.1±15.6	12	19.7±4.0	9	---	

3.2.2 Quantification of cAMP and cGMP levels under adaptive conditions in *R. maderae* females

Keeping females together with a surplus of male cockroaches in colonies changed cyclic nucleotide levels ZT-dependently. While significant differences in cAMP concentrations occurred between ZT 5 (n=12) and ZT 10 (n=4; Mann-Whitney U-test, $p<0.01$; **Fig. 29 A**), no significant cGMP oscillation were detected (Kruskal-Wallis test, $p<0.001$; **Fig. 29 B**). Instead, cGMP concentrations were increased during the whole day with maximum

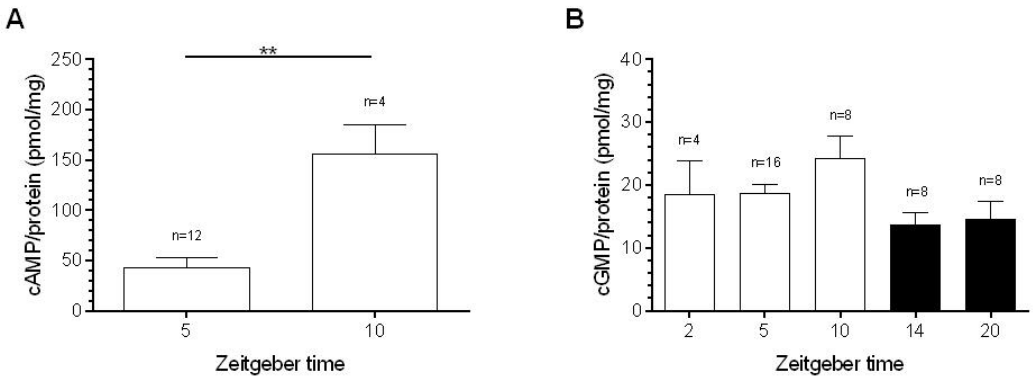

Figure 29. An increase in the male to female ratio overshadows previously measured Zeitgeber time- (ZT-) dependent rhythms in cGMP concentration in antennae of female *Rhyparobia maderae*. While the cAMP baseline level is reduced significantly at ZT 5 as compared to ZT 10 (**A**; Mann-Whitney test, p<0.01 **), no significant differences in cGMP baseline levels were detected (**B**). The incubation buffer contained 10 nM Ca^{2+} (n=1 contained 20 female antennae). Colour of the bars indicates light condition.

at ZT 10 (n=8), while lowest concentrations were found at night (**Fig. 29 B**; **Tab. 5**). Interestingly, cAMP concentrations at ZT 5 (n=16) were significantly reduced, in female antennae if females were raised with a surplus of males (Mann-Whitney U-test, p<0.001; **Fig. 30 A**), but not at ZT 10 (**Fig. 30 B**). Additionally, cGMP concentrations were highly significant increased at ZT 5 and ZT 10 (Mann-Whitney U-test, p<0.001; **Fig. 31**).

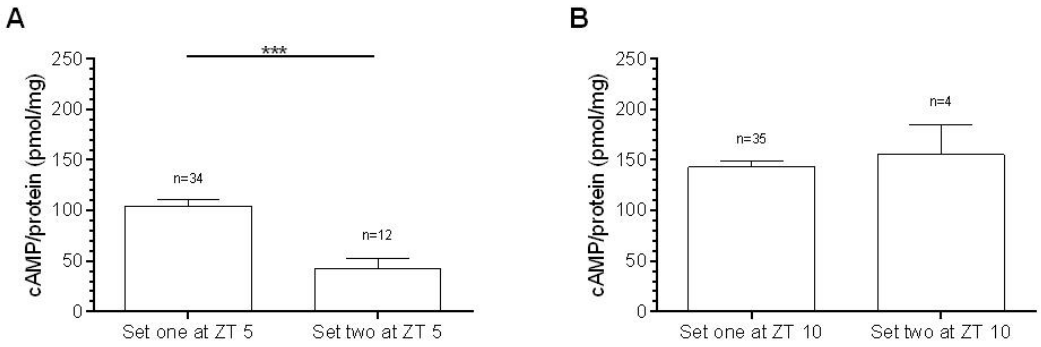

Figure 30. *Rhyparobia maderae* females raised at about equal male to female ratio (set one) demonstrated increased antennal cAMP level at Zeitgeber time (ZT) 5 compared to antennal cAMP level of females raised with surplus of males (set two). Different conditions resulted in significant difference in cAMP concentration at ZT 5 (**A**; Mann-Whitney test, p<0.001 ***), but not at ZT 10 (**B**). The incubation buffer contained 10 nM Ca^{2+}. Colour of the bars indicates light condition (n=1 contained 20 female antennae).

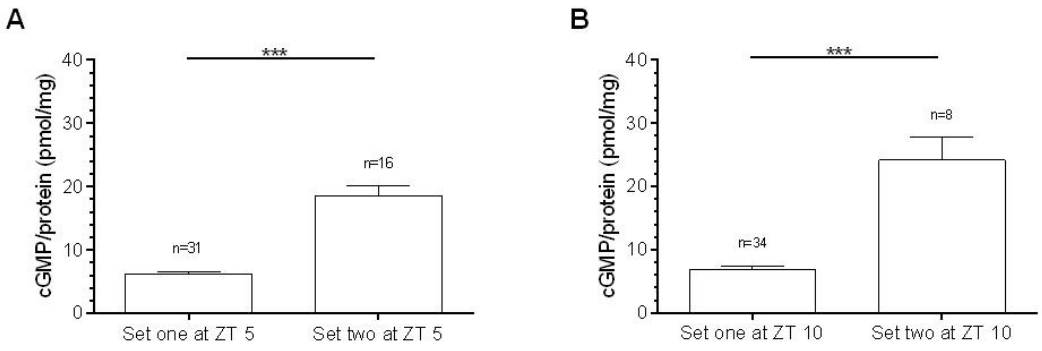

Figure 31. *Rhyparobia maderae* females raised at about equal male to female ratio (set one) demonstrated reduced antennal cGMP level at Zeitgeber time (ZT) 5 and 10 compared to antennal cGMP level of females raised with surplus of males (set two). Different conditions resulted in significant difference in cGMP concentrations at ZT 5 (**A**) and ZT 10 (**B**; Mann-Whitney test, p<0.001 ***). The incubation buffer contained 10 nM Ca^{2+}. Colour of the bars indicates light condition (n=1 contained 20 female antennae).

Table 5. Quantification of antennal cyclic nucleotides (mean±SE) in *Rhyaprobia maderae* at Zeitgeber time (ZT) 2, 5, 10, 14, and 20. Females were raised at excess of males in colonies.

	cAMP (pmol/mg)	n	cGMP (pmol/mg)	n
ZT 2	-		18.5±5.3	4
ZT 5	42.7±10.0	12	18.6±1.6	16
ZT 10	155.5±29.9	4	24.2±3.7	8
ZT 14	-		13.6±2.0	8
ZT 20	-		14.6±2.8	8

3.2.3 Oscillation of antennal cAMP, cGMP, and IP_3 levels in LD cycles in *M. sexta* males

Next, quantification of second messenger concentrations was performed in antennae of male hawk moths (**Fig. 32**; **Tab. 6**). Significant differences were detected between all ZT times in cAMP- and IP_3 baseline levels (Kruskal-Wallis test, p<0.001; **Fig. 32 A,C**), no ZT-dependent effect was observed in antennal cGMP contents (**Fig. 32 B**). At dawn (ZT 1, n=10) and in the middle of the day (ZT 9, n=21) the lowest cAMP baseline levels were detected, before increasing progressively at ZT 16 (n=10) and ZT 18 (n=10). At ZT 20 (n=34) the maximum in cAMP concentration was measured followed by a decrease at the end of the night (ZT 23, n=10). Significant difference occurred between ZT 9 and ZT 16 as well as between ZT 9 and ZT 20 (Dunn's multiple comparison post hoc test, p<0.05; **Fig. 32 A**). On the contrary, the cGMP baseline levels between ZT 9 (n=20), ZT 16 (n=10), ZT 18 (n=14), and ZT 20 (n=23) remained constant. At ZT 23 (n=6) and ZT 1 (n=6) the cGMP contents

slightly, but not significantly differed (**Fig. 32 B**). As observed for cAMP baseline concentrations, also IP_3 concentrations decreased at twilight and day. The lowest IP_3 concentrations were detected during the day (ZT 9, n=25), at dawn (ZT 16, n=16), and at dusk (ZT 1, n=10). The highest antennal IP_3 content was detected at the beginning of the night (ZT 18, n=16), before slightly declining (ZT 20, n=33) and increasing again at the end of the night (ZT 23, n=9). Thus, there was a significant difference between the minimum at ZT 9 and all groups measured during the night (Dunn's multiple comparison post hoc test, $p<0.05$; **Fig. 32 C**). Moreover, at ZT 16 the baseline level was significantly lower as compared to ZT 18 and ZT 20 (Dunn's multiple comparison post hoc test, $p<0.05$; **Fig. 32 C**).

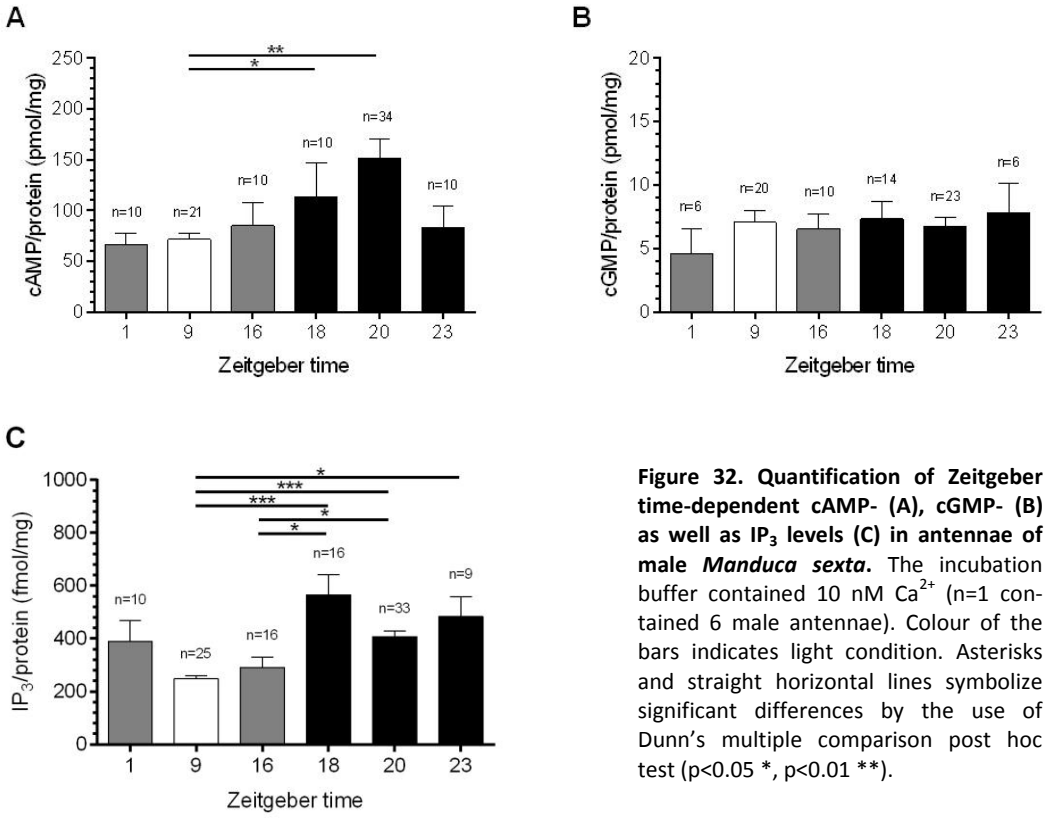

Figure 32. Quantification of Zeitgeber time-dependent cAMP- (A), cGMP- (B) as well as IP_3 levels (C) in antennae of male *Manduca sexta*. The incubation buffer contained 10 nM Ca^{2+} (n=1 contained 6 male antennae). Colour of the bars indicates light condition. Asterisks and straight horizontal lines symbolize significant differences by the use of Dunn's multiple comparison post hoc test ($p<0.05$ *, $p<0.01$ **).

Table 6. Quantification of second messengers (mean±SE) in *Manduca sexta* antennae at Zeitgeber time (ZT) 1, 9 ,16, 18, 20, and 23.

	cAMP (pmol/mg)	n	cGMP (pmol/mg)	n	IP_3 (fmol/mg)	n
ZT 1	66.5±11.1	10	4.6±2.0	6	389.8±79.3	10
ZT 9	71.5±6.5	21	7.1±1.0	20	248.2±11.1	25
ZT 16	84.9±23.1	10	6.5±1.2	10	291.5±39.1	16
ZT 18	113.9±33.4	10	7.3±1.4	14	565.2±77.9	16
ZT 20	151.5±19.5	34	6.7±0.7	23	408.0±20.6	33
ZT 23	83.0±21.4	10	7.8±2.3	6	484.3±75.6	9

3.2.4 Oscillation of antennal cAMP, cGMP, and IP_3 levels in DD in *R. maderae* females

Female cockroach antennae collected on the first day of DD expressed rhythms in cAMP baseline levels (**Fig. 33 A**; **Tab. 7**). Significant difference between all times tested was found (Kruskal-Wallis test, $p<0.05$). As observed in LD highest cAMP levels were detected at ZT 10 (n=13). Thus, there was a significant difference between CT 10 and CT 20 (n=13; Dunn's multiple comparison post hoc test, $p<0.05$; **Fig. 33 A**). Moreover, the continuous decrease in cGMP baseline levels was significant (Kruskal-Wallis test, $p<0.001$; **Fig. 33 B**). The highest cGMP concentration was detected at the beginning of the subjective day (CT 2, n=8), before progressively falling down until CT 20 (n=9, **Tab. 7**). Therefore, cGMP baseline level was significantly reduced at CT 10 (n=10), CT 14 (n=10), and CT 20 as compared to these maximum value at CT 2 (Dunn's multiple comparison post hoc test, $p<0.05$; **Fig. 33 B**). Additionally, a significant difference between CT 5 (n=11) and CT 20 was detected (Dunn's multiple comparison post hoc test, $p<0.01$; **Fig. 33 B**). Also, IP_3 baseline concentrations oscillated significantly (Kruskal-Wallis test, $p<0.05$; **Fig. 33 C**; **Tab.7**). The minimum in IP_3 content, measured at CT 5 (n=10), progressively increased until CT 14 (n=8), before decreasing at CT 20 (n=7) and CT 2 (n=7). There was a significant difference between IP_3 concentrations at CT 5 and CT 14 (Dunn's multiple comparison post hoc test, $p<0.05$; **Fig. 33 C**).

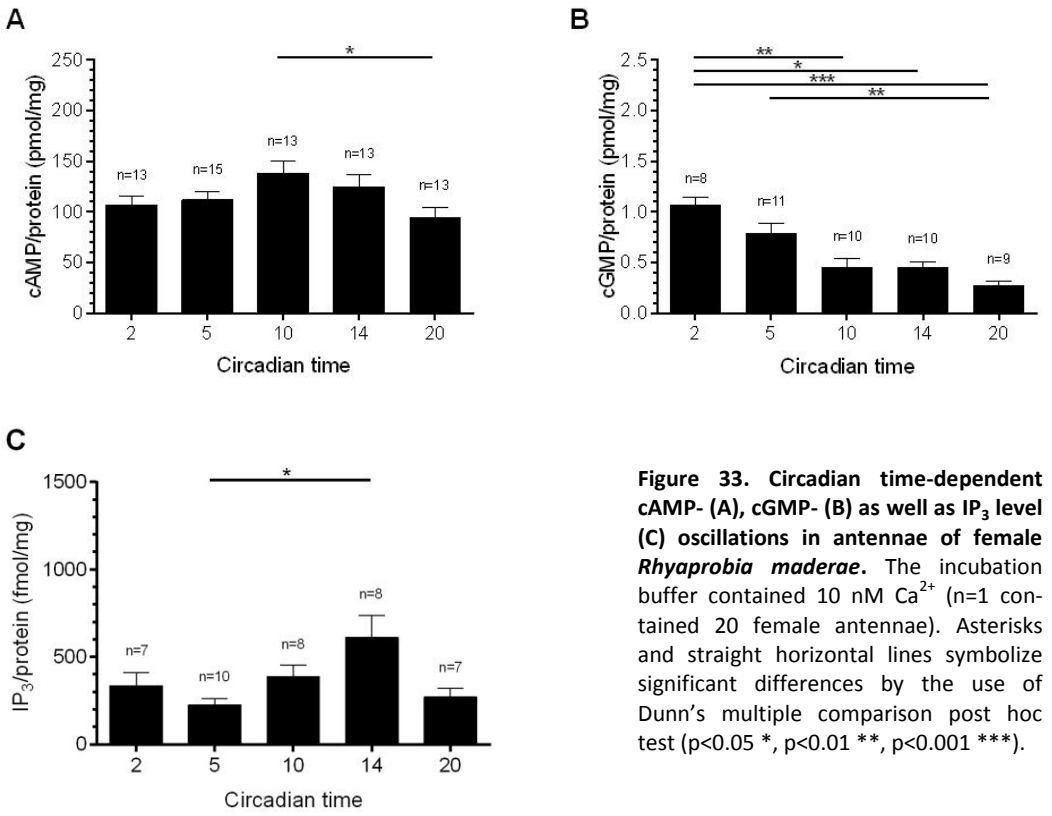

Figure 33. Circadian time-dependent cAMP- (A), cGMP- (B) as well as IP_3 level (C) oscillations in antennae of female *Rhyaprobia maderae*. The incubation buffer contained 10 nM Ca^{2+} (n=1 contained 20 female antennae). Asterisks and straight horizontal lines symbolize significant differences by the use of Dunn's multiple comparison post hoc test ($p<0.05$ *, $p<0.01$ **, $p<0.001$ ***).

Table 7. Quantification of antennal second messengers (mean±SE) in *Rhyparobia maderae* at circadian time (CT) 2, 5, 10, 14, and 20.

	cAMP (pmol/mg)	n	cGMP (pmol/mg)	n	IP_3 (fmol/mg)	n
CT 2	107.2±8.3	13	1.06±0.08	8	335.2±75.7	7
CT 5	111.7±8.3	15	0.79±0.10	11	225.5±35.2	10
CT 10	138.3±11.7	13	0.45±0.09	10	387.0±64.3	8
CT 14	125.1±11.9	13	0.45±0.06	10	613.5±123.6	8
CT 20	93.9±10.3	13	0.27±0.05	9	271.3±49.1	7

3.2.5 Quantification of antennal cAMP, cGMP, and IP_3 levels in DD in *M. sexta* males

As done for the cockroach, circadian experiments were also performed with antennal lysates of male hawk moth antennae. No CT-dependent oscillations of second messengers were found (Kruskal-Wallis test, $p > 0.05$; **Fig. 34**). The means of cAMP baseline concentrations varied between 82.8 pmol/mg and 103.8 pmol/mg (**Tab. 8**). Also, the means of cGMP concentrations amounted approximately 5.0 pmol/mg for each CT time analysed (**Tab. 8**). Small, non significant differences were detected in IP_3 baseline concentrations.

The lowest IP_3 contents were observed at CT 1 (n=10) and CT 18 (n=10), whereas the highest IP_3 levels were detected at CT 20 (n=10) and CT 23 (n=6). In between, CT 9 (n=6) and CT 16 (n=6) values were measured at a moderate level (**Fig. 34 C**; **Tab. 8**).

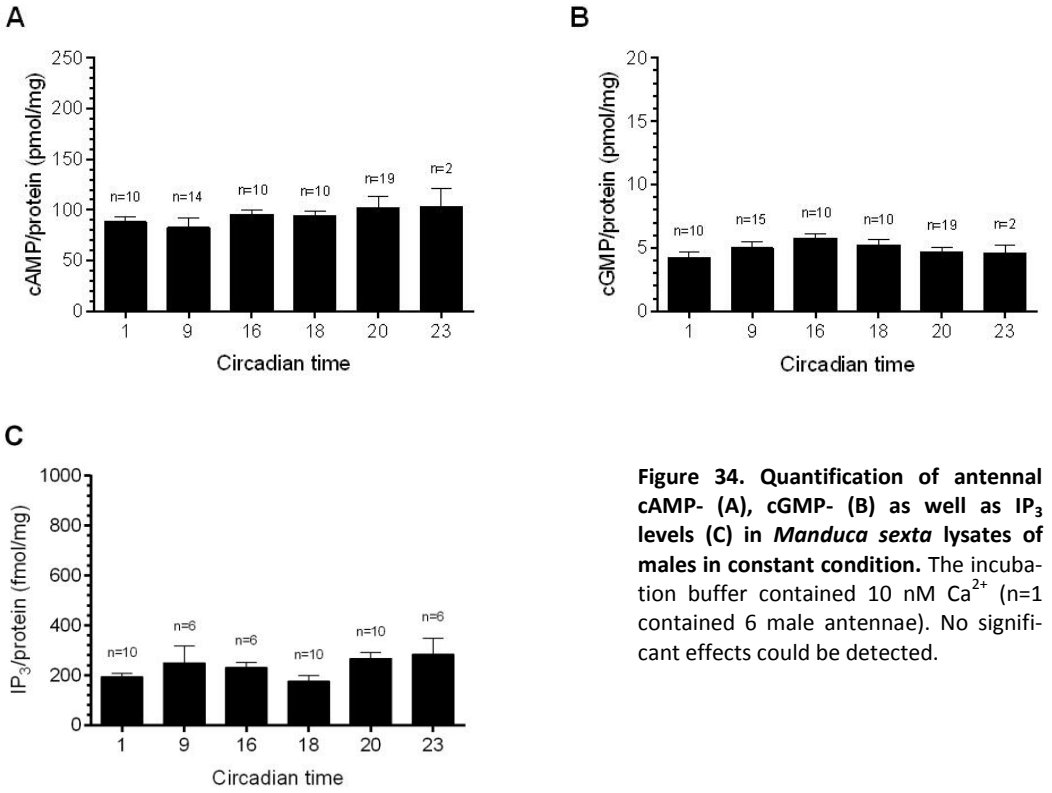

Figure 34. Quantification of antennal cAMP- (A), cGMP- (B) as well as IP_3 levels (C) in *Manduca sexta* lysates of males in constant condition. The incubation buffer contained 10 nM Ca^{2+} (n=1 contained 6 male antennae). No significant effects could be detected.

Table 8. Quantification of antennal second messengers (mean±SE) in *Manduca sexta* at circadian time (CT) 1, 9, 16, 18, 20, and 23.

	cAMP (pmol/mg)	n	cGMP (pmol/mg)	n	IP_3 (fmol/mg)	n
CT 1	88.5±4.3	10	4.3±0.5	10	193.4±14.6	10
CT 9	82.8±9.1	14	5.0±0.5	15	250.7±66.7	6
CT 16	95.5±4.3	10	5.8±0.4	10	231.4±20.9	6
CT 18	94.0±5.3	10	5.2±0.4	10	176.4±22.8	10
CT 20	102.0±11.4	19	4.7±0.3	19	267.1±23.6	10
CT 23	103.8±17.4	2	4.6±0.7	2	283.9±65.3	6

3.3 ZT-dependent effects of OA

OA exerts its effects in insects by binding to α- and β-adrenergic OA receptors which differentially activate cAMP and IP_3 pathways (Farooqui, 2007). Moreover, OA treatment of antenna of *P. americana* as well as *M. sexta* elevated antennal response to pheromone (Zhukovskaya and Kapitsky, 2006; Flecke and Stengl, 2009). Thus, it was tested whether rhythms in antennal cAMP and IP_3 concentrations are driven by OA.

3.3.1 Quantification of OA in male *M. sexta* antenna

Quantification of OA in single male antenna at ZT 1, 9, 16, 18, 20, and 23 revealed significant differences (Kruskal-Wallis test, p<0.001; **Fig. 35**). The lowest OA amount per antenna was detected in the middle of the animals' resting phase at ZT 9 (237.4±10.9 fmol/antenna, n=10), it increased continuously at ZT 16 (272.9±24.6 fmol/antenna, n=10) and ZT 18 (318.2±54.5 fmol/antenna, n=8) until they peaked at ZT 20 (397.4±30.1 fmol/antenna, n=16). Finally, the antennal OA amount decreased at the end of the night (ZT 23, 324.0±6.0 fmol/antenna, n=8) and at dawn (310.4±8.8 fmol/antenna, n=8). Thus, OA amounts at ZT 9 and ZT 16 were significantly lower as compared to the peak level at ZT 20 (Dunn's multiple comparison post hoc test, p<0.05; **Fig. 35**).

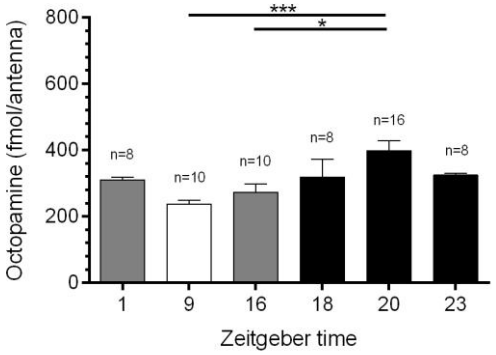

Figure 35. Oscillation of octopamine amount in male hawk moth antenna (n=1 was averaged over 3 female antennae). Colour of the bars indicates light condition. Asterisks and straight horizontal lines symbolize significant differences (Dunn's multiple comparison post hoc test , p<0.05 *, p<0.001 ***).

3.3.2 Effect of OA on AC activity in female *R. maderae* antennae

The effect of OA on AC activity in antennal lysates of *R. maderae* was analyzed at two different ZTs (**Fig. 36**; **Tab. 6**). Control experiments without any pharmaceutical were compared to experiments with addition of epinastine (EPI), EPI and OA, OA and forskolin (FSK) in the animals' resting phase (ZT 5, **Fig. 36 A**) and mating phase (ZT 10, **Fig. 36 B**). At both

ZT times tested significant differences could be demonstrated between all groups analyzed (Kruskal-Wallis test, p<0.001; **Fig. 36**). While the specific OA receptor antagonist EPI did not affect the cAMP baseline at both ZTs (ZT 5, n=4; ZT 10, n=7), OA significantly increased cAMP levels (ZT 5, n=12; ZT 10, n=27; Dunn's multiple comparison post hoc test, p<0.001; **Fig. 36**). When applying OA and EPI, EPI was able to prevent OA-dependent cAMP rises. This effect was more effective at ZT 5, than at ZT 10. Finally, FSK was applied as positive control of AC stimulation. Highly significant increases could be observed at ZT 5 (n=3) and ZT 10 (n=7; Dunn's multiple comparison post hoc test, p<0.01; **Fig. 36**).

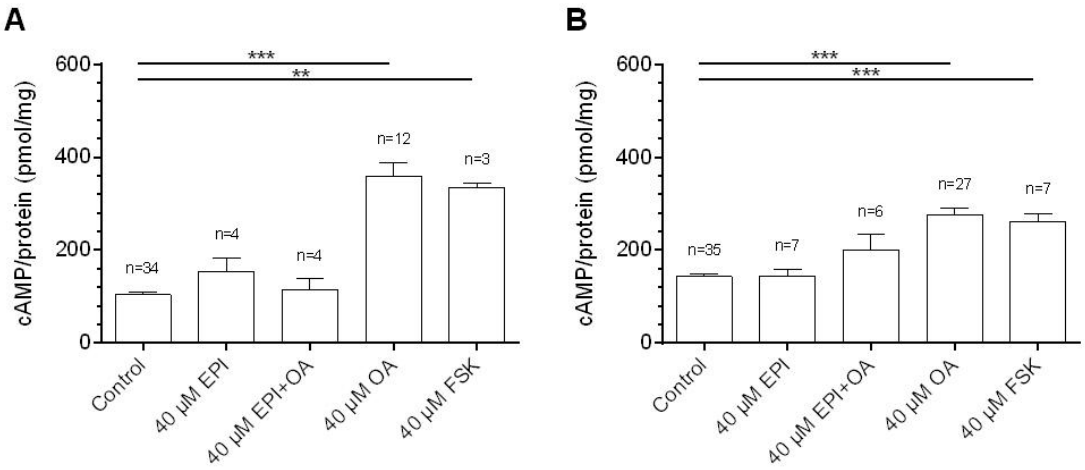

Figure 36. Octopamine (OA) increased adenylyl cyclase activity in female *Rhyparobia maderae* at Zeitgeber time (ZT) 5 (A) and ZT 10 (B). Antennal lysates were treated with control, 40 µM epinastine (EPI), 40 µM EPI and OA, 40 µM OA or 40 µM forskolin (FSK), respectively (n=1 contained 20 female antennae). Colour of the bars indicates light condition. Asterisks and straight horizontal lines symbolize significant differences (Dunn's multiple comparison post hoc test, p<0.01 **, p<0.001 ***).

3.3.3 Effect of OA on AC activity in male *M. sexta* antennae

The effect of OA on the AC activity in antennal lysates of *M. sexta* was also analyzed. The experiments were performed in the hawk moths' resting (ZT 9, **Fig. 37 A**; **Tab. 6**) as well as activity phase (ZT 20, **Fig. 37 B**; **Tab. 6**). Significant differences were observed, when comparing control, EPI, EPI and OA, OA and FSK applications to antennal lysates (Kruskal-Wallis test, p<0.001; **Fig. 37**). While incubation with control, EPI, and EPI and OA buffer did not affect cAMP levels at ZT 9 (control, n=18; EPI, n=12; EPI+OA, n=6) as well as at ZT 20 (control, n=18; EPI, n=6; EPI+OA, n=9), stimulation with OA or FSK increased cAMP levels very effectively at ZT 9 (OA, n=9 ; FSK, n=9) and ZT 20 (OA, n=15 ; FSK, n=15; **Fig. 37**). Although cAMP control levels varied daytime-dependently, stimulation with OA and FSK

resulted in very similar maximal cAMP levels (**Tab. 6**). These cAMP rises were significant at both ZTs (Dunn's multiple comparison post hoc test, p<0.001; **Fig. 37**).

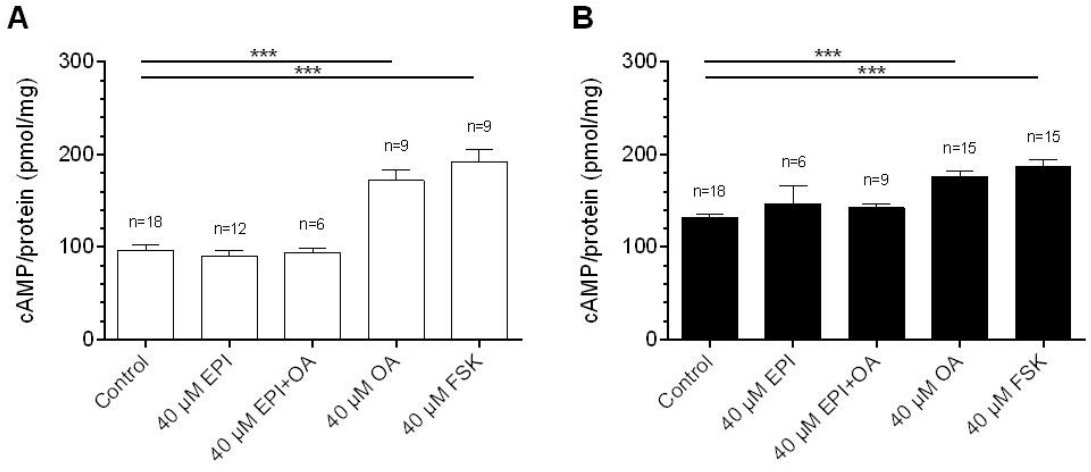

Figure 37. Octopamine (OA) increased adenylyl cyclase activity in male *Manduca sexta* antennae at Zeitgeber time (ZT) 9 (A) and ZT 20 (B). Antennal lysates were treated with control, 40 µM epinastine (EPI), 40 µM EPI and OA, 40 µM OA or 40 µM forskolin (FSK), respectively (n=1 contained 6 male antennae). Colour of the bars indicates light condition. Asterisks and straight horizontal lines symbolize significant differences (Dunn's multiple comparison post hoc test, p<0.001 ***).

Table 9. Effect of control, epinastine (EPI), octopamine (OA), and forskolin (FSK) buffer on antennal cAMP synthesis (mean±SE) in *Rhyparobia maderae* and *Manduca sexta* at various Zeitgeber times (ZT).

	Rhyparobia maderae				***Manduca sexta***			
	cAMP ZT 5 (pmol/mg)	**n**	**cAMP ZT 10 (pmol/mg)**	**n**	**cAMP ZT 9 (pmol/mg)**	**n**	**cAMP ZT 20 (pmol/mg)**	**n**
Control	104.1±6.4	34	143.0±5.5	35	96.3±6.9	18	131.6±4.5	18
EPI	154.8±27.0	4	143.9±15.8	7	90.5±5.6	12	146.6±20.3	6
EPI+OA	113.7±24.4	4	200.2±35.2	6	93.6±5.3	6	142.7.6±3.7	9
OA	358.5±29.5	12	276.3±13.3	27	171.8±11.9	9	176.3±6.4	15
FSK	334.7±8.6	3	261.3±17.0	7	191.7±14.0	9	186.9±7.9	15

3.3.4 Analysis of EC_{50}

To characterise the OA-dependent cAMP rises in more detail, the EC_{50} was calculated at both ZT times investigated. Therefore, antennal lysates of male hawk moths were incubated with buffers, which varied in OA concentration, at ZT 9 and ZT 20 (**Tab. 10**). Control experiments without OA were performed and used as fixed minimum levels for the EC_{50} equation. AT ZT 9 the log EC_{50} was -6.15±0.85 M which is 708.0 nM (**Fig. 38 A**), at ZT 20 the log EC_{50} was -6.63±0.48 M (234.4 nM, **Fig. 38 B**). Top values for cAMP levels of EC_{50} equations were calculated (ZT 9, 187.8 pmol/mg; ZT 20, 191.2 pmol/mg; **Fig. 38**).

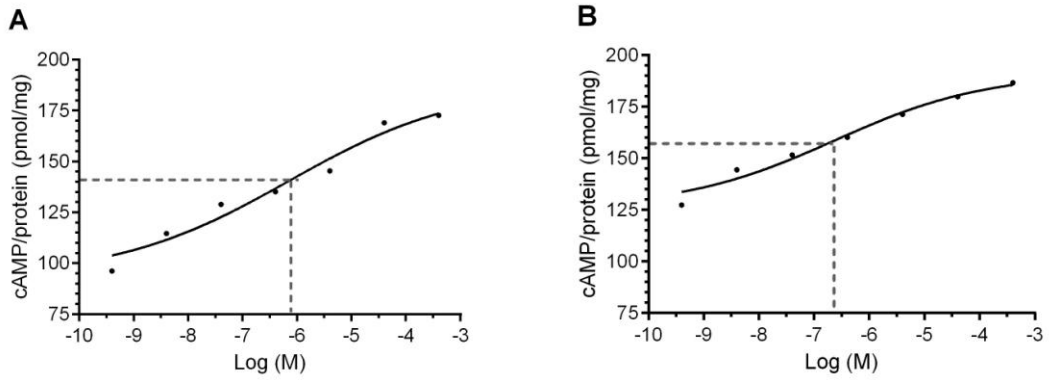

Figure 38. Half maximal effective octopamine (OA) dose (EC_{50}) for OA-dependent antennal cAMP rises at Zeitgeber time (ZT) 9 (A) and ZT 20 (B). The incubation buffers contained 400 pM to 400 µM OA. The log EC_{50} was -6.15±0.85 M at ZT 9 and -6.63±0.48 M at ZT 20 (n=71 at ZT 9; n=84 at ZT 20). The goodness of fit was above 0.95.

Table 10. Effects of octopamine (OA) on cAMP synthesis (mean±SE) in *Manduca sexta* antennae at Zeitgeber time (ZT) 9 and 20.

Concentration (mol/l)	cAMP ZT 9 (pmol/mg)	n	cAMP ZT 20 (pmol/mg)	n
Control	96.3±6.9	18	131.6±4.5	18
4 x 10^{-10} OA	96.2±8.0	6	127.3±6.6	4
4 x 10^{-9} OA	114.6±12.8	6	148.1±13.7	13
4 x 10^{-8} OA	128.9±10.7	6	151.6±20.6	6
4 x 10^{-7} OA	130.0±10.1	5	160.1±16.9	5
4 x 10^{-6} OA	145.4±10.8	12	171.3±15.1	17
4 x 10^{-5} OA	169.4±12.4	12	179.8±5.4	15
4 x 10^{-4} OA	172.6±22.6	6	186.6±12.6	6

3.3.5 Analysis of reaction speed

To determine whether OA receptors signal rapidly on a time scale of milliseconds, fast kinetic methodology (see materials and method section) was developed to quantify OA-dependent cAMP concentration rises (**Fig. 39**; **Tab. 11**). After 25 to 500 ms OA-dependent increases in cAMP concentrations were obtained. Significant rises in cAMP occurred within 50 ms after OA stimulation (Dunn's post hoc test, $p<0.05$), and remained elevated for durations of at least 500 ms (**Fig. 39**; **Tab. 11**).

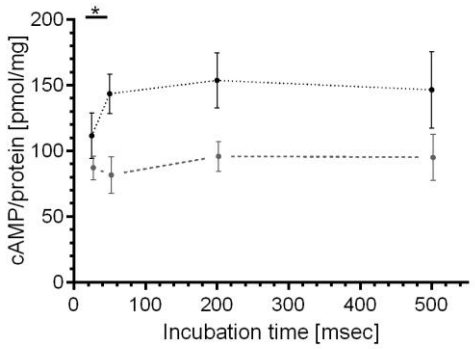

Figure 39. Octopamine (OA) elevated cAMP levels within 50 ms at the animals' resting phase (Zeitgeber time 9). Antennal homogenates were incubated with control buffer (n=9, grey, dashed) or with 40 µM OA buffer (n=9, black, dotted) for 25, 50, 200, and 500 ms. Asterisk symbolizes significant difference between control and OA group (Dunn's multiple comparison post hoc test, $p<0.05$ *; n=1 contained 6 male antennae).

Table 11. Kinetic of octopamine (OA) induced cAMP increases (mean±SE) in antennal lysates of *Manduca sexta*.

Incubation time (ms)	Control (pmol/mg)	n	40 µM OA (pmol/mg)	n
25	87.2±8.9	9	111.6±17.3	9
50	81.8±13.8	9	143.6±15.0	9
200	95.9±11.4	9	153.7±20.8	9
500	95.1±17.4	9	146.5±29.1	9

3.3.6 Effect of OA on antennal IP_3 levels in *R. maderae* females

So far, in both the cockroach as well as the hawk moth it is not known which G-proteins are activated by OA binding to its receptor. Therefore, it was examined whether OA activates PLC causes rises in IP_3 levels in ELISAs. At both ZTs investigated in the cockroach no significant OA effects were observed (Kruskal-Wallis test, $p > 0.05$; **Fig. 40**; **Tab. 12**). In the animals' resting phase (ZT 5), EPI (n=7), EPI+OA (n=6), and OA (n=8) did not affected IP_3 baseline content significantly (**Fig. 40 A**). The strongest, yet still non-significant effect could be observed by the use of the m-3M3FBS (n=5). This increase was about 28 percent compared to control experiments (n=8; **Fig. 40 A**). On the contrary, in the animals' activity

phase (ZT 10), EPI+OA (n=5), OA (n=7), and m-3M3FBS (n=10) did not effected IP_3 concentration at all, but EPI alone reduced it about 20 percent (n=7; **Fig. 40 B**).

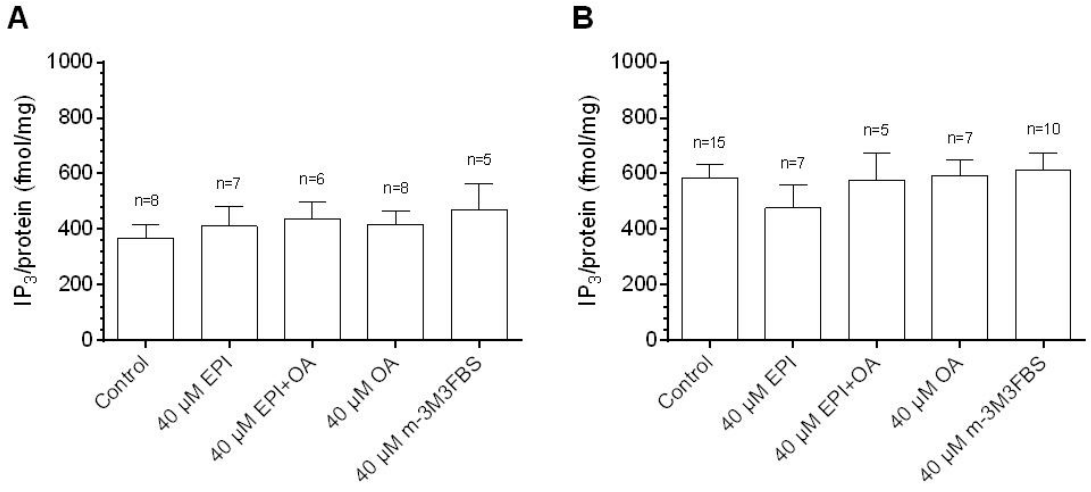

Figure 40. Octopamine (OA) did not affected IP_3 concentration at Zeitgeber time (ZT) 5 (A) and ZT 10 (B) in female *Rhyparobia maderae* antennae. Antennal lysates of *Rhyparobia maderae* were treated with control, 40 µM epinastine (EPI), 40 µM EPI and OA, 40 µM OA or 40 µM m-3M3FBS (phospholipase C activator), respectively (n=1 contained 20 female antennae). Colour of the bars indicates light condition. No significant effects could be observed.

3.3.7 Effect of OA on antennal IP_3 content in male *M. sexta* antennae

Comparably to previous investigations in the cockroach, OA experiments were performed in the hawk moth. EPI, EPI+OA, OA, and m-3M3FBS effects on IP_3 levels were compared with control groups at ZT 9 (n=25) and ZT 20 (n=33; **Fig. 41**; **Tab. 12**). While, pharmaceuticals could not induce any effects at ZT 20 (**Fig. 41 A**), significant effects were detected at the animals' resting phase (Kruskal-Wallis test, $p<0.01$; **Fig. 41 B**). Although, the control IP_3 level (ZT 9) was the same state as in the presence of EPI (n=10) and EPI+OA (n=9), an increase over 20 percent could be obtained when OA (n=28) or m-3M3FBS (n=19) were applied. These effects were significant (Dunn's multiple comparison post hoc test, $p<0.05$; **Fig. 41 B**).

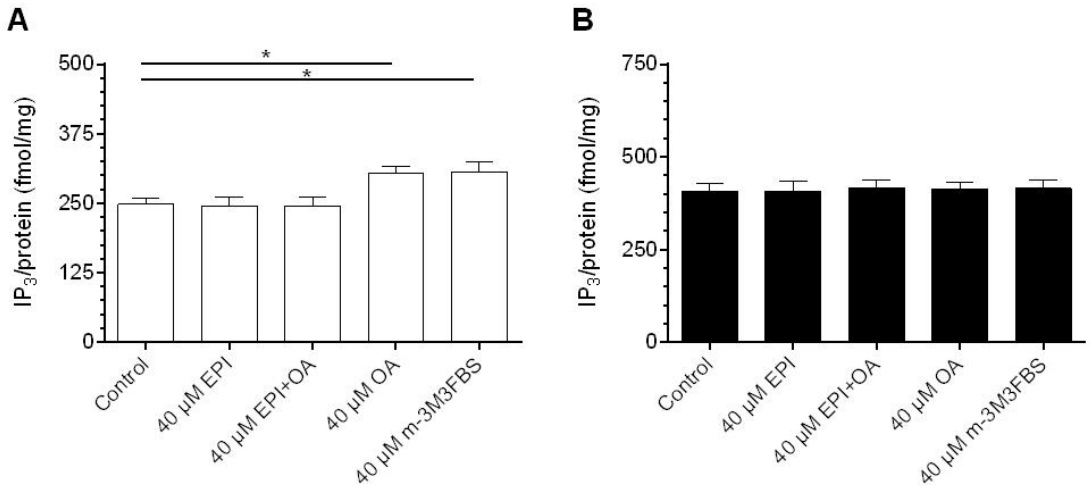

Figure 41. **Octopamine (OA) increased IP_3 concentration at Zeitgeber time (ZT) 9 (A) but not at ZT 20 (B) in male *Manduca sexta* antennae.** Antennal lysates of *Manduca sexta* were stimulated with control, 40 µM epinastine (EPI), 40 µM EPI and OA, 40 µM OA or 40 µM m-3M3FBS (phospholipase C activator), respectively (n=1 contained 6 male antennae). Colour of the bars indicates light condition. Asterisks symbolize significant difference between control and drug group (Dunn's multiple comparison post hoc test, $p<0.05$ *).

Table 12. Effects of control-, epinastine- (EPI), octopamine- (OA), and m-3M3FBS (phospolipase C activator) buffer on antennal IP_3 concentration (mean±SE) in *Rhyparobia maderae* and *Manduca sexta* antennae at various Zeitgeber times (ZTs).

	Rhyparobia maderae				***Manduca sexta***			
	IP_3 ZT 5 (fmol/mg)	**n**	**IP_3 ZT 10 (fmol/mg)**	**n**	**IP_3 ZT 9 (fmol/mg)**	**n**	**IP_3 ZT 20 (fmol/mg)**	**n**
Control	367.3±48.9	8	582.9±49.7	15	248.2±11.1	25	408.0±20.6	33
EPI	411.5±72.52	7	476.1±87.8	7	245.8±15.4	10	407.4±28.7	7
EPI+OA	438.1±60.1	6	576.9±97.8	5	245.7±14.9	9	416.7±20.4	8
OA	418.0±45.4	8	591.9±57.1	7	303.8±12.5	28	414.2±18.2	28
m-3M3FBS	470.2±92.0	5	613.6±60.6	10	306.0±17.4	19	416.0±20.5	17

3.4 ZT-dependent effects of calcium concentrations

Since some enzymes as ACs, GCs, and PLCs were demonstrated to be modulated in their activity by Ca^{2+} (Sunahara et al., 1996; Rebecchi and Pentyala, 2000; Sharma, 2010), the influence of this cation was investigated in antennae of *R. maderae* and *M. sexta.*

3.4.1 Effect of changes in the free Ca^{2+} concentration on AC activity in *R. maderae*

To test Ca^{2+} dependency of antennal ACs in cockroach antenna, variable free Ca^{2+} concentrations were applied and cAMP synthesis was measured (**Fig. 42**; **Tab. 13**). No significant effects were detected at ZT 5 (**Fig. 42 A**), whereas a significant effect was observed at ZT 10 (Kruskal-Wallis test, $p<0.05$). An increase in free Ca^{2+} concentration decreased cAMP contents from 0 nM Ca^{2+} (n=6) to 60 nM Ca^{2+} (n=5) before they increased with Ca^{2+} levels higher than 60 nM. Comparing AC activity of Ca^{2+} free solution with 60 nM Ca^{2+} shared significant differences (Dunn's multiple comparison post hoc test, $p<0.05$; **Fig. 42 B**).

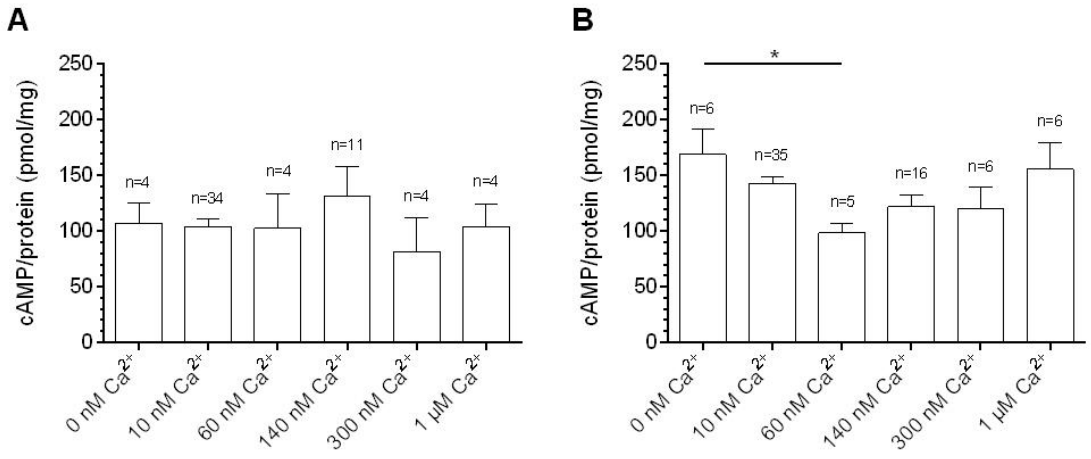

Figure 42. Adenylyl cyclase activity was reduced with 60 nM free calcium (Ca^{2+}) concentration at Zeitgeber time (ZT) 10 (B) but not at ZT 5 (A) in female *Rhyparobia maderae* antennae (n=1 contained 20 female antennae). Colour of the bars indicates light condition. Asterisk symbolizes significant difference between control (0 nM Ca^{2+}) and 60 nM Ca^{2+} at ZT 10 (Dunn's multiple comparison post hoc test, $p<0.05$ *).

3.4.2 Effect of changes in the free Ca^{2+} concentration on AC activity in *M. sexta*

Next, it was investigated whether Ca^{2+} could also affect AC activity in the hawk moth antennae (**Fig. 43**; **Tab. 13**). No Ca^{2+}-dependent effects could be observed at ZT 9 (**Fig. 43 A**). As previously described in cockroach experiments, an inverse bell shaped Ca^{2+} induced cAMP reduction was observed in the hawk moths' activity phase (Kruskal-Wallis test, $p<0.001$). Furthermore, this reduction reached its significant minimum with 60 nM Ca^{2+} (n=9; Dunn's multiple comparison post hoc test, $p<0.05$; **Fig. 43 B**).

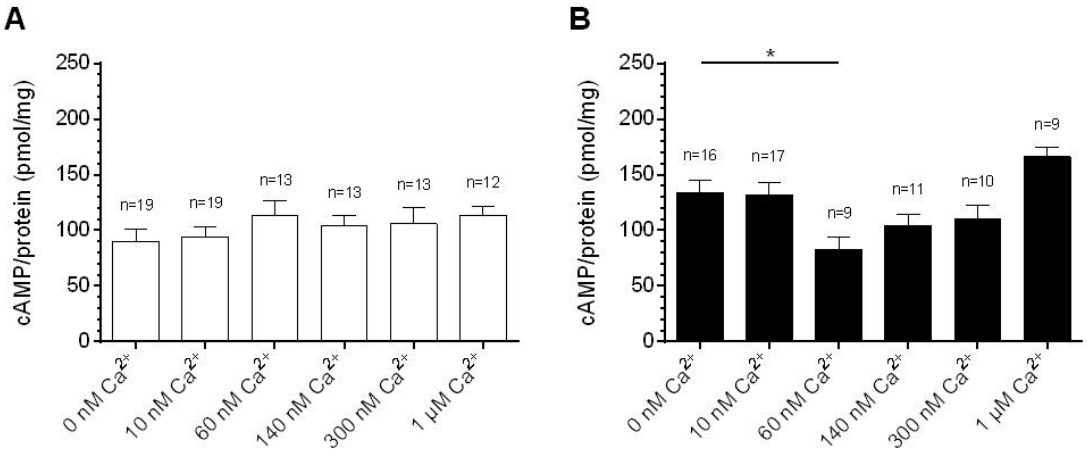

Figure 43. Adenylyl cyclase activity was reduced with 60 nM free calcium (Ca^{2+}) concentration at Zeitgeber time (ZT) 20 (B) but not at ZT 9 (A) in male *Manduca sexta* antennae (n=1 contained 6 male antennae). Colour of the bars indicates light condition. Asterisk symbolize significant difference between control (0 nM Ca^{2+}) and 60 nM Ca^{2+} at ZT 20 (Dunn's multiple comparison post hoc test, $p<0.05$ *).

Table 13. Effects of 0 nM free calcium (Ca^{2+}) concentrations on cAMP synthesis (mean±SE) in *Rhyparobia maderae* and *Manduca sexta* antennae at various Zeitgeber times (ZTs).

	Rhyparobia maderae				***Manduca sexta***			
	cAMP ZT 5 (pmol/mg)	**n**	**cAMP ZT 10 (pmol/mg)**	**n**	**cAMP ZT 9 (pmol/mg)**	**n**	**cAMP ZT 20 (pmol/mg)**	**n**
0 nM Ca^{2+}	107.2±18.0	4	169.1±22.8	6	90.3±10.6	19	134.3±11.2	16
10 nM Ca^{2+}	104.1±6.4	34	143.0±5.5	35	94.0±8.9	19	132.0±11.1	17
60 nM Ca^{2+}	102.9± 30.8	4	98.43±8.2	5	113.4±13.2	13	82.8±11.2	9
140 nM Ca^{2+}	131.7±26.9	11	122.2±10.2	16	103.8±9.9	13	104.3±10.3	11
300 nM Ca^{2+}	81.47±30.4	4	120.8±18,7	6	106.2±13.9	13	110.3±12.7	10
1 µM Ca^{2+}	103.9±19.9	4	156.0±23.9	6	113.4±7.7	12	166.1±8.2	9

3.4.3 Effect of changes in the free Ca^{2+} concentration on GC activity in *R. maderae*

To test whether antennal GCs activity are modulated by Ca^{2+}, incubations of antennal lysates were performed with variable free Ca^{2+} concentrations. Contrarily to AC activity, GC activity was not Ca^{2+}-dependent in the cockroach antennae (**Fig. 44**; **Tab. 14**). At ZT 5, the highest cGMP concentrations were induced with 10 nM Ca^{2+} (n=31) and 1 µM Ca^{2+} (n=3). Further free Ca^{2+} concentrations tested resulted in lower cGMP baseline levels (**Fig. 44 A**). Also, during the animals' mating phase (ZT 10), no significant effects were recognized. Almost all free Ca^{2+} concentrations tested resulted in a stable cGMP content of approximately 6.5 pmol/mg (**Fig. 44 B**).

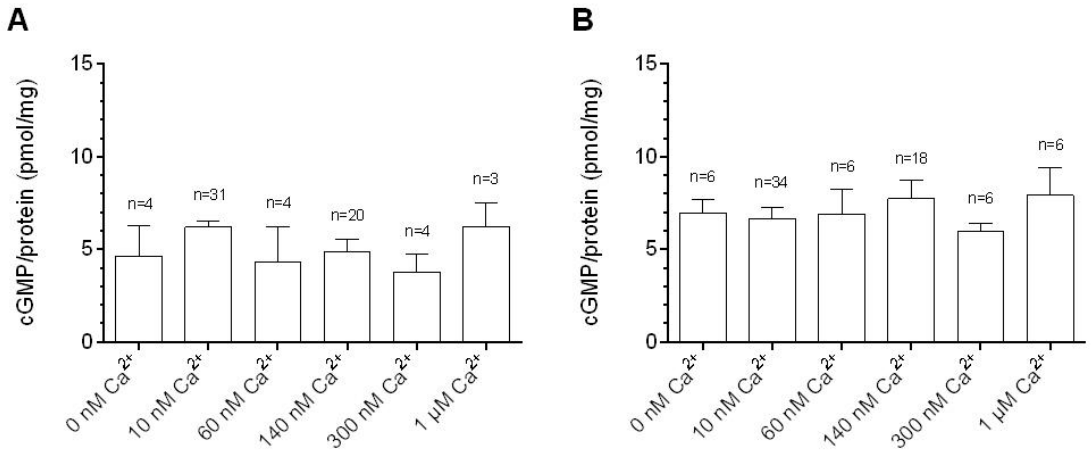

Figure 44. Guanylyl cyclase activity was not affected by calcium (Ca^{2+}) at Zeitgeber time (ZT) 5 (A) and ZT 10 (B) in female *Rhyparobia maderae* antennae (n=1 contained 20 female antennae). Colour of the bars indicates light condition. No significant differences were observed.

3.4.4 Effect of changes in the free Ca^{2+} concentration on GC activity in *M. sexta*

The Ca^{2+} dependence of GCs was tested in antennal tissues of the hawk moth. An increase in Ca^{2+} only activated GCs significant at the animals' resting phase (**Fig. 45**; **Tab. 14**; Kruskal-Wallis test, $p<0.05$). While the lowest GC activity was observed without Ca^{2+} (n=16), 60 nM Ca^{2+} (n=10) induced a maximum in cGMP concentrations at ZT 9 (Dunn's multiple comparison post hoc test, $p<0.01$; **Fig. 45 A**). At ZT 20 the highest, but not significant, GC activity was detected with 60 nM Ca^{2+} (n=12; **Fig. 45 B**).

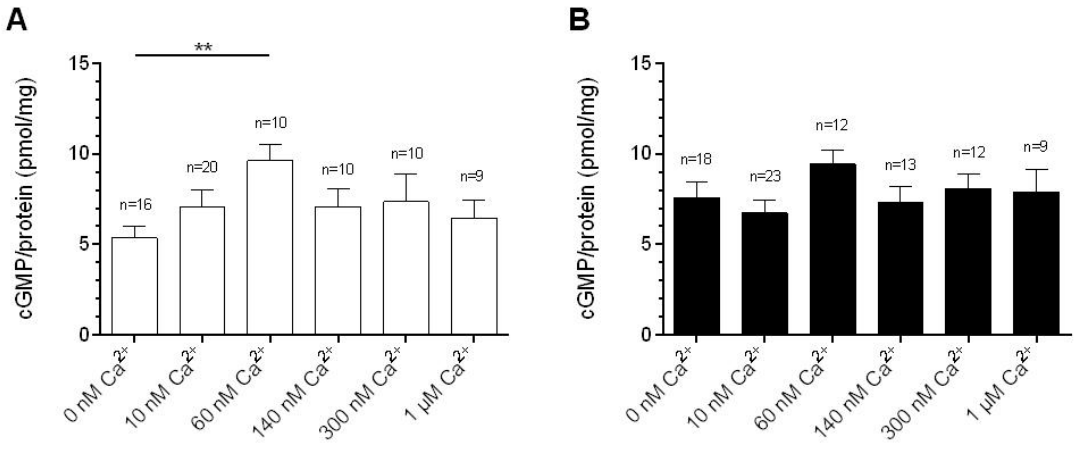

Figure 45. Guanylyl cyclase activity was increased with 60 nM free calcium (Ca^{2+}) concentration at Zeitgeber time (ZT) 9 (A) but not at ZT 20 (B) in male *Manduca sexta* antennae (n=1 contained 6 male antennae). Colour of the bars indicates light condition. Asterisk symbolizes significant difference between control (0 nM Ca^{2+}) and 60 nM Ca^{2+} at ZT 9 (Dunn's multiple comparison post hoc test, $p<0.01$ **).

Table 14. Effects of 0 nM and varying free calcium (Ca^{2+}) concentrations on cGMP synthesis (mean±SE) in *Rhyparobia maderae* and *Manduca sexta* antennae at various Zeitgeber times (ZTs).

	Rhyparobia maderae				***Manduca sexta***			
	cGMP ZT 5 (pmol/mg)	**n**	**cGMP ZT 10 (pmol/mg)**	**n**	**cGMP ZT 9 (pmol/mg)**	**n**	**cGMP ZT 20 (pmol/mg)**	**n**
0 nM Ca^{2+}	4.7±1.6	4	7.0±0.7	6	5.4±0.6	16	7.6±0.8	18
10 nM Ca^{2+}	6.2±0.4	31	6.7±0.6	34	7.1±1.0	20	6.7±0.7	23
60 nM Ca^{2+}	4.3±1.9	4	6.9±1.3	6	9.6±0.9	10	9.5±0.8	12
140 nM Ca^{2+}	4.9±0.7	20	7.7±1.0	18	7.1±1.0	10	7.3±0.9	13
300 nM Ca^{2+}	3.8±1.0	4	6.0±0.5	6	7.4±1.5	10	8.1±0.8	12
1 µM Ca^{2+}	6.2±1.3	3	7.9±1.5	6	6.5±1.5	9	7.9±1.3	9

3.4.5 Effect of changes in the free Ca^{2+} concentration on IP_3 levels in *R. maderae*

Since, next to ACs and GCs, PLCs are known to be Ca^{2+} modulated, the effect of different Ca^{2+} concentrations on antennal IP_3 content was analysed in both species. Although a 31 percent rise in IP_3 concentration was observed in antennal tissue of the cockroach by increasing Ca^{2+} concentration to 1 µM (n=8) at ZT 5, the effect was not significant (**Fig. 46 A**; **Tab. 15**). At ZT 10 a non significant increase of about 40 percent was found, when comparing 0 nM Ca^{2+} (n=4) to 1 µM Ca^{2+} (n=3; **Fig. 46 B**; **Tab. 15**).

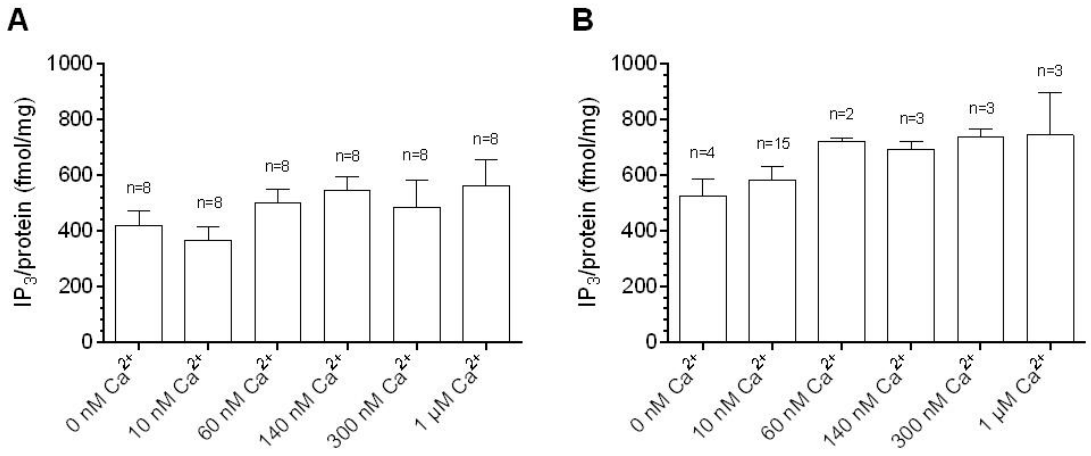

Figure 46. Antennal IP_3 concentration was not affected by calcium (Ca^{2+}) at Zeitgeber time (ZT) 5 (A) and ZT 10 (B) in female *Rhyparobia maderae* antennae (n=1 contained 20 female antennae). Colour of the bars indicates light condition. No significant effects could be observed.

3.4.6 Effect of changes in the free Ca^{2+} concentration on IP_3 levels in *M. sexta*

Next, Ca^{2+} effects on IP_3 concentrations in antennae of the hawk moth were investigated (**Fig. 47 A**; **Tab. 15**). The experimental strategy was modified in these experiments. While in the previous experiments variable Ca^{2+} buffer were incubated with lysates of different animals, here each lysate was separated into six parts and all tested free Ca^{2+} concentrations were incubated with each sample. Therefore, a direct pairwise comparison was obtained. At the animals' resting time no Ca^{2+}-dependent effects on IP_3 concentrations could be detected (**Fig. 47 A**). However, significant effects could be detected at ZT 20 (Friedman test, $p<0.01$; **Fig. 47 B**). When applying 140 nM Ca^{2+} (n=9) IP_3 was significant increased compared to Ca^{2+} free buffer (n=9; Dunn's multiple comparison post hoc test for paired samples, $p<0.01$; **Fig. 47 B**).

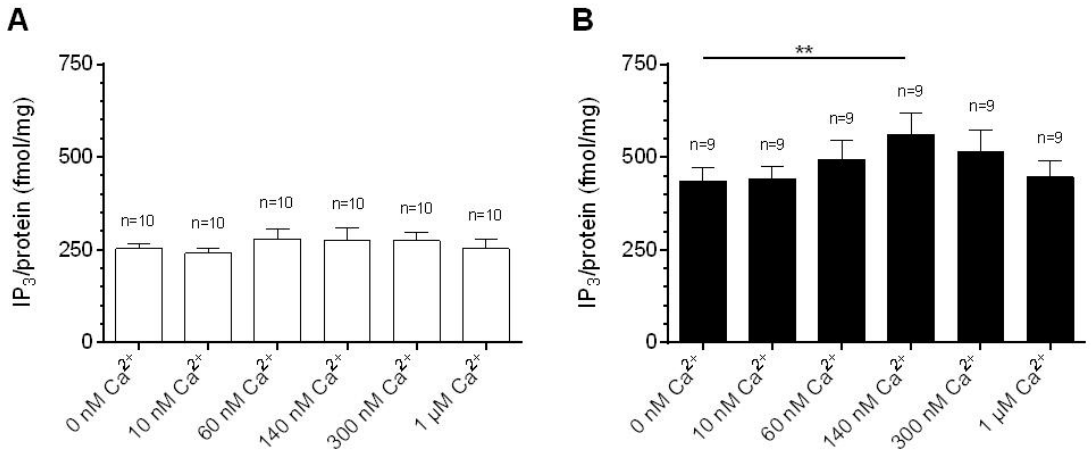

Figure 47. Antennal IP_3 concentration was increased by 140 nM free calcium (Ca^{2+}) concentration at Zeitgeber time (ZT) 20 (B) but not at ZT 9 (A) in male *Manduca sexta* antennae (n=1 contained 6 male antennae). Colour of the bars indicates light condition. Asterisk symbolizes significant difference between control (0 nM Ca^{2+}) and 140 nM Ca^{2+} at ZT 9 (Dunn's multiple comparison post hoc test for paired samples, $p<0.01$ **).

Table 15. Effects of 0 nM and varying free calcium (Ca^{2+}) concentrations on IP_3 concentrations (mean±SE) in *Rhyparobia maderae* and *Manduca sexta* antennae at various Zeitgeber times (ZTs).

	Rhyparobia maderae				***Manduca sexta***			
	IP_3 ZT 5 (fmol/mg)	**n**	**IP_3 ZT 10 (fmol/mg)**	**n**	**IP_3 ZT 9 (fmol/mg)**	**n**	**IP_3 ZT 20 (fmol/mg)**	**n**
0 nM Ca^{2+}	417.5±53.2	8	526.4±59.7	4	252.5±13.5	10	435.2±37.9	9
10 nM Ca^{2+}	367.3±48.9	8	582.9±49.7	15	240.1±13.9	10	440.4±35.0	9
60 nM Ca^{2+}	501.9±49.5	8	723.9±9.5	2	278.2±29.2	10	492.8±51.0	9
140 nM Ca^{2+}	546.5±46.9	8	695.0±27.5	3	276.0±33.6	10	560.9±58.4	9
300 nM Ca^{2+}	485.3±96.3	8	736.7±32.1	3	274.9±21.1	10	515.2±58.8	9
1 µM Ca^{2+}	563.2±91.8	8	744.9±151.4	3	252.9±26.0	10	445.8±44.2	9

3.5 Cyclic nucleotides effects in the circadian pacemaker of *R. maderae*

Cyclic nucleotide oscillations were demonstrated in antennae of *M. sexta* and *R. maderae* which are putative peripheral circadian pacemaker (Schuckel et al., 2007; Saifullah and Page, 2009). Thus, it was investigated whether cAMP and cGMP oscillations also occur in the central circadian pacemaker of the Madeira cockroach, the AMe (Reischig and Stengl, 2003a), and whether PDF, the most important coupling factor of the circadian system in insects (Stengl and Homberg, 1994), could drive these rhythms.

3.5.1 Effect of PDF on cyclic nucleotides

Optic lobe tissue collected in the middle of the night was incubated with 1 µM *Rhyparobia*-PDF. Incubation with this peptide increased the cAMP baseline level highly significant (control, 4.7±1.0 nmol/mg, n=13; peptide, 8.3±1.6 nmol/mg, n=13; Mann-Whitney U-test, p<0.01; **Fig. 48 A**). Contrarily, no effect on cGMP content was observed (control, 208.5±38.3 pmol/mg, n=15; peptide, 232.9±61.9 mol/mg, n=13; **Fig. 48 B**).

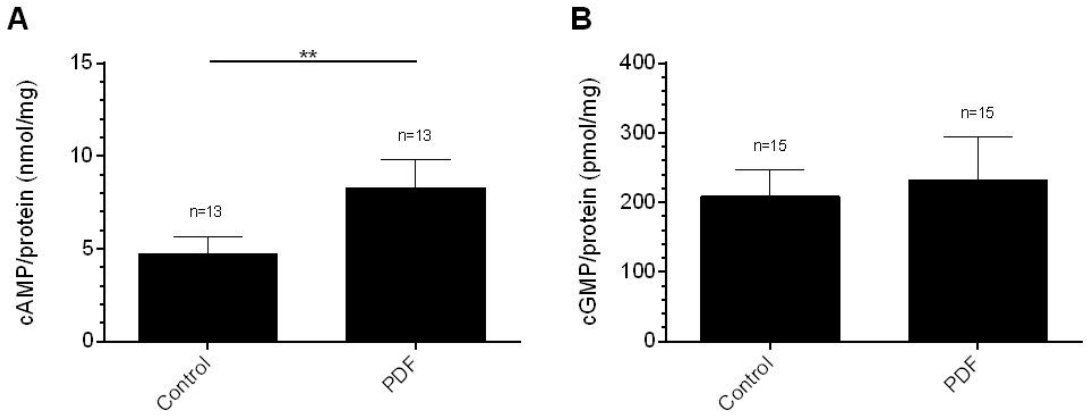

Figure 48. Effect of *Rhyparobia*-PDF on cyclic nucleotide content in optic lobe tissue. Asterisks and straight horizontal lines symbolize significant difference by the use of Mann-Whitney U-test (p<0.01 **). The incubation buffer contained 10 nM Ca^{2+} (n=1 contained 6 optic lobes).

3.5.2 Biphasic oscillations of cAMP concentrations in LD and DD2 in the AMe

In LD in the AMe cAMP concentrations oscillated with a minimum at ZT 18 and two maxima at dusk and dawn (**Fig. 49 A**; **Tab. 16**). Significantly lower cAMP levels were measured at ZT 18 as compared to ZT 12 and ZT 24 (Dunn's post hoc test, $p<0.01$). At DD1 cAMP concentrations were elevated as compared to LD and no significant differences were observed at different CTs (**Fig. 49 B**; **Tab. 16**). However, at DD2 a bimodal oscillation of cAMP became apparent with minima at CT 6 and CT 18 and maxima at CT 12 and CT 24 (**Fig. 49 C**; **Tab. 16**). The means of CT 6 and CT 18 significantly differed when compared to CT 12 and CT 24 (Dunn's post hoc test, $p<0.05$).

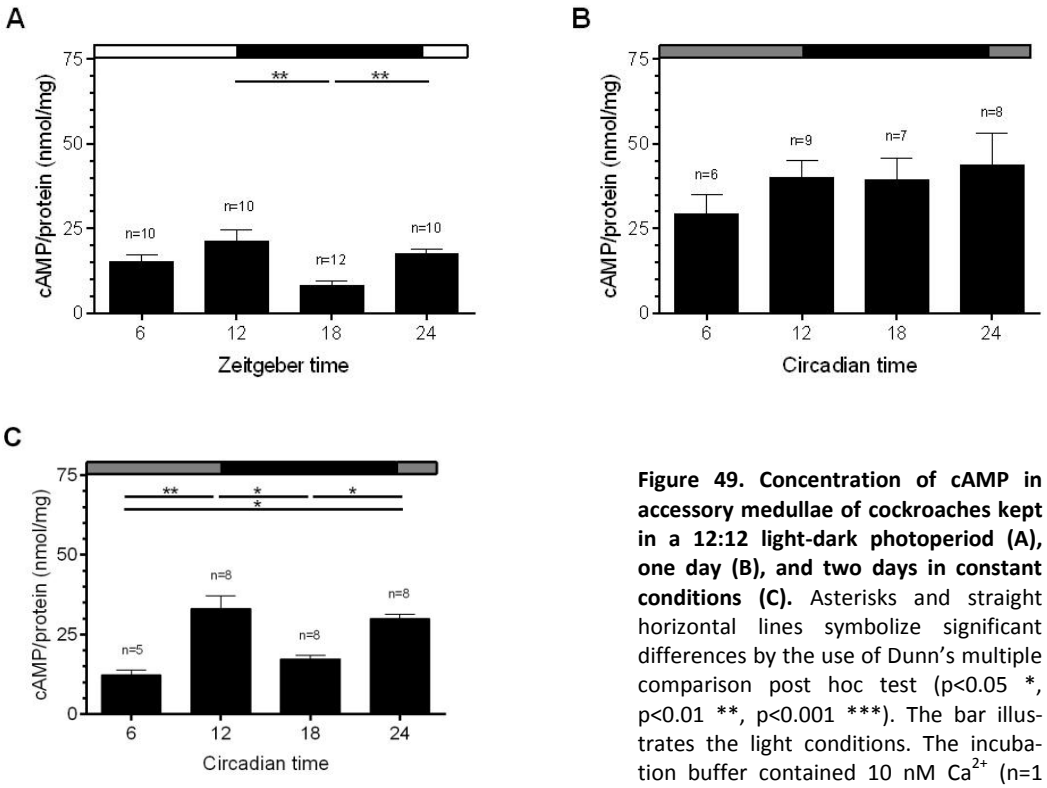

Figure 49. Concentration of cAMP in accessory medullae of cockroaches kept in a 12:12 light-dark photoperiod (A), one day (B), and two days in constant conditions (C). Asterisks and straight horizontal lines symbolize significant differences by the use of Dunn's multiple comparison post hoc test ($p<0.05$ *, $p<0.01$ **, $p<0.001$ ***). The bar illustrates the light conditions. The incubation buffer contained 10 nM Ca^{2+} (n=1 contained 20 accessory medullae).

3.5.3 Biphasic oscillations of cAMP concentrations only in DD2 in optic lobe neuropils

Measurements of cAMP levels in optic lobes (without AMae) under LD revealed no significant oscillation (**Fig. 50 A**; **Tab. 16**), but mean values at ZT 12 and ZT 18 were approximately half the values measured at ZT 6 and ZT 24. At DD1, cAMP levels strongly increased at all CTs with a significant maximum at CT 18 (Dunn's post hoc test, $p<0.01$; **Fig. 50 B**; **Tab. 16**). In DD2, cAMP levels oscillated with minima at CT 6 and CT 18 (**Fig. 50 C**; **Tab. 16**). In DD2 mean cAMP values at CT 6 were significantly lower in comparison to CT 12 and CT 18 as well as to CT 24 (Dunn's post hoc test, $p<0.01$).

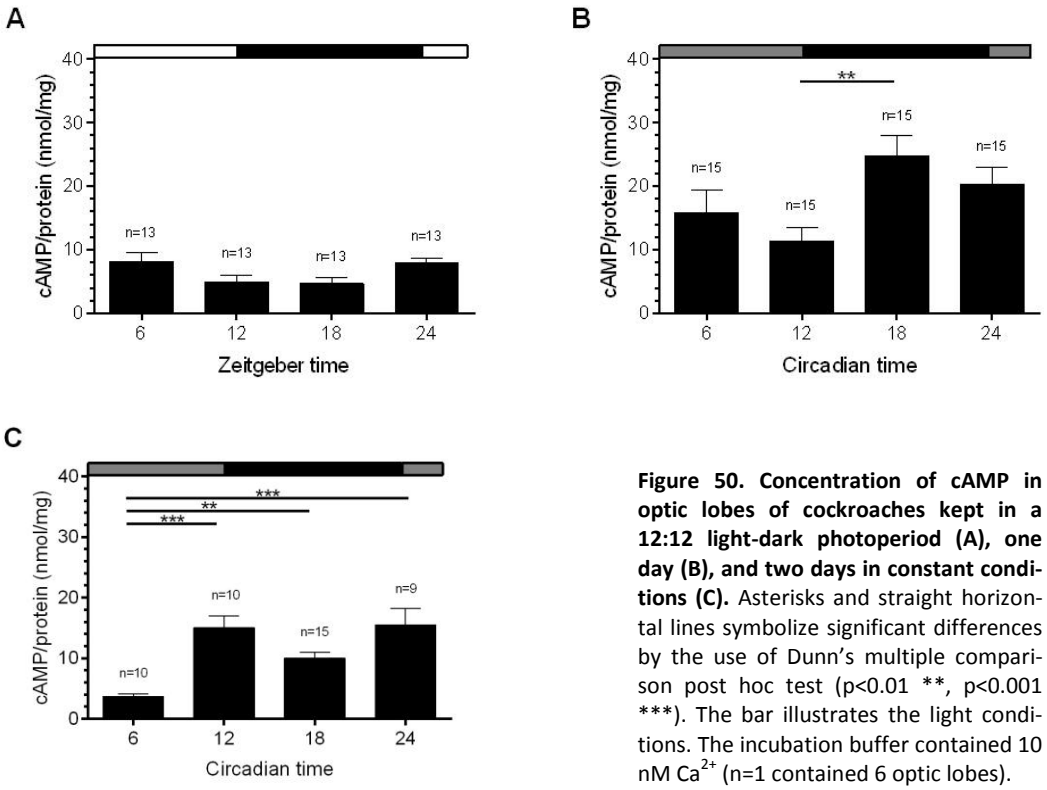

Figure 50. Concentration of cAMP in optic lobes of cockroaches kept in a 12:12 light-dark photoperiod (A), one day (B), and two days in constant conditions (C). Asterisks and straight horizontal lines symbolize significant differences by the use of Dunn's multiple comparison post hoc test ($p<0.01$ **, $p<0.001$ ***). The bar illustrates the light conditions. The incubation buffer contained 10 nM Ca^{2+} (n=1 contained 6 optic lobes).

3.5.4 Biphasic oscillations of cGMP concentrations only in LD in AMae

Under LD also concentrations of cGMP oscillated in AMae with a significant minimum at ZT 18 and maxima at dusk and dawn (**Fig. 51 A**; **Tab. 16**). Significant differences in cGMP concentrations were measured between ZT 18 and ZT 12 as well as between ZT 18 and ZT 24 (Dunn's post hoc test, $p<0.05$). An almost tripling of cGMP concentrations at DD1 was detected at all CTs (**Fig. 51 B**; **Tab. 16**). During DD2 cGMP concentrations remained constant at a lower level as compared to DD1 (**Fig. 51 C**; **Tab. 16**).

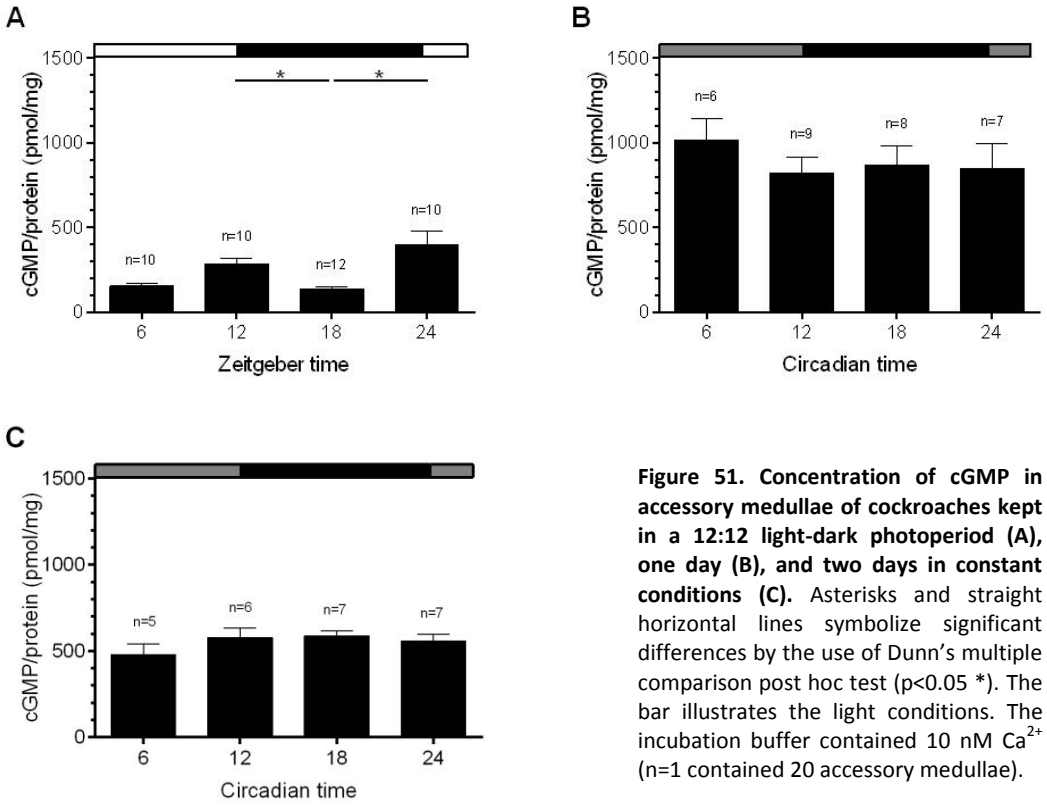

Figure 51. Concentration of cGMP in accessory medullae of cockroaches kept in a 12:12 light-dark photoperiod (A), one day (B), and two days in constant conditions (C). Asterisks and straight horizontal lines symbolize significant differences by the use of Dunn's multiple comparison post hoc test ($p<0.05$ *). The bar illustrates the light conditions. The incubation buffer contained 10 nM Ca^{2+} (n=1 contained 20 accessory medullae).

3.5.5 Monophasic oscillation of cGMP levels in LD and DD1 in optic lobe neuropils

In optic lobe neuropils (without AMae) in LD and DD1 cGMP levels oscillated with a single, significant maximum at ZT/CT 12 (Dunn's post hoc test, $p<0.05$; **Fig. 52 A,B**; **Tab. 16**). The concentration of cGMP at DD2 remained constant at a lower level as compared to the maximum in DD1 (**Fig. 52 C**; **Tab. 16**).

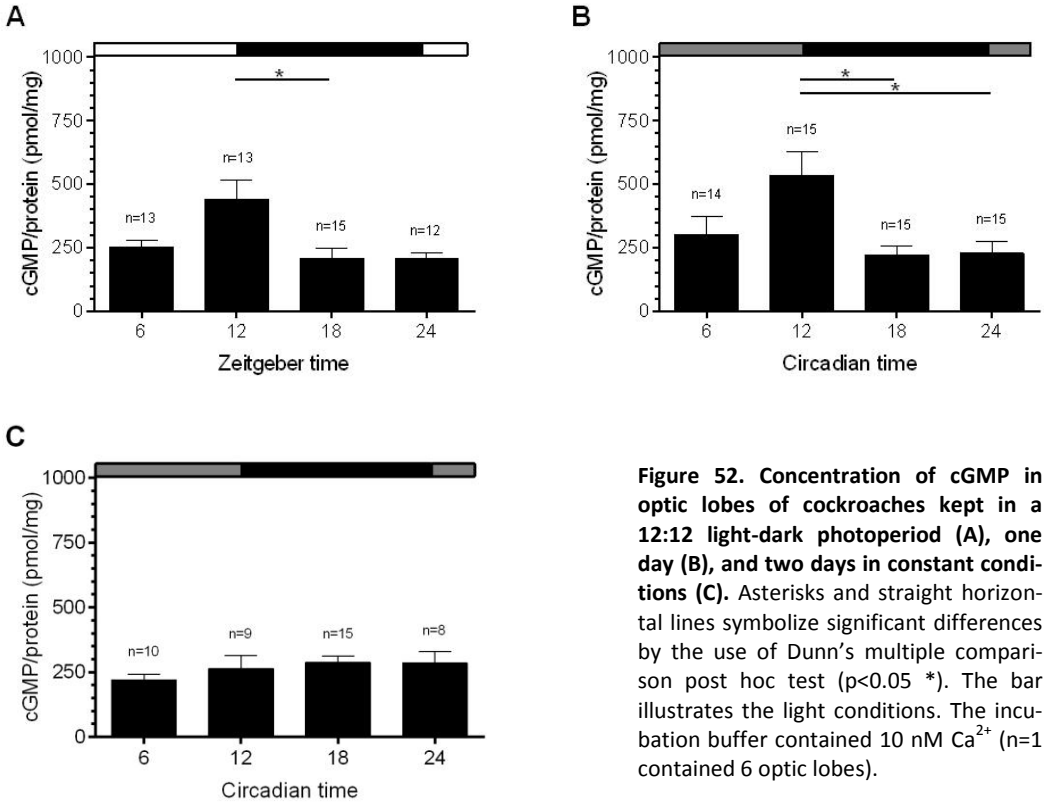

Figure 52. Concentration of cGMP in optic lobes of cockroaches kept in a 12:12 light-dark photoperiod (A), one day (B), and two days in constant conditions (C). Asterisks and straight horizontal lines symbolize significant differences by the use of Dunn's multiple comparison post hoc test ($p<0.05$ *). The bar illustrates the light conditions. The incubation buffer contained 10 nM Ca^{2+} (n=1 contained 6 optic lobes).

Table 16. Concentrations of cAMP and cGMP (mean±SE) in accessory medullae and optic lobes at different Zeitgeber times (ZT) or circadian times (CT) of animals kept in a 12:12 light-dark photoperiod (LD), one day (DD 1), and two days in constant conditions (DD 2).

		Accessory medullae				Optic lobes			
		cAMP (nmol/mg)	n	cGMP (pmol/mg)	n	cAMP (nmol/m)	n	cGMP (pmol/mg)	n
LD	ZT 6	15.2±2.2	10	154.0±19.7	10	8.2±1.3	13	251.6±26.5	13
	ZT 12	21.4±3.3	10	282.5±37.2	10	4.9±1.0	13	441.7±72.8	13
	ZT 18	8.3±1.2	12	139.3±12.1	12	4.7±1.0	13	208.5±38.3	15
	ZT24	17.5±1.5	10	398.8±83.2	10	7.9±0.8	13	207.1±24.4	12
DD 1	CT 6	29.3±5.6	6	1017.0±128.8	6	15.9±3.6	15	304.0±70.2	14
	CT 12	40.2±4.8	9	823.0±94.0	9	11.3±2.2	15	535.6±94.2	15
	CT 18	39.5±6.3	7	868.4±112.9	8	24.8±3.2	15	222.1±33.6	15
	CT 24	43.8±9.3	8	848.5±148.3	7	20.4±2.6	15	229.7±43.2	15
DD 2	CT 6	12.3±1.6	5	478.4±63.6	5	3.7±0.4	10	219.9±22.2	10
	CT 12	33.1±4.1	8	577.6±55.9	6	15.0±2.0	10	262.6±51.1	9
	CT 18	17.4±1.2	8	587.7±30.9	7	10.0±1.0	15	287.9±24.1	15
	CT 24	30.0±1.4	8	558.7±37.6	7	15.5±2.7	9	285.6±44.7	8

3.5.6 Cyclic nucleotide concentrations usually increased in DD1

Mean values of cAMP- and cGMP concentrations of all samples tested per day were combined and statistically evaluated (**Fig. 53**; **Tab. 17**). In AMae, cAMP- and cGMP levels increased significantly at DD1 as compared to LD (Dunn's post hoc test, p<0.001; **Fig. 53 A,C**). At DD2, both cAMP and cGMP levels decreased significantly as compared to DD1 (Dunn's post hoc test, p<0.05; **Fig. 53 A,C**) but remained elevated as compared to LD levels (Dunn's post hoc test, p<0.01; **Fig. 53 A,C**). In optic lobes (without AMae), mean cAMP levels increased significantly at DD1 as compared to LD (Dunn's post hoc test, p<0.001; **Fig. 53 B**). DD2 values decreased significantly as compared to DD1, while still remaining elevated as compared to LD values (Dunn's post hoc test, p<0.01; **Fig. 53 B**). The mean cGMP concentrations in optic lobes remained constant at low levels (**Fig. 53 D**).

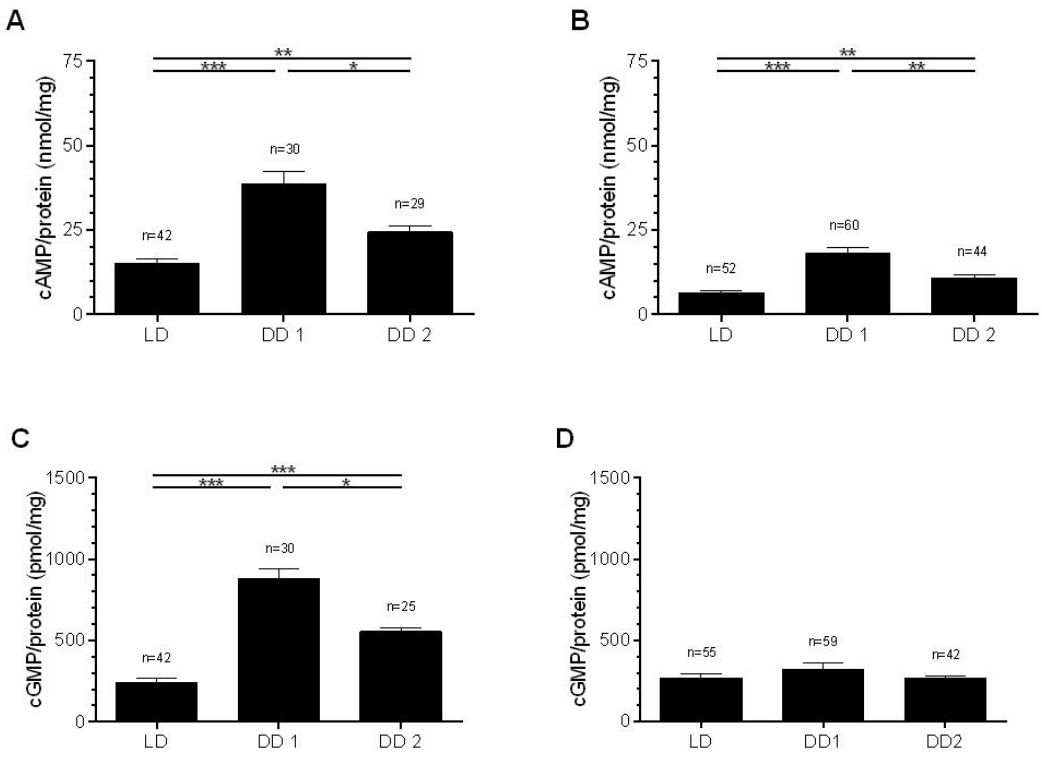

Figure 53. Transfer from 12:12 light-dark cycle (LD) to constant conditions (DD) influences the cAMP- as well as the cGMP content of accessory medullae (A,C) and optic lobes (B,D). Measured data sets from each day were combined for comparison. Asterisks and straight horizontal lines symbolize significant differences by the use of Dunn's multiple comparison post hoc test (p<0.05 *, p<0.01 **, p<0.001 ***). The used incubation buffer contained 10 nM Ca^{2+} (n=1 contained 20 accessory medullae or 6 optic lobes, respectively).

Table 17. Pooled cAMP- and cGMP concentrations (mean±SE) of accessory medullae and optic lobes of animals kept in a 12:12 light-dark photoperiod (LD), one day (DD 1), and two days in constant conditions (DD 2).

	Accessory medullae				Optic lobes			
	cAMP (nmol/mg)	n	cGMP (pmol/mg)	n	cAMP (nmol/m)	n	cGMP (pmol/mg)	n
LD	15.2±2.2	42	154.0±19.7	42	8.2±1.3	52	251.6±26.5	55
DD 1	21.4±3.3	30	282.5±37.2	30	4.9±1.0	60	441.7±72.8	59
DD 2	8.3±1.2	29	139.3±12.1	25	4.7±1.0	44	208.5±38.3	42

3.5.7 Injection of 8-br-cAMP induced a biphasic PRC with phase delays at the late subjective day and phase advances at the end of the subjective night

Injections of 8-br-cAMP phase-shifted circadian locomotor activity rhythms measured in running-wheel assays significantly (Kruskal-Wallis test, $p<0.01$; **Tab. 18**). Between CT 7.5 (-1.52 h_{CT}), CT 10.5 (-2.18 h_{CT}), and CT 13.5 (-1.58 h_{CT}) as compared to CT 22.5 (2.01 h_{CT}) significant phase shifts were obtained (Dunn's post hoc test, $p < 0.01$). Moreover, CT 10.5 and 13.5 significantly differed from CT 1.5 (1.08 h_{CT}). While maximal phase delays were induced at CT 10.5, maximal phase advances occurred at CT 22.5 after 8-br-cAMP injections (**Fig. 54 A**). Saline-dependent phase shifts at all CTs did not differ significantly from each other (Kruskal-Wallis test, $p>0.05$). Comparing 8-br-cAMP- with saline injections revealed significant differences (Kruskal-Wallis test, $p<0.001$). At CT 10.5 8-br-cAMP induced significant phase delays and at CT 22.5 significant phase advances (Dunn's post hoc test, $p<0.05$; **Fig. 54 A**).

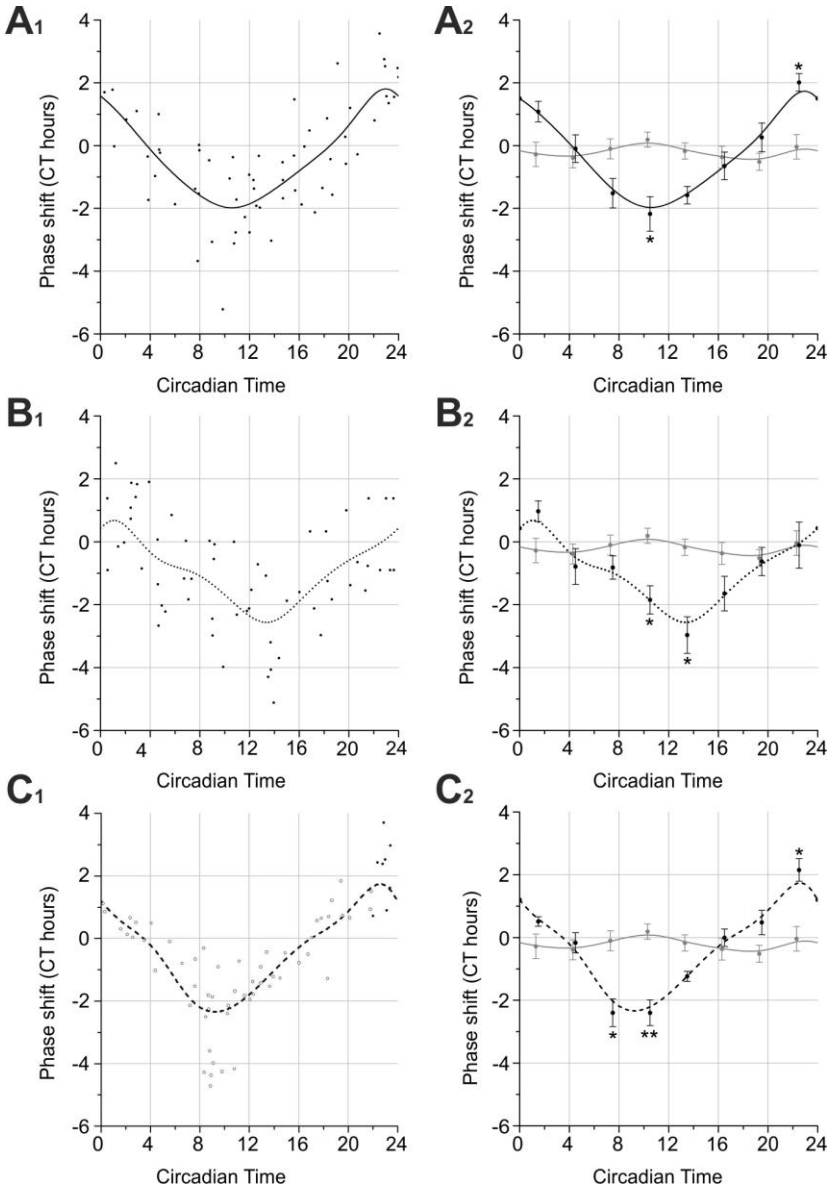

Figure 54. Phase response curves (PRC) of 8-br-cAMP (black line; A_1, A_2), 8-br-cGMP (dotted line; B_1, B_2), and PDF (dashed line; C_1, C_2) compared with insect saline injections (grey line; A_2, B_2, C_2). Data were presented as scatter plots and b-spline curves (**A_1, B_1, C_1**) and 3-h merged bins (mean circadian hours±SE; **A_2, B_2, C_2**). 8-br-cAMP injections caused significant phase delays at CT 10.5 as well as significant phase advances at CT 22.5 compared to control injections (Dunn's post hoc test, $p<0.05$ *, asterisks; **A_2**). 8-br-cGMP injections resulted in significant phase delays at CT 10.5 and CT 13.5 compared to control injections (Dunn's post hoc test, $p<0.05$ *; **B_2**). Next to significant phase delays at the end of subjective night published in Petri and Stengl, 1997 (open dots), *Rhyparobia*-PDF induced significant phase advances at CT 22.5 (filled dots; Dunn's post hoc test, $p<0.05$ *; **C_2**).

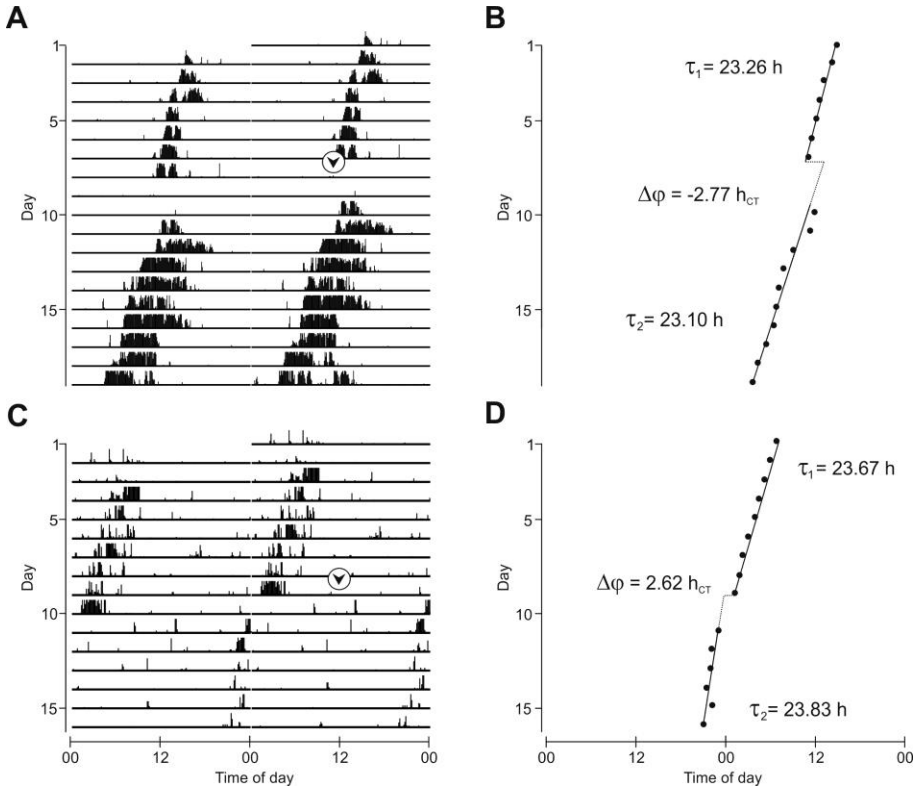

Figure 55. Running-wheel recordings (A,C) and regression analysis through consecutive activity onsets (B,D) of the circadian locomotor activity of the cockroach *Rhyparobia maderae* after injections of 2 x 10^{-10} mol 8-br-cAMP. A,B: A phase shift (Δϕ) of -2.77 circadian hours (h_{CT}) was induced after an injection at CT 10.5 of day 8 (arrowhead). **C,D:** A phase advance of 2.62 h_{CT} was observed after injection at CT 22.5 of day 9 (arrowhead). No effects on the period length (tau = τ) of the cockroaches' activity rhythm were observed in both cases (modified after Schendzielorz, 2013).

Table 18. Effects of 2 x 10^{-10} mol 8-br-cAMP, 2 x 10^{-10} mol 8-br-cGMP, 2 x 10^{-12} mol PDF, and saline (control) injections at different circadian times on the phase of the circadian locomotor activity (Δϕ; mean±SE) of the cockroach *Rhyparobia maderae*.

CT time (hours)	8-br-cAMP		8-br-cGMP		PDF		saline	
	Δϕ	n	Δϕ	n	Δϕ	n	Δϕ	n
00:00-03:00	1.08±0.33	5	0.97±0.33	10	0.51±0.15[x]	7	-0.28±0.39	6
03:00-06:00	-0.10±0.44	7	-0.79±0.57	8	-0.18±0.32[x]	4	-0.39±0.32	7
06:00-09:00	-1.52±0.47	8	-0.82±0.37	5	-2.42±0.44[x,a]	12	-0.10±0.32	7
09:00-12:00	-2.18±0.55[a]	8	-1.85±0.45[a]	9	-2.40±0.41[x,b]	10	0.19±0.24	6
12:00-15:00	-1.58±0.28	10	-2.97±0.58[a]	8	-1.24±0.16[x]	10	-0.17±0.26	7
15:00-18:00	-0.65±0.44	8	-1.65±0.55	5	-0.01±0.28[x]	5	-0.37±0.35	7
18:00-21:00	0.26±0.46	8	-0.63±0.45	6	0.48±0.40[x]	7	-0.52±0.27	11
21:00-00:00	2.01±0.28[a]	9	-0.11±0.73	9	2.15±0.36[a]	8	-0.04±0.39	9

[a] Significant difference (Dunn's post hoc test, $p<0.05$) compared with saline induced phase-shifts.
[b] Significant difference (Dunn's post hoc test, $p<0.01$) compared with saline induced phase-shifts.
[x] Published data (Petri and Stengl, 1997).

3.5.8 The 8-br-cAMP-dependent phase shifts at the late subjective day were dose-dependent

Between CT 9 to 12 dose-dependent phase-shifts were obtained with injections of 2 x 10^{-7} mol, 2 x 10^{-10} mol, 2 x 10^{-13} mol, and 2 x 10^{-16} mol 8-br-cAMP (**Fig. 56 A_1**; **Tab. 19**). The 8-br-cAMP- and saline injections differed significantly (Kruskal-Wallis test, $p<0.05$). At a concentration of 2 x 10^{-13} mol 8-br-cAMP phase delayed by -0.91 h_{CT}, while injections of 2 x 10^{-16} mol 8-br-cAMP phase delayed by -0.09 h_{CT}. Phase shifts induced by higher concentration of 8-br-cAMP such as 2 x 10^{-10} mol (-2.18 h_{CT}) and 2 x 10^{-7} mol (-1.99 h_{CT}) revealed significant differences as compared to saline injections (Dunn's post hoc test, $p<0.05$, **Fig. 54 A_1**). Moreover, EC_{50} of 8-br-cAMP was 6.5 x 10^{-13} mol 8-br-cAMP (**Fig. 54 A_2**).

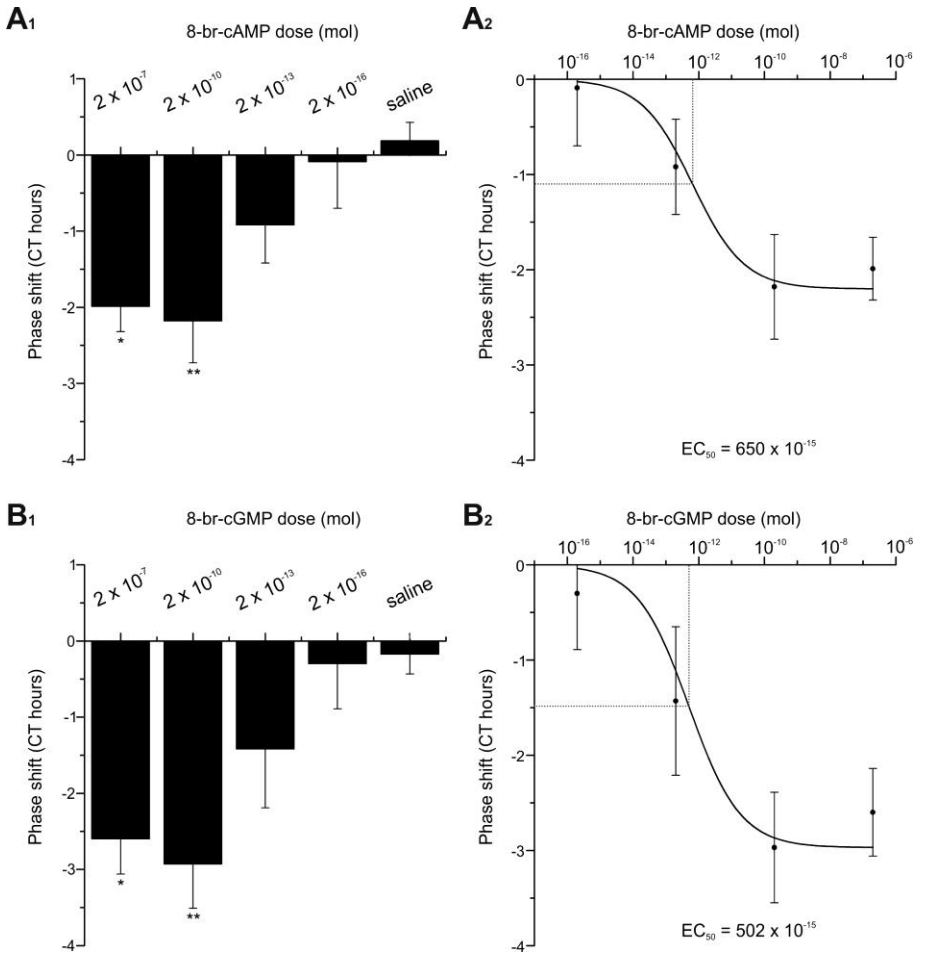

Figure 56. Injections of 8-br-cAMP into optic lobes of Madeira cockraches dose-dependently phase delayed locomotor activity rhythms in running-wheel assays (A) between CT 9 and CT 12, comparably to 8-br-cGMP injections (B) between CT 12 and CT 15. Bars represent the mean phase shifts (in circadian hours ± SE). **A_1**: Injections of saline (n = 6), 2 x 10^{-16} mol (n = 4), 2 x 10^{-13} mol (n = 5), 2 x 10^{-10} mol (n = 8), and 2 x 10^{-7} mol 8-br-cAMP (n = 7). **B_1**: Injections of saline (n = 7), 2 x 10^{-16} mol (n = 3), 2 x 10^{-13} mol (n = 4), 2 x 10^{-10} mol (n = 8), and 2 x 10^{-7} mol 8-br-cGMP (n = 6). **A_2, B_2**: Calculation of half maximal effective dose (EC_{50}) for 8-br-cAMP (EC_{50} = 650 x 10^{-15} mol) as well as 8-br-cGMP (EC_{50} = 502 x 10^{-15} mol).

Table 19. Effects of injections of different amounts of 8-br-cAMP as well as 8-br-cGMP on the phase of the circadian locomotor activity (Δϕ; mean±SE) of the cockroach *R. maderae*.

Dose (mol)	8-br-cAMP		8-br-cGMP	
	Δϕ	n	Δϕ	n
2 x 10^{-16}	-0.09±0.61	4	-0.30±0.59	3
2 x 10^{-13}	-0.92±0.50	5	-1.43.±0.77	4
2 x 10^{-10}	-2.18±0.55[b]	8	-2.97±0.58[b]	8
2 x 10^{-7}	-1.99±0.33[a]	7	-2.60±0.46[a]	6

[a] Significant difference (Dunn's post hoc test, p<0.05) compared with saline induced phase shifts.
[b] Significant difference (Dunn's post hoc test, p<0.01) compared with saline induced phase shifts.

3.5.9 Injections of 8-br-cGMP revealed a monophasic all-delay PRC with maximum at the late subjective day and early subjective night

Significant differences between all CTs were observed after injections of 2 x 10^{-10} mol 8-br-cGMP (Kruskal-Wallis test, p<0.01; **Tab. 18**). Phase shifts between CT 1.5 (0.97 h_{CT}) and CT 10.5 (-1.85 h_{CT}) as well as between CT 1.5 and CT 13.5 (-2.97 h_{CT}) were highly significantly different from each other (Dunn's post hoc test, p<0.01). Maximal phase delays of -2.97 h_{CT} were induced at CT 13.5. (**Fig. 57**). Highly significant differences were detected between 8-br-cGMP- and saline-injections (Kruskal-Wallis test, p<0.01). At CT 10.5 and 13.5 significant phase delays were induced by 8-br-cGMP (Dunn's post hoc test, p<0.05; **Fig. 54 B**).

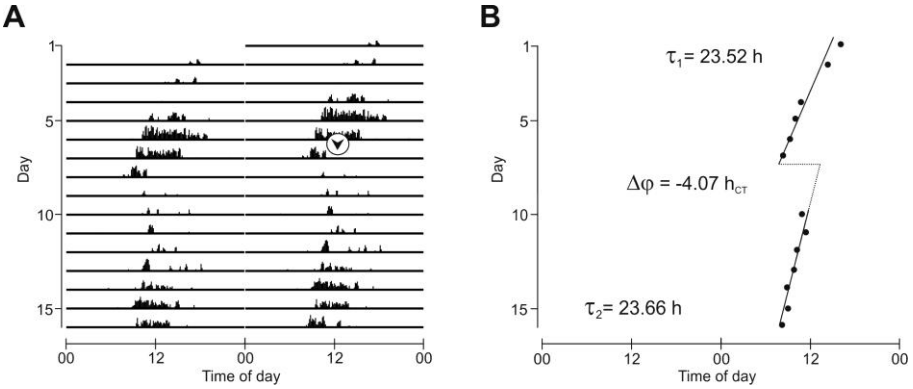

Figure 57. Running-wheel recording (A) and regression analysis through consecutive activity onsets (B) of the circadian locomotor activity of the cockroach *Rhyparobia maderae*. After injection of 2 x 10^{-10} mol 8-br-cGMP at CT 10.5 of day 7 (arrowhead) a phase shift (Δϕ) of -4.07 circadian hours (hCT) was induced without affecting the period length (tau = τ). Modified after Schendzielorz, 2013.

3.5.10 8-br-cGMP injections induced dose-dependent delays at the late subjective day/early subjective night

Application of 8-br-cGMP at four different doses (2 x 10^{-7} mol, 2 x 10^{-10} mol, 2 x 10^{-13} mol, and 2 x 10^{-16} mol) produced dose-dependent phase delays between CT 12 to 15 (Kruskal-Wallis test, $p<0.05$; **Tab. 19**). With 2 x 10^{-13} mol 8-br-cGMP phase delays of -1.43 h_{CT} were obtained while injections of 2 x 10^{-16} mol 8-br-cGMP revealed phase delays of -0.30 h_{CT}. Between 2 x 10^{-10} mol as well as 2 x 10^{-7} mol 8-br-cGMP- and saline induced phase shifts highly significant differences were detected (Dunn's post hoc test, $p<0.05$; **Fig. 56 B_1**). The resulting EC_{50} of 8-br-cGMP was 5.0 x 10^{-13} mol 8-br-cGMP (**Tab. 19**; **Fig. 56 B_2**).

3.5.11 Injection of *Rhyparobia*-PDF induced a biphasic PRC with phase delay at dusk and phase advance at dawn

Next to significant phase delays at the end of the subjective day (Petri and Stengl, 1997), now for the first time also significant phase advances of up to 2.15 h_{CT} were obtained at CT 22.5 as compared to control injections (Dunn's post hoc test, $p<0.05$; **Fig. 54 C**; **Fig. 58**; **Tab. 18**).

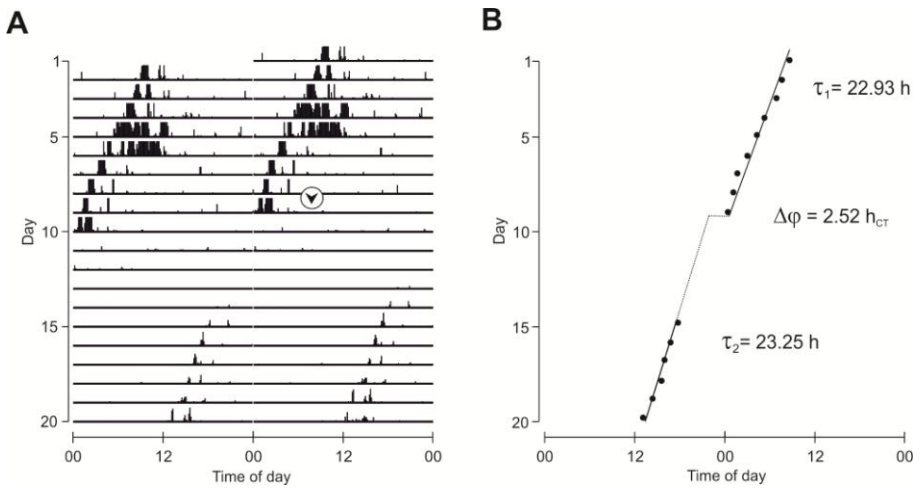

Figure 58. **Running-wheel recording (A) and regression analysis through consecutive activity onsets (B) of the circadian locomotor activity of the cockroach *Rhyparobia maderae*.** Injections of 2 x 10^{-12} mol *Rhyparobia*-pigment dispersing factor at CT 22.5 of day 9 (arrowhead) resulted in a phase shift (Δφ) of 2.52 circadian hours (hCT) after the injections without affecting the period length (tau=τ).

3.5.12 All tested substances did not affect the period length of the circadian locomotor activity

In all groups examined no significant differences of the period of circadian locomotor activity rhythms were detected after injections of 8-br-cAMP, 8-br-cGMP, *Rhyparobia*-PDF and saline (Mann-Whitney U-test, $p>0.05$; **Tab. 20**). Before 8-br-cAMP injections the average period length was 23.53 h and after injections 23.54 h. An average period length of 23.50 h was determined before 8-br-cGMP injections and 23.59 h after the injections. Also, *Rhyparobia*-PDF did not affect these parameters. The period length was 23.23 h before and 23.31 h after injection. The Chi-Square periodogram analysis of controls before saline injections was 23.58 h and 23.65 h after saline injections.

Table 20. Effects of 2 x 10^{-10} mol 8-br-cAMP, 2 x 10^{-10} mol 8-br-cGMP, 2 x 10^{-12} mol *Rhyparobia*-pigment dispersing factor (PDF), and saline (control) injections on the period length (τ; mean±SE) of the circadian locomotor activity of the cockroach *Rhyparobia maderae.*

CT time (hours)	8-br-cAMP	8-br-cGMP	PDF	saline
τ_{before} (hours)	23.53±0.05	23.50±0.05	23.23±0.10[x]	23.58±0.04
τ_{after} (hours)	23.54±0.05	23.59±0.05	23.31±0.09[x]	23.65±0.05

[x] For calculation results of injections at time bin CT 21:00-00:00 were used.

Discussion

4.1 Rhythmic behaviour of *R. maderae* and *M. sexta* is synchronized by LD cycles and odours

The cockroach *R. maderae* expresses locomotion activity at night as a multifunctional behaviour depending on numerous external factors such as search for food, mating, or avoiding predators (Wiedenmann, 1980). Since locomotion behaviour of female cockroaches was shown to be more erratic and ovarian cycles are superimposed on it, usually males were taken for circadian experiments (Roberts, 1960; Wiedenmann and Martin, 1980). However, females as the recipient of the male pheromone were employed for olfactory experiments (Sreng, 1993; Saifullah and Page, 2009). In running-wheel assays male cockroaches demonstrated peak activity directly after light-to-dark transitions (evening peak = E peak) which progressively decreased at night during 12:12 LD conditions and remained under DD. Additionally, a much smaller peak at the end of the night (morning peak = M peak) was described which occurred under prolong photoperiod, constant red- or day-light conditions (Roberts, 1962; Wiedenmann, 1980). The locomotor pattern of male cockroaches in Noldus tracking assays with larger arenas for movement exhibited also two activity peaks under 12:12 LD cycles (**Fig. 24 B**). Thereby, the M peak at the end of the night was as large as the E peak at the beginning of the night, most probably due to continuously applied red light which was necessary for detection. Thus, it appears that the M peak is favoured (activated) by more light.

Moreover, it was shown that the activity pattern of female and male cockroaches resembled each other (**Fig. 24**). Since females were kept in isolation without copulation partners or predators their activity pattern closely resembled their feeding behaviour (**Fig. 25 A**) comparable to the American cockroach *P. americana* (Lipton and Sutherland, 1970). If not feeding, females were drinking (**Fig. 25 B**). Interestingly, isolated females spend most time per day in the pheromone zone (at the end of the day until middle of the night) in correlation to the maximum in males' calling behaviour in colonies (**Fig. 25 C**, **Fig. 26 A**). Under the assumption that attraction of female cockroaches to male pheromone is guided by the sensitivity of their ORNs this would indicated that males' pheromone release is synchronized with females' sensitivity for pheromone.

Similarly to the hemimetabolous Madeira cockroach, the holometabolous hawk moth M. sexta is a nocturnal species. Both, male hawk moths in the wild and in isolation expressed maxima in feeding activity at twilight, while increased flight activity was observed throughout the night. Even in the absence of females, increased flight activity was observed at night when mating flights occurred (**Fig. 27 A**; Sasaki and Riddiford, 1984). However, in the wild hawk moth feeding rhythms are phase-shifted for a few hours into the night apparently due to olfactory and visual cues which synchronize moth behaviour with nectar production of their food plants (Thom et al., 2004; Goyret and Raguso, 2006; Goyret et al., 2008; Riffell et al., 2009). The preferred plants for hawk moth feeding are *Datura wrightii* which opens trumpet-shaped flowers at dusk, producing most nectar about 1-2 hours thereafter when maximal feeding by its moth pollinators occurred (Guerenstein et al., 2004; Riffell et al., 2008) and *Nicotina attenuate,* which opens flowers at dusk or dawn (Kessler et al., 2010). After feeding at dusk, at the beginning of the night male moths start searching for females (Sasaki and Riddiford, 1984). Therefore, male moths activity rhythms are synchronized with rhythms of antennal pheromone-sensitivity. In addition, males are synchronized with their species-specific females which express rhythmic pheromone production in LD and DD (Madden and Chamberlin, 1945; Sasaki and Riddiford, 1984; Itagaki and Conner, 1988; Flecke et al., 2010). However, it is still not resolved which circadian clocks and which coupling signals control the rest-activity rhythms of the hawk moths (Lindgren et al., 1977; Sasaki and Riddiford, 1984). Furthermore, it remains to be studied which circadian pacemakers and coupling factors synchronize both sexes and respective pollinator-plant interactions. From studies in the fruit fly *D. melanogaster* it is known that many different central and peripheral circadian pacemakers such as sensory neuron pacemakers coexist which are coupled with each other and with external Zeitgebers (Plautz *et al.*, 1997). Also in the hawk moth, ORNs appear to be peripheral circadian pacemakers, since they express the circadian clock gene *period* (Schuckel *et al.*, 2007).

The circadian clock work of the ORNs appears to control the ORN's olfactory sensitivity which expressed maxima during the activity phase of the hawk moth (Sasaki and Riddiford, 1984; Flecke et al., 2010). Previously, in *D. melanogaster* and *R. maderae* circadian rhythms in olfactory sensitivity were observed. In the fruit fly normal antennal clock gene expression was required for normal circadian rhythms in olfactory responses

(Krishnan et al., 1999; Tanoue et al., 2004; Zhou et al., 2005). In addition, in cockroaches circadian rhythms were observed in odour-dependent behaviour such as mating and feeding (Lipton and Sutherland, 1970; Rymer et al., 2007). However, unexpectedly mating rhythms were not synchronized with olfactory sensitivity rhythms in the antenna (Page and Koelling, 2003; Saifullah and Page, 2009).

4.2 Second messenger oscillations in the antenna are coupled with behavioural rhythms

As was shown previously in electrophysiological studies in moths cyclic nucleotide levels modulate olfactory sensitivity in a ZT-dependent manner (Villet, 1978; Flecke et al., 2006; Flecke et al., 2010). While cAMP perfusions of pheromone-sensitive trichoid sensilla in hawk moths sensitized pheromone responses (Flecke et al., 2010), cGMP perfusions adapted it (Flecke et al., 2006). Correspondingly, adapting odour concentrations increased cGMP levels in antennal homogenates of different insects (Ziegelberger et al., 1990; Boekhoff et al., 1993). These antennal cGMP rises took place in pheromone-dependent ORNs and supporting cells of trichoid sensilla as was shown in immunocytochemical studies combined with minute-long adapting pheromone stimulation (Stengl et al., 2001). How cAMP levels are controlled in hawk moth antenna remained elusive, but it was suggested that the stress hormone octopamine signals via cAMP rises in the antenna (Flecke and Stengl 2009).

Also IP_3 concentration changes appeared to be important for odour detection since pheromone-dependent ion channels were also activated via IP_3 in ORNs of *M. sexta* (Stengl, 2010). In addition, ORCO which is necessary for OR insertion in ORN membrane was suggested to be a pacemaker channel in *M. sexta,* which controls intracellular Ca^{2+} concentration and thereby modulating PLC activity (Rebecchi and Pentyala, 2000; Stengl and Funk, 2013). Moreover, adapting pheromone concentration seemed to increase PKC activity which inhibit PLC action (Stengl, 1993, 1994; Krannich, 2008; Stengl, 2010). Therefore, it was examined whether in antennae of male *M. sexta* and female *R. maderae* cyclic nucleotides and IP_3 concentrations vary in a ZT-dependent manner.

Indeed, for the first time antennal cyclic nucleotide and IP_3 concentrations in insect were shown to differ ZT-dependently in phase with previously observed rhythms of

odour-dependent behaviour (**Fig. 28**; **Fig. 32**; Sasaki and Riddiford, 1984; Decker et al. 2007; Rymer et al. 2007). In the hawk moth cAMP concentration peaked in the middle of the night correlating with its mating rhythms (**Fig. 59**; Sasaki and Riddiford, 1984), whereas IP_3 levels were increased during the whole night peaking at ZT 18 and ZT 23 as observed for animals' flight activity in isolation (**Fig. 27 A**; **Fig. 32**).

Also, in female cockroaches an increased cAMP concentration was detected at the animals mating time (Rymer et al., 2007). Moreover, antennal IP_3 concentrations were also increased at this ZT (**Fig. 28**). However, since IP_3 quantifications were performed with antennae of female cockroaches taken from laboratory colonies without recording their activity patterns, a direct correlation between IP_3 levels and rhythms in female behaviour can only be assumed.

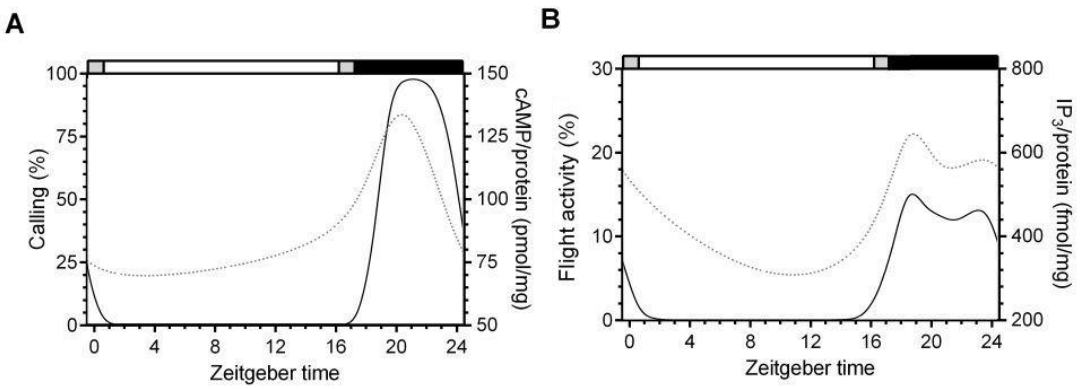

Figure 59. Correlation between antennal cAMP oscillation (A; grey dotted line) and calling behaviour (A; black solid line; modified after Sasaki and Riddiford, 1984) as well as antennal IP_3 oscillation (B; grey dotted line) and flight activity (B; black solid line) in *Manduca sexta* males. Polynomial fit of averaged values.

In addition, evidence was provided for an inverse correlation between cAMP- and cGMP concentration changes in antennae from female cockroaches taken directly from colonies (**Fig. 28**). Moreover, since cAMP oscillations persisted in DD they were controlled by a circadian clock (**Fig. 33**). However, it remains unknown where this clock was located and how it controlled cAMP levels. Contrarily to cAMP, cGMP concentrations expressed no circadian rhythm since they progressively decreased in DD (**Fig. 33**). Under the assumption that only adapting pheromone concentrations cause rises in antennal cGMP levels (Ziegelberger et al., 1990; Boekhoff et al., 1993; Stengl et al., 2001), the lack of pheromone could be responsible for the decline in cGMP concentrations in the isolated females (in DD experiments females were isolated for 2, 5, 10, 14, and 20 hours from males).

Correspondingly, in male hawk moths, which were never before in contact with their species-specific pheromones, antennal cGMP concentrations remained at low baseline levels in LD cycles and in DD (**Fig. 32**; **Fig. 34**). In contrast to cockroaches in *M.* sexta neither cAMP- nor IP_3 level oscillations were detected in DD. Thus, either these second messengers are not circadian clock-controlled or, which is more likely, the respective rhythms desynchronized rapidly in the absence of coupling signal. This assumption is further supported by the finding of rhythmic clock gene expression in hawk moth antenna (Schuckel et al., 2007).

4.2.1 Cyclic nucleotide concentrations in antennae of female Madeira cockroaches depended on male to female ratios

Previously, a puzzling phase difference was found between circadian rhythms in pheromone-dependent behaviour and antennal pheromone-sensitivity (Sreng, 1993; Page and Koelling, 2003; Decker et al., 2007; Farine et al., 2007; Rymer et al., 2007; Saifullah and Page, 2009). Thus, it was suggested that sensory adaptation due to prolonged pheromone-stimulation modulated antennal pheromone detection and masked underlying phase-coupled circadian rhythms. Indeed, excess males in the cockroach colonies increased the duration of males´ calling behaviour (**Fig. 26 B**) and affected rhythms in cyclic nucleotides (**Fig. 29**). Since cAMP- and cGMP levels were affected in opposite ways ZT-dependently via excess males in the cockroach colonies this mechanism could be caused by excessive stimulation of pheromone receptors. Male cockroaches produced sex-pheromones as well as contact pheromones (Sreng, 1993) and, thus, it is very likely that the surplus of males compared to the number of females in the insect colonies resulted in overstimulation of females via adapting male pheromone concentrations. Therefore, it is likely that adapting pheromone stimuli masked underlying cGMP rhythms in the Madeira cockroach.

4.3 Oscillation of OA drives rhythms in cAMP and partially IP_3

The neuromodulator, neurotransmitter, and neurohormone OA is involved in almost every physiological and behavioural process in invertebrates (Roeder, 1999, 2005; Wicher, 2007; Rillich et al., 2011). Moreover, it plays an important role during the daily

rest activity cycle (Saraswati et al., 2004). In hawk moth antennae OA allowed sensitive and fast pheromone detection during the moth´s activity phase and was a prerequisite to pheromone responses during the rest phase (Flecke and Stengl, 2009). Also, in the cockroach *P. americana* OA elevated the spontaneous and pheromone-dependent action potential frequency in antennal sensory neurons (Zhukovskaya and Kapitsky, 2006). Thus, OA appeared to signal via cAMP concentration rises since OA perfusions of pheromone-sensitive antenna were partly mimicked by cAMP perfusion (Flecke and Stengl, 2009; Flecke et al., 2010). However, cAMP did not mimic all effects of OA in moth antennae which suggested that there is an additional second messenger involved (Flecke and Stengl, 2009; Flecke et al., 2010). Thus, with ELISAs OA signalling was examined in *M. sexta* and *R. maderae* antennae. Generally, two types of G-protein-dependent OA receptors are known (Roeder, 1999; Balfanz et al., 2005; Farooqui, 2007). The α-adrenergic-like OA receptor (OctαR) modulates IP3- as well as cAMP levels. In contrast, activation of β-adrenergic-like OA receptors (OctβR) only affects cAMP levels (Farooqui, 2007). Since a previous study only found evidence for one putative OA receptor in hawk moths it is possible that this is the only OA-receptor present (Dacks et al., 2006). Its amino acid sequence expressed a high degree of homology to OctαR type OA receptors from the honey bee *Apis mellifera* and *P. americana* (Grohmann et al., 2003; Bischof and Enan, 2004; Dacks et al., 2006). Since OA increased cAMP and IP3 levels in antennal lysates of the hawk moth which could be blocked by the OA recpeptor antagonist epinastine (EPI) (**Fig. 37**; **Fig. 41**), the data of this study support the presence of OctαR type in hawk moth antennae. Unexpectedly, antennal OA- and cAMP- but not IP_3 baseline oscillations closely resembled each other peaking both at the animals calling phase (**Fig. 9**; **Fig. 32**; **Fig. 35**; **Fig. 41**). Therefore, there must be additional factors responsible for IP_3 concentration rises, which correlated with starts of flight. Interestingly, also the transepithelial potential of ORNs changed during hawk moth's flight activity (Dolzer et al., 2001). This effect could be mimicked by OA perfusions (Dolzer et al., 2001). Thus, different mechanisms depending on OA release are assumed. Possibly, centrifugal OA neurons contacting the sensory cell layer of the antenna were activated during flight and then directly modulated antennal sensory neurons, and/or odours detected during flight were responsible for the correlation of IP_3 level changes with flight activity. Whereas daily rhythms of OA in the hemo-

lymph could modulate mostly cAMP levels. Contrarily, OA increased only cAMP concentration in *R. maderae* antennae indicative for OctβR types (**Fig. 36**; **Fig. 40**).

While most of the known OA receptors were expressed in mammalian cell lines and showed an EC_{50} in the low micromolar range (von Nickisch-Rosenegk et al., 1996; Grohmann et al., 2003; Bischof and Enan, 2004; Ohtani et al., 2006), only *D. melanogaster* DmOA2 showed a higher affinity with an EC_{50} at 3 x 10-8 M (Balfanz et al., 2005). Thus, EC_{50} values of 708.0 nM and 234.4 nM in *M. sexta* (**Fig. 38**) are consistent with previous studies in other insects.

4.3.1 Hemolymph born- and centrifugal OA

In accordance with the hypotheses above, ZT-dependent changes of OA levels occur in the hemolymph of *M. sexta* (Lehman, 1990), with maximal OA concentrations during the night when moths mate (Sasaki and Riddiford, 1984; Itagaki and Conner, 1988). Also, antennal OA amounts varied ZT-dependently closely resembling cAMP level oscillations (**Fig. 32**; **Fig. 35**). Thus, OA seems to be responsible for rhythms in baseline levels of cAMP in the antenna of the hawk moth. However, a distinction between hemolymph-born and neuronally derived OA concentrations could not be obtained in the experiments of this study. In the brain of *M. sexta* widespread OA-immunoreactivity was observed (Dacks et al., 2005), but so far it was not known whether octopaminergic fibers projected out into the antenna to the moth's ORNs. Also In the brain of the honeybee two octopaminergic fibers called VUMmx3 and VUMmd3 innervate the antennal nerves but it remained unknown whether they project into the antenna (Schroter et al., 2007). In *M. sexta* immoncytochemical studies against the OA precursor tyramine showed that two tyraminergic centrifugal neurons project into the antenna which appeared to directly contact the sensory neurons (Stolte, 2010). Furthermore, electrophysiological studies indicated that both OA and TA bind to the same receptors in the antenna. Since tyramine perfusions in trichoid sensilla of *M. sexta* partly mimicked OA actions (Flecke and Stengl, 2009). It is likely that these tyraminergic centrifugal neurons are also synthesizing OA. Additionally, it could be demonstrated that antennal OA receptor could also relay fast signalling on a time scale of ms (**Fig. 39**).

Based on these findings two main sources of OA are predicted which regulate cAMP- and IP_3-levels in the antenna: hemolymph-derived OA controlled by central cir-

cadian pacemaker cells might set baseline levels of second messengers which regulate the sensitivity of the antennal sensory neurons during the rest activity cycle. In addition to the circadian control of the antenna, two octopaminergic centrifugal neurons are suggested to release OA during flight activity thereby allowing for mechanisms of active sensing (Wachowiak, 2011). In addition to behaviour-dependent modulation of antennal sensitivity these centrifugal neurons might modulate antennal sensory neurons during learning and in response to acute stimuli (Peters, 2010; Behrends and Scheiner, 2012; Kim et al., 2013).

4.4 Calcium affects second messenger levels ZT-dependently

Physiological data suggested a daily rhythm in Ca^{2+}-baseline levels in *M. sexta* ORNs with a maximum at the rest phase which adapted transient pheromone-dependent ion channels (Stengl, 1994, 2010). This hypothesis is supported by ample evidence that Ca^{2+} concentration changes affect numerous cellular targets such as ACs, GCs, and PLCs, thereby orchestrating the internal state of ORNs (Sunahara et al., 1996; Rebecchi and Pentyala, 2000; Sharma, 2010; Stengl, 2010). Indeed, ZT-dependent effects of calcium on antennal IP_3-, cAMP-, and cGMP concentration in the hawk moth antenna were found suggesting several cross talks between second messenger cascades (**Fig. 43**; **Fig. 45**; **Fig. 47**). Respective Ca^{2+}-dependent cross talk also occurred in the antenna of the Madeira cockroach, indicative for conserved mechanisms during evolution (**Fig. 42**; **Fig. 44**; **Fig. 46**). In both, cockroach and hawk moth antennae 60 nM Ca^{2+} reduced AC activity during the time when animals mating were maximal, but was ineffective during their time of rest (**Fig. 42**, **Fig. 43**). Since higher or lower Ca^{2+} concentrations did not affect cAMP synthesis this type of Ca^{2+}-dependent regulation of AC activity is reminiscent of AC 5 regulation (Yoshimura and Cooper, 1992; Kawabe et al., 1994; Newton, 1997). Initially an increase in Ca^{2+} inhibited AC activity, followed by PKC activation by higher Ca^{2+} concentrations which led to phosphorylation and thereby activation of ACs. The presence of other ACs as AC 1, 2, 3, 4, 7, and 8 is unlikely because their activity can only be increased by Ca^{2+} (**Fig. 19**). A similar bell-shaped Ca^{2+}-dependence appears to regulate IP_3-production, since only 140 nM Ca^{2+} increased IP_3 concentrations significantly (**Fig. 47**). Generally, all isoforms of PLCs require Ca^{2+} for activation. Since PLCβ function as effector of G-protein-coupled receptors, these

PLC was assumed to be activated by pheromones in the hawk moth and cockroach (Boekhoff et al., 1990a; Boekhoff et al., 1990b; Boekhoff et al., 1993; Stengl, 2010). Thus, PLCβ could be activated by 140 nM Ca^{2+} resulting in increased IP_3 synthesis, further increase in Ca^{2+} might activate PKC, leading to a feedback mechanism (Newton, 1997; Rebecchi and Pentyala, 2000; Strassheim and Williams, 2000; Stengl, 2010). Contrarily to cAMP-, antennal cGMP concentration was increased by 60 nM Ca^{2+} at the resting phase of the hawk moth (**Fig. 45**). This is in accordance with a negative feedback mechanism observed in retinal rod cells (Koch and Stryer, 1988). Guanylyl cyclase activating proteins (GCAPs) activated GCs at low concentration of Ca^{2+} (50nM). Further increase in Ca^{2+} concentration (200 nM) inhibited GCAP activity (Koch and Stryer, 1988; Dizhoor et al., 1995; Laura et al., 1996).

Thus, cellular Ca^{2+} concentration is assumed to be a critical factor for adjusting ORNs sensitivity. Whether Ca^{2+} concentration of ORNs are indeed under circadian control as known for circadian pacemaker neurons of the suprachiasmatic nucleus remains to be examined. The vertebrate primary circadian pacemaker demonstrated Ca^{2+} oscillations in correlation with the rhythmic light-dark cycle (Colwell, 2000; Ikeda et al., 2003). For the hawk moth as well as for other insects it was shown that ORNs are circadian pacemaker neurons which express circadian clock genes such as *per* (Tanoue *et al.*, 2004; Merlin *et al.*, 2007; Schuckel *et al.*, 2007). Whether circadian clock proteins regulate circadian changes in intracellular Ca^{2+} baseline levels, which underlie circadian changes in olfactory sensitivity, remains to be examined in both the hawk moth and the cockroach (Stengl, 2010).

4.5 Signal transduction

In insects odour transduction is still under debate since there are contradicting findings even in the same species. One hypothesis suggests that ORs together with the conserved ion channel ORCO underlie an ionotropic signal transduction cascade (Sato *et al.*, 2008). Alternatively, either a sole metabotropic or a mixed ionotropic and metabotropic odour transduction cascade was suggested (Wicher et al., 2008; Nakagawa and Vosshall, 2009; Stengl, 2010; Nolte et al., 2013; Stengl and Funk, 2013). In the hawk moth *M. sexta* so far, no evidence for an ORCO-based ionotropic signal transduction cascade was found (Nolte

et al., 2013). ORCO was suggested to be a pacemaker channel controlling spontaneous activity and, thereby, threshold and temporal resolution of pheromone detection (Stengl and Funk, 2013). In moths, pheromone-receptors appear to couple to PLCβ, increasing IP_3 levels resulting in Ca^{2+} channel opening (Breer et al., 1990; Boekhoff et al., 1993; Stengl, 1994, 2010). So far, pheromone-dependent rises of cAMP were not observed in moth antennae, but adapting pheromone concentrations caused slow, sustained rises in cGMP levels which correlated with processes of odour-dependent adaptation (Ziegelberger et al., 1990; Boekhoff et al., 1993; Stengl et al., 2001). The observation of maximal IP_3 base-line levels before and after OA maxima (**Fig. 32**; **Fig. 35**), while moths were feeding or flying (**Fig. 27**) is consistent with an IP_3-dependent odour transduction cascade in *M. sexta*. Co-application of OA during moth pheromone detection appears to increase the sensitivity and temporal resolution of pheromone detection (Pophof, 2000; Grosmaitre et al., 2001; Flecke and Stengl, 2009; Stengl, 2010). Elevations of cAMP might further boost sensitivity and temporal resolution of the pheromone transduction cascade of the hawk moth via activation of cAMP-dependent transient Ca^{2+} channels (Krannich and Stengl, 2008; Flecke et al., 2010). Alternatively or concurrently, OA-dependent second messenger changes might affect opening probability of the pacemaker channel ORCO, since OA-receptor antagonists deleted spontaneous activity of ORNs (Flecke and Stengl, 2009). Future experiments will distinguish between these different hypotheses of OA actions for odour detection and will examine whether octopaminergic centrifugal neurons are implicated in stress-signal-dependent control of odour sensitivity and/or in reward-dependent learning at the periphery.

4.6 Bimodal oscillations of cyclic nucleotide concentrations in the circadian system of the Madeira cockroach *R. maderae*

With ELISAs it was examined whether the neuropeptide PDF, the major circadian coupling factor in the fruit fly as well as in the Madeira cockroach (Helfrich-Förster and Homberg, 1993; Stengl and Homberg, 1994; Helfrich-Förster et al., 1998), signals via cAMP elevations in the AMe, the cockroaches' circadian clock, and in the optic lobes as the clock's prominent input and output region (Reischig and Stengl, 2003b). Rhythmic maxima in

cyclic nucleotide levels were presumed to be indicative of maxima in neurotransmitter- or neuropeptide release of the circadian pacemaker network.

Consistent with findings in the fruit fly (Shafer et al., 2008; Duvall and Taghert, 2012, 2013) application of *Rhyparobia*-PDF increased cAMP- but not cGMP-levels (**Fig. 48**). Reminiscent for the mammalian circadian clock the AMe expressed maxima in cAMP- and cGMP concentrations at ZT 12 (dusk) and ZT 24 (dawn) (**Fig. 49**; **Fig. 51**; Prosser and Gillette, 1991), suggestive of light-dependent neuropeptide release via two synchronized populations of circadian pacemaker circuits, the E- and M-oscillators, coupled at 12 hours phase difference. The rhythms were lost at DD1 apparently due to disrupted homeostasis between inputs and endogenous rhythms (**Fig. 49**). Since cAMP levels significantly increased at DD1 and DD2 as compared to LD in both tissues investigated, light appeared to suppress AC activity (**Fig. 53**). At DD2, a bimodal oscillation in cAMP concentration with peaks at dusk and dawn returned both in the AMe and in other optic lobe neuropils, resembling the rhythm observed in the AMe in LD conditions (**Fig. 49**; **Fig. 50**). The presence of two coupled endogenous circadian oscillator networks could account for this finding. Most likely these oscillator networks are located in the AMe, the circadian pacemaker which controls circadian locomotor activity (Stengl and Homberg, 1994; Reischig and Stengl, 2003a). However, it cannot be excluded that additional oscillators located in other areas of the brain, are also involved in the generation of these rhythms (Helfrich-Förster, 2009).

In LD maxima of cGMP concentrations were found in the optic lobes at dusk apparently depending on photic stimuli (**Fig. 52**). In DD1 and to a lesser extend also in DD2 cGMP levels were constant and elevated as expected for mostly inhibitory photic input into the clock (Eskin et al., 1984). In optic lobes neuropils a cGMP peak at dusk dampened out at DD2 indicating that it resulted from photic input and not from endogenous clocks (**Fig. 52**). We hypothesize that cGMP concentration changes in the clock are mostly controlled via photic inputs delaying locomotor activity rhythms at dusk (**Fig. 54 B**). In contrast cAMP levels appeared to be light- and clock-controlled signals which might be mediated via light-dependent PDF release at dusk and dawn (**Fig. 54 A,C**).

4.6.1 PDF-neurons serve different functions in the circadian clock

In the Madeira cockroach about 12 PDF-immunoreactive neurons are located anterior to the AMe (aPDFMes) and about 3-6 large cells are located more posteriorly (pPDFMes). In addition, two larger PDF-ir cell groups are located dorsally and ventrally to the lamina (PDFLas) in the optic lobes (Petri et al., 1995; Reischig and Stengl, 2003b). Mostly the 12 aPDFMes were intensely investigated. The largest aPDFMe appears to connect all targets of PDF cells in the brain and optic lobes via the anterior and posterior optic commissure as possible circadian coupling pathway (Reischig et al., 2004; Soehler et al., 2011; Wei et al., submitted). Together with 3 medium sized aPDFMe which colocalize PDF-, orcokinin-, and FMRFamide-immunoreactivity it directly connects both AMae with each other (Hofer and Homberg, 2006; Soehler et al., 2011). Since they are affected distinctly by short and long photoperiods the different PDF-dependent input pathways into the clock are assumed to specifically synchronize different groups of pacemakers of the bilaterally symmetric pacemaker centers in response to light (Wei and Stengl, 2011). In addition, they are also assumed to gate outputs of the clock to locomotor control centers via ensemble formation (Schneider and Stengl, 2005). Furthermore, since PDFMes and PDFLas connect the AMe with the medulla and lamina the optic lobes appear to be both input and output regions of the circadian clock. Therefore, PDF appears to be the major coupling factor of the circadian clock in the Madeira cockroach which is expected to be released in a circadian rhythm comparably to PDF in *D. melanogaster* (Helfrich-Förster 2014).

4.6.2 PDF signals via AC activation

Experiments in *D. melanogaster* demonstrated PDF-dependent rises in intracellular cAMP levels in most circadian pacemaker neurons via activation of different ACs and an increase of intracellular calcium in a subset of clock neurons (Shafer et al., 2008; Duvall and Taghert, 2012, 2013; Seluzicki et al., 2014). Also in the Madeira cockroach calcium imaging experiments showed that PDF can modulate intracellular calcium levels of circadian pacemaker neurons mostly via activation of AC (Wei et al., submitted). Since incubation of optic lobe tissue with *Rhyparobia*-PDF resulted in an elevation of cAMP, these findings provide further evidence for PDF-dependent AC activation most likely via $G_{\alpha s}$ (**Fig. 48**). In accordance, the PDF-receptor of *D. melanogaster* is a class II G-protein-coupled receptor

which activates AC (Hyun et al., 2005; Lear et al., 2005). Furthermore, in both the Madeira cockroach and the fruit fly a $G_{\alpha s}$ independent signaling pathway is assumed. This is further supported by the resemblance of the PDF-receptor with the VPAC-2 receptor of vasoactive intestinal peptide (VIP) which couples to both AC and PLCβ (Meyer-Spasche and Piggins, 2004; Dickson and Finlayson, 2009; An et al., 2011; Agrawal et al., 2013; Wei et al., submitted).

However, since cAMP- and cGMP elevations do not change in synchrony with the same phase neither in the AMe nor in other optic lobe neuropils under DD it is likely that cGMP levels depend on additional excitatory photic inputs (**Fig. 51**; **Fig. 52**). Accordingly, accumulation of cGMP concentrations were obtained after exposure to light in the eyes of the mollusk *Aplysia* (Eskin et al., 1984). It was assumed that light-dependent excitatory neurotransmitters such as acetylcholine or other neuropeptides and -transmitters result in activation of guanylyl cyclases (Prosser et al., 1989). Therefore, receptor-type guanylyl cyclases or intracellular calcium levels might be affected, which activated calcium-sensitive nitric oxide synthase resulting in increased nitric oxide sensitive guanylyl cyclase activity. A candidate for such a neuropeptide is *Rhyparobia*-MIP-1 since injections resulted in an all delay PRC resembling the cGMP-dependent PRC (Schulze et al., 2013). To test whether acetylcholine affects the circadian locomotor activity in cGMP-dependent manner, injection experiments need to be performed.

4.6.3 PDF appears to be released by morning and evening oscillators in the circadian pacemaker center of the Madeira cockroach

The M and E dual oscillator model is a very useful concept (Aschoff, 1966; Pittendrigh and Daan, 1976) which can explain adaptations to different photoperiods as well as internal desynchronization into two free-running activity components with long or short period (Grima et al., 2004; Stoleru et al., 2004; Inagaki et al., 2007; Naito et al., 2008; Helfrich-Forster, 2009). The M-oscillator couples to dawn and is advanced (accelerated) by light resulting in a shorter period, while the E-oscillator with a longer period is delayed (decelerated) by light and synchronizes to dusk. While in the fruit fly the M-oscillator, but not the E-oscillator is assumed to consist of PDF-releasing neurons of the AMe (Yoshii et al., 2009; Peschel and Helfrich-Forster, 2011), in the cockroach the cellular and molecular natures of M- and E-oscillators are not known. However, as two maxima of cAMP concen-

trations were observed, dual oscillator circuits also might be present in the Madeira cockroach (**Fig. 49**). Thus, the first cAMP peak at CT 12 seems to be associated with an E- and the second peak at CT 24 with a M-oscillator circuit. In agreement with the assumption of two oscillator circuits controlling PDF release is our finding of the resemblance of the cAMP-dependent PRC and the Rhyparobia-PDF-dependent PRC (**Fig. 54 A,C**; Petri and Stengl, 1997). Thus, we hypothesize that circadian pacemaker neurons, which form phase-coupled ensembles (Schneider and Stengl, 2005), are either recruited as M- or E-oscillators via PDF as the major coupling factor which is released via photic inputs at dusk and dawn. It needs to be examined further whether additional neuropeptides and neurotransmitters are involved also.

Consistent with the assumption of light-controlled PDF-neurons, photoperiod-dependent changes in the number of medium-sized and posterior PDFMes was observed (Wei and Stengl, 2011). Thus, light appears to affect the expression of PDF in the aPDFMes, making them ideal candidates for adjustment to annual changes in photoperiods (Wei and Stengl, 2011). Furthermore, in agreement with this hypothesis light controls cyclic nucleotide concentrations, decreasing them in LD. Possibly, the strong inhibitory input into the AMe during the day is a light-dependent gain control mechanism preventing light-dependent overstimulation. A good candidate for light-dependent inhibition is the neurotransmitter GABA. The GABAergic distal tract connects the AMe to the ipsilateral medulla and lamina and could function as either entrainment pathway (Petri et al., 2002) or as gain control mechanism keeping light-dependent circuits in their response range. Furthermore, metabotropic GABA receptors (GABAB) couple to G_i proteins which reduce AC activity (Hamasaka et al., 2005b).

Whether the same or different PDFMes can be inhibited and/or excited by light, depending on the internal state of the cells and depending on additional environmental signals is not known but is likely. Thus, it is not surprising that we found evidence that PDF can both be excitatory or inhibitory for AMe pacemakers (Wei et al., submitted). Current experiments examine whether input-dependent activation of circadian pacemaker neurons results in phase advances and short periods and whether inhibitions result in delays and longer periods in the circadian clock of the Madeira cockroach.

Abbreviations

AC	adenylyl cyclase
ACh	acetylcholine
Ame	accessory medulla
aPDFMe	PDF neurons located anteriorly to the medulla
APF	action potential frequency
AT	allatotropin
B0	maximum binding
BAL	bombykal
BB	blocking buffer
$CaCl_2$	calcium chloride
CaM	calmodulin
cAMP	cyclic adenosine monophosphate
cGMP	cyclic guanosine monophosphate
clk	*clock*
CLK	CLOCK
COS-7 cells	cells from the kidney of the African Green Monkey
CRY 1	CRYPTOCHROME 1
CT	circadiane time
cyc	*cycle*
CYC	CYCLE
DAG	diacylglycerol
DD	constant conditions
disco	*disconnected*
DN	dorsal neurons
dPDFLa	PDF neurons located in the distal lamina
DTT	DL-1,4-dithiothreitol
E	evening
EAG	antennal electroantennogram
EC_{50}	half maximal effective dose
EDTA	ethylenediaminetetraacetic acid
EPAC	exchange proteins activated by cAMP
EPI	epinastine
FSK	forskolin
GABA	γ-aminobutyric acid
GABAB	metabotropic GABA receptors
GC	guanylyl cyclase
GTP	guanosin triphosphate
HB	homogenization buffer
HRP	horseradish peroxidase
IB	incubation buffer
IBMX	3-isobutyl-1-methylxanthine

IP_3	inositol trisphosphate
ir	immunoreactive
IR	glutamate-like receptor
K_m	substrate concentration at half-maximal enzyme activity
LD	light-dark
lLN_vs	large ventro-lateral neurons
LN_ds	dorso-lateral neurons
LPNs	posterior-lateral neurons
M	morning
m-3M3FBS	PLC activator
$MgCl_2$	magnesium chloride
MIP	myoinhibitory peptide
MOPS	3-(N-morpholino)propanesulfonic acid
NaCl	sodium chloride
NADPH diaphorase	amide adenine dinucleotide phosphate diaphorase
NO	nitric oxide
NSB	non-specific binding
OA	octopamine
OR	olfactory receptor
ORC	orcokinin
ORCO	OR-coreceptor
ORN	olfactory receptor neuron
PBP	pheromone-binding protein
PBS	phosphate buffer
PDE	phosphodiesterase
PDF	pigment-dispersing factor
PDFR	PDF receptor
PDH	β-pigment-dispersing hormone
per	*period*
PER	PERIOD
PIP2	phosphatidylinositol bisphosphate
PKA	protein kinase A
PKC	protein kinase C
PKG	protein kinase G
PLC	phospholipase
PLCβ	phospholipase Cβ
pPDFMe	PDF neurons located posteriorly to the medulla
PRC	phase response curve
rAC	receptor adenylyl cyclase
rGC	receptor guanylyl cyclase
RT	room temperature
sAC	soluble adenylyl cyclase
sGC	soluble guanylyl cyclase
sLN_vs	small ventro-lateral neurons
SPA	sensillar potential amplitude

τ	period length
tim	*timeless*
TIM	TIMELESS
VIP	vasoactive intestinal peptide
vPDFLa	PDF neurons located in the ventral lamina
WB	washing buffer
ZT	Zeitgeber time

References

Agrawal T, Sadaf S, Hasan G (2013) A genetic RNAi screen for IP(3)/Ca(2)(+) coupled GPCRs in *Drosophila* identifies the PdfR as a regulator of insect flight. PLoS Genet 9:e1003849.

Allada R, White NE, So WV, Hall JC, Rosbash M (1998) A mutant *Drosophila* homolog of mammalian Clock disrupts circadian rhythms and transcription of period and timeless. Cell 93:791-804.

An S, Irwin RP, Allen CN, Tsai C, Herzog ED (2011) Vasoactive intestinal polypeptide requires parallel changes in adenylate cyclase and phospholipase C to entrain circadian rhythms to a predictable phase. J Neurophysiol 105:2289-2296.

Aschoff AJ (1954) Zeitgeber der tierischen Tagesperiodik. Die Naturwissenschaften 41.

Aschoff J (1966) Circadian activity pattern with two peaks. Ecology:657-662.

Aschoff J (1969) Desynchronization and resynchronization of human circadian rhythms. Aerospace Med 40:844.

Balfanz S, Strunker T, Frings S, Baumann A (2005) A family of octopamine receptors that specifically induce cyclic AMP production or Ca^{2+} release in *Drosophila melanogaster*. J Neurochem 93:440-451.

Beavo JA (1995) Cyclic nucleotide phosphodiesterases: functional implications of multiple isoforms. Physiol Rev 75:725-748.

Behrends A, Scheiner R (2012) Octopamine improves learning in newly emerged bees but not in old foragers. J Exp Biol 215:1076-1083.

Bell RA, Joachim FA (1976) Techniques for rearing laboratory colonies of tobacco hornworms and pink bollworms. Ann Entomol Soc Am 69:365–373.

Bell WJ, Gorton Jr. RE, Tuortellot MK, Breed MD (1979) Comparison of male agonistic behavior in five species of cockroaches. Insect Soc 26:252-263.

Benton R, Sachse S, Michnick SW, Vosshall LB (2006) Atypical membrane topology and heteromeric function of *Drosophila* odorant receptors in vivo. PLoS Biol 4:e20.

Bischof LJ, Enan EE (2004) Cloning, expression and functional analysis of an octopamine receptor from *Periplaneta americana*. Insect Biochem Mol Biol 34:511-521.

Block GD, Page TL (1978) Circadian pacemakers in the nervous system. Annu Rev of Neurosci 1:19-34.

Boeckh J, Kaissling KE, Schneider D (1965) Insect olfactory receptors. In: Cold Spring Harbor Symposia on Quantitative Biology, pp 263-280: Cold Spring Harbor Laboratory Press.

Boekhoff I, Breer H (1992) Termination of second messenger signaling in olfaction. Proc Natl Acad Sci U S A 89:471-474.

Boekhoff I, Raming K, Breer H (1990a) Pheromone-induced stimulation of inositol-trisphosphate formation in insect antennae is mediated by G-proteins. Journal of comparative physiology B, Biochemical, systemic, and environmental physiology 160:99-103.

Boekhoff I, Strotmann J, Raming K, Tareilus E, Breer H (1990b) Odorant-sensitive phospholipase C in insect antennae. Cell Signal 2:49-56.

Boekhoff I, Seifert E, Göggerle S, Lindemann M, Krüger B-W, Breer H (1993) Pheromone-induced second maessenger signaling in insect antennae. Insect Biochem Mol Biol 23:757-762.

Bradford MM (1976) A rapid and sensitive method for the quantitation of microgram quantities of protein utilizing the principle of protein-dye binding. Anal Biochem 72:248-254.

Breer H, Boekhoff I, Tareilus E (1990) Rapid kinetics of second messenger formation in olfactory transduction. Nature 345:65-68.

Cermakian N, Sassone-Corsi P (2000) Multilevel regulation of the circadian clock. Nature Rev Mol Cell Biol 1:59-67.

Chen YQ, Cann MJ, Litvin TN, Iourgenko V, Sinclair ML, Levin LR, Buck J (2000) Soluble adenylyl cyclase as an evolutionarily conserved bicarbonate sensor. Science 289:625-628.

Chrisman TD, Garbers DL, Parks MA, Hardman JG (1975) Characterization of particulate and soluble guanylate cyclases from rat lung. J Biol Chem 250:374-381.

Colwell CS (2000) Circadian modulation of calcium levels in cells in the suprachiasmatic nucleus. Eur J Neurosci 12:571-576.

Conti M (2000) Phosphodiesterases and cyclic nucleotide signaling in endocrine cells. Mol Endocrinol 14:1317-1327.

Cooper DM (2003) Regulation and organization of adenylyl cyclases and cAMP. Biochem J 375:517-529.

Corbet PS (1960) Patterns of circadian rhythms in insects. In: Cold Spring Harbor symposia on quantitative biology, pp 357-360: Cold Spring Harbor Laboratory Press.

Dacks AM, Dacks JB, Christensen TA, Nighorn AJ (2006) The cloning of one putative octopamine receptor and two putative serotonin receptors from the tobacco hawkmoth, *Manduca sexta*. Insect Biochem Mol Biol 36:741-747.

Dacks AM, Christensen TA, Agricola HJ, Wollweber L, Hildebrand JG (2005) Octopamine-immunoreactive neurons in the brain and subesophageal ganglion of the hawkmoth *Manduca sexta*. J Comp Neurol 488:255-268.

Daly JW (1984) Forskolin, adenylate cyclase, and cell physiology: an overview. Adv Cyclic Nucl Prot 17:81-89.

Decker S, McConnaughey S, Page TL (2007) Circadian regulation of insect olfactory learning. Proc Natl Acad Sci U S A 104:15905-15910.

Dickson L, Finlayson K (2009) VPAC and PAC receptors: From ligands to function. Pharmacol Ther 121:294-316.

Dizhoor AM, Olshevskaya EV, Henzel WJ, Wong SC, Stults JT, Ankoudinova I, Hurley JB (1995) Cloning, sequencing, and expression of a 24-kDa Ca(2+)-binding protein activating photoreceptor guanylyl cyclase. J Biol Chem 270:25200-25206.

Dolzer J, Krannich S, Stengl M (2008) Pharmacological investigation of protein kinase C- and cGMP-dependent ion channels in cultured olfactory receptor neurons of the hawkmoth *Manduca sexta*. Chem Senses 33:803-813.

Dolzer J, Krannich S, Fischer K, Stengl M (2001) Oscillations of the transepithelial potential of moth olfactory sensilla are influenced by octopamine and serotonin. J Exp Biol 204:2781-2794.

Dunlap JC (1999) Molecular bases for circadian clocks. Cell 96:271-290.

Dushay MS, Rosbash M, Hall JC (1989) The disconnected visual system mutations in *Drosophila melanogaster* drastically disrupt circadian rhythms. J Biol Rhythm 4:1-27.

Duvall LB, Taghert PH (2012) The circadian neuropeptide PDF signals preferentially through a specific adenylate cyclase isoform AC3 in M pacemakers of *Drosophila*. PLoS Biol 10:e1001337.

Duvall LB, Taghert PH (2013) E and M circadian pacemaker neurons use different PDF receptor signalosome components in *Drosophila*. J Biol Rhythms 28:239-248.

Eskin A, Takahashi JS, Zatz M, Block GD (1984) Cyclic guanosine 3':5'-monophosphate mimics the effects of light on a circadian pacemaker in the eye of aplysia. J Neurosci 4:2466-2471.

Essayan DM (2001) Cyclic nucleotide phosphodiesterases. J Allergy Clin Immun 108:671-680.

Farine JP, Sirugue D, Abed-Vieillard D, Everaerts C, Le Quere JL, Bonnard O, Brossut R (2007) The male abdominal glands of *Leucophaea maderae*: chemical identification of the volatile secretion and sex pheromone function. J Chem Ecol 33:405-415.

Farooqui T (2007) Octopamine-mediated neuromodulation of insect senses. Neurochem Res 32:1511-1529.

Fitzpatrick DA, O'Halloran DM, Burnell AM (2006) Multiple lineage specific expansions within the guanylyl cyclase gene family. Bmc Evol Biol 6.

Flecke C, Stengl M (2009) Octopamine and tyramine modulate pheromone-sensitive olfactory sensilla of the hawkmoth *Manduca sexta* in a time-dependent manner. J Comp Physiol A 195:529-545.

Flecke C, Nolte A, Stengl M (2010) Perfusion with cAMP analogue affects pheromone-sensitive trichoid sensilla of the hawkmoth *Manduca sexta* in a time-dependent manner. J Exp Biol 213:842-852.

Flecke C, Dolzer J, Krannich S, Stengl M (2006) Perfusion with cGMP analogue adapts the action potential response of pheromone-sensitive sensilla trichoidea of the hawkmoth *Manduca sexta* in a daytime-dependent manner. J Exp Biol 209:3898-3912.

Gesteland RC (1971) Neural coding in olfactory receptor cells. In: Olfaction, pp 132-150: Springer.

Giebultowicz JM (2001) Peripheral clocks and their role in circadian timing: insights from insects. Philos T Roy Soc B 356:1791-1799.

Golombek DA, Rosenstein RE (2010) Physiology of circadian entrainment. Physiol Rev 90:1063-1102.

Goyret J, Raguso RA (2006) The role of mechanosensory input in flower handling efficiency and learning by *Manduca sexta*. J Exp Biol 209:1585-1593.

Goyret J, Pfaff M, Raguso RA, Kelber A (2008) Why do *Manduca sexta* feed from white flowers? Innate and learnt colour preferences in a hawkmoth. Naturwissenschaften 95:569-576.

Grima B, Chelot E, Xia R, Rouyer F (2004) Morning and evening peaks of activity rely on different clock neurons of the *Drosophila* brain. Nature 431:869-873.

Grohmann L, Blenau W, Erber J, Ebert PR, Strunker T, Baumann A (2003) Molecular and functional characterization of an octopamine receptor from honeybee (*Apis mellifera*) brain. J Neurochem 86:725-735.

Grosmaitre X, Marion-Poll F, Renou M (2001) Biogenic amines modulate olfactory receptor neurons firing activity in *Mamestra brassicae*. Chem Senses 26:653-661.

Guerenstein PG, E AY, Van Haren J, Williams DG, Hildebrand JG (2004) Floral CO_2 emission may indicate food abundance to nectar-feeding moths. Naturwissenschaften 91:329-333.

Hamasaka Y, Wegener C, Nässel DR (2005b) GABA modulates *Drosophila* circadian clock neurons via $GABA_B$ receptors and decreases in calcium. J Neurobiol 65:225-240.

Hamasaka Y, Mohrherr CJ, Predel R, Wegener C (2005a) Chronobiological analysis and mass spectrometric characterization of pigment-dispersing factor in the cockroach *Leucophaea maderae*. J Insect Sci 5:43.

Hanoune J, Defer N (2001) Regulation and role of adenylyl cyclase isoforms. Annu Rev Pharmacol Toxicol 41:145-174.

Hardin PE (2005) The circadian timekeeping system of *Drosophila*. Curr Biol 15:R714-R722.

Helfrich-Forster C (1995) The Period Clock Gene Is Expressed in Central-Nervous-System Neurons Which Also Produce a Neuropeptide That Reveals the Projections of Circadian Pacemaker Cells within the Brain of *Drosophila Melanogaster*. P Natl Acad Sci USA 92:612-616.

Helfrich-Forster C (1998) Robust circadian rhythmicity of *Drosophila melanogaster* requires the presence of lateral neurons: a brain-behavioral study of disconnected mutants. J Comp Physiol A 182:435-453.

Helfrich-Forster C (2009) Does the morning and evening oscillator model fit better for flies or mice? J Biol Rhythms 24:259-270.

Helfrich-Forster C, Edwards T, Yasuyama K, Wisotzki B, Schneuwly S, Stanewsky R, Meinertzhagen IA, Hofbauer A (2002) The extraretinal eyelet of Drosophila: development, ultrastructure, and putative circadian function. J Neurosci 22:9255-9266.

Helfrich-Förster C (1996) *Drosophila* rhythms: from brain to behavior. In: Semin Cell Dev Biol pp 791-802: Elsevier.

Helfrich-Förster C (2003) The neuroarchitecture of the circadian clock in the brain of *Drosophila melanogaster*. Microsc Res Techniq 62:94-102.

Helfrich-Förster C (2006) The neural basis of *Drosophila*'s circadian clock*. Sleep Biol Rhythms 4:224-234.

Helfrich-Förster C, Homberg U (1993) Pigment-dispersing hormone-immunoreactive neurons in the nervous system of wild-type *Drosophila melanogaster* and of several mutants with altered circadian rhythmicity. J Comp Neurol 337:177-190.

Helfrich-Förster C, Stengl M, Homberg U (1998) Organization of the circadian system in insects. Chronobiol Int 15:567-594.

Hofbauer A, Buchner E (1989) Does Drosophila have seven eyes? Naturwissenschaften 76:335-336.

Hofer S, Homberg U (2006) Evidence for a role of orcokinin-related peptides in the circadian clock controlling locomotor activity of the cockroach Leucophaea maderae. J Exp Biol 209:2794-2803.

Homberg U, Würden S, Dircksen H, Rao KR (1991) Comparative anatomy of pigment-dispersing hormone-immunoreactive neurons in the brain of orthopteroid insects. Cell Tissue Res 266:343-357.

Huber I, Edward PM, Rao BR (1990) Cockroaches as Model for Neurobiology: Application in Biomedical Research. Boca Raton, Florida, USA: CRC Press, Inc.

Hyun S, Lee Y, Hong ST, Bang S, Paik D, Kang J, Shin J, Lee J, Jeon K, Hwang S, Bae E, Kim J (2005) *Drosophila* GPCR Han is a receptor for the circadian clock neuropeptide PDF. Neuron 48:267-278.

Ikeda M, Sugiyama T, Wallace CS, Gompf HS, Yoshioka T, Miyawaki A, Allen CN (2003) Circadian dynamics of cytosolic and nuclear Ca^{2+} in single suprachiasmatic nucleus neurons. Neuron 38:253-263.

Inagaki N, Honma S, Ono D, Tanahashi Y, Honma K (2007) Separate oscillating cell groups in mouse suprachiasmatic nucleus couple photoperiodically to the onset and end of daily activity. Proc Natl Acad Sci USA 104:7664-7669.

Insel PA, Ostrom RS (2003) Forskolin as a tool for examining adenylyl cyclase expression, regulation, and G protein signaling. Cell Mol Neurobiol 23:305-314.

Ishikawa T, Matsumoto A, Kato T, Jr., Togashi S, Ryo H, Ikenaga M, Todo T, Ueda R, Tanimura T (1999) DCRY is a *Drosophila* photoreceptor protein implicated in light entrainment of circadian rhythm. Genes to cells : devoted to molecular & cellular mechanisms 4:57-65.

Itagaki H, Conner WE (1988) The calling behavior of *Manduca sexta* (*L.*) (*Lepidoptera:Sphingidae*) with notes on the morphology of the pheromone gland. Ann Entomol Soc 81:798-807.

Kain P, Chakraborty TS, Sundaram S, Siddiqi O, Rodrigues V, Hasan G (2008) Reduced odor responses from antennal neurons of G(q)alpha, phospholipase Cbeta, and rdgA mutants in *Drosophila* support a role for a phospholipid intermediate in insect olfactory transduction. J Neurosci 28:4745-4755.

Kaissling KE (2013) Kinetics of olfactory responses might largely depend on the odorant-receptor interaction and the odorant deactivation postulated for flux detectors. J Comp Physiol A Neuroethol Sens Neural Behav Physiol.

Kalinova B, Hoskovec M, Liblikas I, Unelius CR, Hansson BS (2001) Detection of sex pheromone components in *Manduca sexta* (L.). Chem Senses 26:1175-1186.

Kaneko M, Hall JC (2000) Neuroanatomy of cells expressing clock genes in Drosophila: transgenic manipulation of the period and timeless genes to mark the perikarya of circadian pacemaker neurons and their projections. J Comp Neurol 422:66-94.

Karlson P, Lüscher M (1959) 'Pheromones': a new term for a class of biologically active substances.

Karlson P, Butenandt A (1959) Pheromones (ectohormones) in insects. Ann Rev Entomol 4:39-58.

Kawabe J, Iwami G, Ebina T, Ohno S, Katada T, Ueda Y, Homcy CJ, Ishikawa Y (1994) Differential activation of adenylyl cyclase by protein kinase C isoenzymes. J Biol Chem 269:16554-16558.

Keil TA (1989) Fine structure of the pheromone-sensitive sensilla on the antenna of the hawkmoth, *Manduca sexta*. Tissue Cell 21:139-151.

Kessler D, Diezel C, Baldwin IT (2010) Changing pollinators as a means of escaping herbivores. Curr Biol 20:237-242.

Kim YC, Lee HG, Lim J, Han KA (2013) Appetitive learning requires the alpha1-like octopamine receptor OAMB in the Drosophila mushroom body neurons. J Neurosci 33:1672-1677.

Kimura H, Murad F (1974) Evidence for two different forms of guanylate cyclase in rat heart. J Biol Chem 249:6910-6916.

Koch KW, Stryer L (1988) Highly Cooperative Feedback-Control of Retinal Rod Guanylate-Cyclase by Calcium-Ions. Nature 334:64-66.

Konopka RJ, Benzer S (1971) Clock mutants of *Drosophila melanogaster*. P Nat Acad Sci USA 68:2112-2116.

Krannich S (2008) Electrophysiological and Pharmacological Characterization of Ion Channels Involved in Moth Olfactory Transduction Cascades. In: Dissertation, University of Marburg, 1–114.

Krannich S, Stengl M (2008) Cyclic nucleotide-activated currents in cultured olfactory receptor neurons of the hawkmoth *Manduca sexta*. J Neurophysiol 100:2866-2877.

Krishnan B, Dryer SE, Hardin PE (1999) Circadian rhythms in olfactory responses of *Drosophila melanogaster*. Nature 400:375-378.

Kuhn M (2003) Structure, regulation, and function of mammalian membrane guanylyl cyclase receptors, with a focus on guanylyl cyclase-A. Circ Res 93:700-709.

Larsson MC, Domingos AI, Jones WD, Chiappe ME, Amrein H, Vosshall LB (2004) Or83b encodes a broadly expressed odorant receptor essential for *Drosophila* olfaction. Neuron 43:703-714.

Laura RP, Dizhoor AM, Hurley JB (1996) The membrane guanylyl cyclase, retinal guanylyl cyclase-1, is activated through its intracellular domain. J Biol Chem 271:11646-11651.

Lear BC, Merrill CE, Lin JM, Schroeder A, Zhang L, Allada R (2005) A G protein-coupled receptor, groom-of-PDF, is required for PDF neuron action in circadian behavior. Neuron 48:221-227.

Lee JK, Strausfeld NJ (1990) Structure, distribution and number of surface sensilla and their receptor cells on the olfactory appendage of the male moth *Manduca sexta*. J Neurocytol 19:519-538.

Lehman HK (1990) Circadian control of *Manduca sexta* flight. Soc Neurosci Abstracts 16:1334.

Lindgren PD, Greene GL, Davis DR, Baumhover AH, Henneberry T (1977) Nocturnal behavior of four lepidopteran pests that attack tobacco and other crops. Ann Ent Soc Am. 70:161-167.

Linn CE, Roelofs WL (1986) Modulatory effects of octopamine and serotonin on male sensitivity and periodicity of response to sex pheromone in the cabbage looper moth; *Trichoplusia ni*. Arch Insect Biochem Physiol 3:161-171.

Lipton GR, Sutherland DJ (1970) Feeding rhythms in the american cockroach, *Periplaneta americana*. J Insect Physiol 16:1757-1767.

Loesel R, Homberg U (1999) Histamine-immunoreactive neurons in the brain of the cockroach *Leucophaea maderae*. Brain Res 842:408-418.

Loesel R, Homberg U (2001) Anatomy and physiology of neurons with processes in the accessory medulla of the cockroach *Leucophaea maderae*. J Comp Neurol 439:193-207.

Lucas KA, Pitari GM, Kazerounian S, Ruiz-Stewart I, Park J, Schulz S, Chepenik KP, Waldman SA (2000) Guanylyl cyclases and signaling by cyclic GMP. Pharmacol Rev 52:375-413.

Lugnier C (2006) Cyclic nucleotide phosphodiesterase (PDE) superfamily: A new target for the development of specific therapeutic agents. Pharmacol Ther 109:366-398.

Madden AH, Chamberlin FS (1945) Biology of the Tobacco Hornworm in the Southern Cigar-Tobacco District. United States Department of Agriculture Washington, DC Technical Bulletin No. 896.

Merlin C, Lucas P, Rochat D, Francois MC, Maibeche-Coisne M, Jacquin-Joly E (2007) An antennal circadian clock and circadian rhythms in peripheral pheromone reception in the moth Spodoptera littoralis. J Biol Rhythms 22:502-514.

Mertens I, Vandingenen A, Johnson EC, Shafer OT, Li W, Trigg JS, De Loof A, Schoofs L, Taghert PH (2005) PDF receptor signaling in Drosophila contributes to both circadian and geotactic behaviors. Neuron 48:213-219.

Meyer-Spasche A, Piggins HD (2004) Vasoactive intestinal polypeptide phase-advances the rat suprachiasmatic nuclei circadian pacemaker in vitro via protein kinase A and mitogen-activated protein kinase. Neurosci Lett 358:91-94.

Morton DB, Nighorn A (2003) MsGC-II, a receptor guanylyl cyclase isolated from the CNS of *Manduca sexta* that is inhibited by calcium. J Neurochem 84:363-372.

Myers MP, Wager-Smith K, Rothenfluh-Hilfiker A, Young MW (1996) Light-induced degradation of TIMELESS and entrainment of the Drosophila circadian clock. Science 271:1736-1740.

Naito E, Watanabe T, Tei H, Yoshimura T, Ebihara S (2008) Reorganization of the suprachiasmatic nucleus coding for day length. J Biol Rhythms 23:140-149.

Nakagawa T, Vosshall LB (2009) Controversy and consensus: noncanonical signaling mechanisms in the insect olfactory system. Curr Opin Neurobiol 19:284-292.

Nathanson JA, Greengard P (1973) Octopamine-sensitive adenylate cyclase: evidence for a biological role of octopamine in nervous tissue. Science 180:308-310.

Newton AC (1997) Regulation of protein kinase C. Curr Opin Cell Biol 9:161-167.

Niehaus M, Gewecke M (1978) The antennal movement apparatus in the small tortoiseshell (Aglais urticae L., Insecta, Lepidoptera). Zoomorphologie 91:19-36.

Nighorn A, Byrnes KA, Morton DB (1999) Identification and characterization of a novel beta subunit of soluble guanylyl cyclase that is active in the absence of a second subunit and is relatively insensitive to nitric oxide. J Biol Chem 274:2525-2531.

Nighorn A, Gibson NJ, Rivers DM, Hildebrand JG, Morton DB (1998) The nitric oxide-cGMP pathway may mediate communication between sensory afferents and projection neurons in the antennal lobe of *Manduca sexta*. J Neurosci 18:7244-7255.

Nishiitsutsuji-Uwo J, Pittendrigh CS (1968) Central nervous system control of circadian rhythmicity in the cockroach. Zeitschrift für vergleichende Physiologie 58:1-46.

Nolte A, Funk NW, Mukunda L, Gawalek P, Werckenthin A, Hansson BS, Wicher D, Stengl M (2013) In situ Tip-Recordings Found No Evidence for an Orco-Based Ionotropic Mechanism of Pheromone-Transduction in Manduca sexta. PLoS One 8.

Ohtani A, Arai Y, Ozoe F, Ohta H, Narusuye K, Huang J, Enomoto K, Kataoka H, Hirota A, Ozoe Y (2006) Molecular cloning and heterologous expression of an alpha-adrenergic-like octopamine receptor from the silkworm *Bombyx mori*. Insect Mol Biol 15:763-772.

Page TL (1982) Transplantation of the cockroach circadian pacemaker. Science 216:73-75.

Page TL (1987) Serotonin phase-shifts the circadian rhythm of locomotor activity in the cockroach. J Biol Rhythms 2:23-34.

Page TL, Koelling E (2003) Circadian rhythm in olfactory response in the antennae controlled by the optic lobe in the cockroach. J Insect Physiol 49:697-707.

Pelosi P, Zhou JJ, Ban LP, Calvello M (2006) Soluble proteins in insect chemical communication. Cell Mol Life Sci 63:1658-1676.

Peschel N, Helfrich-Forster C (2011) Setting the clock--by nature: circadian rhythm in the fruitfly Drosophila melanogaster. FEBS Lett 585:1435-1442.

Peters W (2010) Analyse des zyklischen Nukleotids cAMP im olfaktorischen System im Tagesverlauf bei *Rhyparobia maderae*. In: Animal physiology. Kassel: University of Kassel.

Petri B, Stengl M (1997) Pigment-dispersing hormone shifts the phase of the circadian pacemaker of the cockroach *Leucophaea maderae*. J Neurosci 17:4087-4093.

Petri B, Homberg U, Loesel R, Stengl M (2002) Evidence for a role of GABA and Mas-allatotropin in photic entrainment of the circadian clock of the cockroach *Leucophaea maderae*. J Exp Biol 205:1459-1469.

Pittendrigh C, Daan S (1976) A functional analysis of circadian pacemakers in nocturnal rodents. J Comp Physiol 106:223-252.

Pittendrigh CS (1960) Circadian rhythms and the circadian organization of living systems. In: Cold Spring Harbor symposia on quantitative biology, pp 159-184: Cold Spring Harbor Laboratory Press.

Plautz JD, Kaneko M, Hall JC, Kay SA (1997) Independent photoreceptive circadian clocks throughout Drosophila. Science 278:1632-1635.

Pophof B (2000) Octopamine modulates the sensitivity of silkmoth pheromone receptor neurons. J Comp Physiol A 186:307-313.

Prosser RA, Gillette MU (1991) Cyclic Changes in Camp Concentration and Phosphodiesterase Activity in a Mammalian Circadian Clock Studied Invitro. Brain Research 568:185-192.

Prosser RA, McArthur AJ, Gillette MU (1989) cGMP induces phase shifts of a mammalian circadian pacemaker at night, in antiphase to cAMP effects. Proc Natl Acad Sci USA 86:6812-6815.

Rebecchi MJ, Pentyala SN (2000) Structure, function, and control of phosphoinositide-specific phospholipase C. Physiol Rev 80:1291-1335.

Refinetti R (2010) Circadian physiology: CRC press.

Reischig T, Stengl M (1996) Morphology and pigment-dispersing hormone immunocytochemistry of the accessory medulla, the presumptive circadian pacemaker of the cockroach *Leucophaea maderae*: a light- and electron- microscopic study. Cell Tissue Res 285:305-319.

Reischig T, Stengl M (2002) Optic lobe commissures in a three-dimensional brain model of the cockroach Leucophaea maderae: a search for the circadian coupling pathways. J Comp Neurol 443:388-400.

Reischig T, Stengl M (2003a) Ectopic transplantation of the accessory medulla restores circadian locomotor rhythms in arrhythmic cockroaches (Leucophaea maderae). J Exp Biol 206:1877-1886.

Reischig T, Stengl M (2003b) Ultrastructure of pigment-dispersing hormone-immunoreactive neurons in a three-dimensional model of the accessory medulla of the cockroach *Leucophaea maderae*. Cell Tissue Res 314:421-435.

Reischig T, Petri B, Stengl M (2004) Pigment-dispersing hormone (PDH)-immunoreactive neurons form a direct coupling pathway between the bilaterally symmetric circadian pacemakers of the cockroach Leucophaea maderae. Cell Tissue Res 318:553-564.

Renn SC, Park JH, Rosbash M, Hall JC, Taghert PH (1999) A pdf neuropeptide gene mutation and ablation of PDF neurons each cause severe abnormalities of behavioral circadian rhythms in Drosophila. Cell 99:791-802.

Rieger D, Stanewsky R, Helfrich-Forster C (2003) Cryptochrome, compound eyes, Hofbauer-Buchner eyelets, and ocelli play different roles in the entrainment and masking pathway of the locomotor activity rhythm in the fruit fly Drosophila melanogaster. J Biol Rhythms 18:377-391.

Riffell JA, Lei H, Christensen TA, Hildebrand JG (2009) Characterization and coding of behaviorally significant odor mixtures. Curr Biol 19:335-340.

Riffell JA, Alarcon R, Abrell L, Davidowitz G, Bronstein JL, Hildebrand JG (2008) Behavioral consequences of innate preferences and olfactory learning in hawkmoth-flower interactions. Proc Natl Acad Sci U S A 105:3404-3409.

Rillich J, Schildberger K, Stevenson PA (2011) Octopamine and occupancy: an aminergic mechanism for intruder-resident aggression in crickets. Proc Biol Sci 278:1873-1880.

Roberts SK (1965) Photoreception and entrainment of cockroach activity rhythms. Science 148:958-959.

Roberts SK (1974) Circadian rhythms in cockroaches. Effects of optic lobe lesions. J comp Physiol 88:21-30.

Roberts SKdF (1960) Circadian activity rhythms in cockroaches. I. The freerunning rhythm in steady state. J Cell Comp Physiol 55:99-110.

Roberts SKDF (1962) Circadian Activity Rhythms in Cockroaches II. Entrainment and phase shifting. J Cell Comp Physiol 59:175-186.

Robinson G, Butcher RW, Sutherland EW (1968) Cyclic amp. Annu Rev Biochem 37:149-174.

Roeder T (1999) Octopamine in invertebrates. Prog Neurobiol 59:533-561.

Roeder T (2005) Tyramine and octopamine: ruling behavior and metabolism. Annu Rev Entomol 50:447-477.

Rutila JE, Suri V, Le M, So WV, Rosbash M, Hall JC (1998) CYCLE is a second bHLH-PAS clock protein essential for circadian rhythmicity and transcription of *Drosophila* period and timeless. Cell 93:805-814.

Rymer J, Bauernfeind AL, Brown S, Page TL (2007) Circadian rhythms in the mating behavior of the cockroach, *Leucophaea maderae*. J Biol Rhythms 22:43-57.

Saifullah AS, Page TL (2009) Circadian regulation of olfactory receptor neurons in the cockroach antenna. J Biol Rhythms 24:144-152.

Sanes JR, Hildebrand JG (1976) Structure and development of antennae in a moth, *Manduca sexta*. Dev Biol 51:280-299.

Saraswati S, Fox LE, Soll DR, Wu C-F (2004) Tyramine and octopamine have opposite effects on the locomotion of *Drosophila* larvae. J Neurobiol 58:425-441.

Sargsyan V, Getahun MN, Llanos SL, Olsson SB, Hansson BS, Wicher D (2011) Phosphorylation via PKC Regulates the Function of the Drosophila Odorant Co-Receptor. Front Cell Neurosci 5:5.

Sasaki M, Riddiford LM (1984) Regulation of reproductive behaviour and egg maturation in the tobacco hawk moth, *Manduca sexta*. Physiol Entomol 9:315-327.

Sato K, Pellegrino M, Nakagawa T, Vosshall LB, Touhara K (2008) Insect olfactory receptors are heteromeric ligand-gated ion channels. Nature 452:1002-1006.

Saunders DS (2002) Insect clocks: Elsevier.

Schafer R (1971) Antennal sense organs of the cockroach, Leucophaea maderae. Journal of Morphology 134:91-103.

Schendzielorz J (2013) Analysis of the circadian system of the cockroach *Rhyparobia (Leucophaea) maderae*. In: Animal physiology. Kassel: University of Kassel.

Schendzielorz J, Stengl M (2014) Candidates for the light entrainment pathway to the circadian clock of the Madeira cockroach Rhyparobia maderae. Cell Tissue Res 355:447-462.

Schendzielorz T, Peters W, Boekhoff I, Stengl M (2012) Time of Day Changes in Cyclic Nucleotides Are Modified via Octopamine and Pheromone in Antennae of the Madeira Cockroach. J Biol Rhythms 27:388-397.

Schneider NL, Stengl M (2005) Pigment-dispersing factor and GABA synchronize cells of the isolated circadian clock of the cockroach *Leucophaea maderae*. J Neurosci 25:5138-5147.

Schroter U, Malun D, Menzel R (2007) Innervation pattern of suboesophageal ventral unpaired median neurones in the honeybee brain. Cell Tissue Res 327:647-667.

Schuckel J, Siwicki KK, Stengl M (2007) Putative circadian pacemaker cells in the antenna of the hawkmoth *Manduca sexta*. Cell Tissue Res 330:271-278.

Schulze J, Schendzielorz T, Neupert S, Predel R, Stengl M (2013) Neuropeptidergic input pathways to the circadian pacemaker center of the Madeira cockroach analysed with an improved injection technique. Eur J Neurosci 38:2842-2852.

Schulze J, Neupert S, Schmidt L, Predel R, Lamkemeyer T, Homberg U, Stengl M (2012) Myoinhibitory peptides in the brain of the cockroach *Leucophaea maderae* and colocalization with pigment-dispersing factor in circadian pacemaker cells. J Comp Neurol 520:1078-1097.

Seamon KB, Daly JW (1981) Forskolin: a unique diterpene activator of cyclic AMP-generating systems. J Cyclic Nucleotide Res 7:201-224.

Sehgal A, Price JL, Man B, Young MW (1994) Loss of circadian behavioral rhythms and per RNA oscillations in the Drosophila mutant timeless. Science 263:1603-1606.

Seluzicki A, Flourakis M, Kula-Eversole E, Zhang L, Kilman V, Allada R (2014) Dual PDF signaling pathways reset clocks via TIMELESS and acutely excite target neurons to control circadian behavior. PLoS Biol 12:e1001810.

Shafer OT, Kim DJ, Dunbar-Yaffe R, Nikolaev VO, Lohse MJ, Taghert PH (2008) Widespread receptivity to neuropeptide PDF throughout the neuronal circadian clock network of Drosophila revealed by real-time cyclic AMP imaging. Neuron 58:223-237.

Sharma RK (2010) Membrane guanylate cyclase is a beautiful signal transduction machine: overview. Mol Cell Biochem 334:3-36.

Shaw SR (1981) Anatomy and physiology of identified non-spiking cells in the photoreceptor-lamina complex of the compound eye of insects, especially Diptera. Neurons without impulses Cambridge University Press, Cambridge:61-116.

Soehler S, Stengl M, Reischig T (2011) Circadian pacemaker coupling by multi-peptidergic neurons in the cockroach Leucophaea maderae. Cell Tissue Res 343:559-577.

Soehler S, Neupert S, Predel R, Stengl M (2008) Examination of the role of FMRFamide-related peptides in the circadian clock of the cockroach *Leucophaea maderae*. Cell Tissue Res 332:257-269.

Sokolove PG (1975) Localization of the cockroach optic lobe circadian pacemaker with microlesions. Brain Res 87:13-21.

Sreng L (1993) Cockroach Mating Behaviors, Sex Pheromones, and Abdominal Glands (*Dictyoptera*: *Blaberidae*). J Insect Behav 6.

Stanewsky R, Kaneko M, Emery P, Beretta B, Wager-Smith K, Kay SA, Rosbash M, Hall JC (1998) The cryb mutation identifies cryptochrome as a circadian photoreceptor in Drosophila. Cell 95:681-692.

Steinbrecht RA (1998) Odorant-binding proteins: expression and function. Ann N Y Acad Sci 855:323-332.

Steinbrecht RA, Gnatzy W (1984) Pheromone receptors in Bombyx mori and Antheraea pernyi. I. Reconstruction of the cellular organization of the sensilla trichodea. Cell Tissue Res 235:25-34.

Stengl M (1993) Intracellular-messenger-mediated cation channels in cultured olfactory receptor neurons. J Exp Biol 178:125-147.

Stengl M (1994) Inositol-trisphosphate-dependent calcium currents precede cation currents in insect olfactory receptor neurons in vitro. J Comp Physiol A 174:187-194.

Stengl M (2010) Pheromone transduction in moths. Front Cell Neurosci 4:133.

Stengl M, Homberg U (1994) Pigment-dispersing hormone-immunoreactive neurons in the cockroach *Leucophaea maderae* share properties with circadian pacemaker neurons. J Comp Physiol A 175:203-213.

Stengl M, Zintl R (1996) NADPH diaphorase activity in the antennae of the hawkmoth *Manduca sexta*. J Exp Biol 199:1063-1072.

Stengl M, Funk NW (2013) The role of the coreceptor Orco in insect olfactory transduction. J Comp Physiol A Neuroethol Sens Neural Behav Physiol 199:897-909.

Stengl M, Zintl R, De Vente J, Nighorn A (2001) Localization of cGMP immunoreactivity and of soluble guanylyl cyclase in antennal sensilla of the hawkmoth *Manduca sexta*. Cell Tissue Res 304:409-421.

Stoleru D, Peng Y, Agosto J, Rosbash M (2004) Coupled oscillators control morning and evening locomotor behaviour of *Drosophila*. Nature 431:862-868.

Stolte P (2010) Untersuchung von Tyramin in der Antenne des Tabakschwärmers *Manduca sexta*. In: Tierphysiologie. Marburg: Universität Marburg.

Strassheim D, Williams CL (2000) P2Y2 purinergic and M3 muscarinic acetylcholine receptors activate different phospholipase C-beta isoforms that are uniquely susceptible to protein kinase C-dependent phosphorylation and inactivation. J Biol Chem 275:39767-39772.

Sunahara RK, Dessauer CW, Gilman AG (1996) Complexity and diversity of mammalian adenylyl cyclases. Annu Rev Pharmacol Toxicol 36:461-480.

Sutherland E, Butcher R, Robison G, Hardman J, Karlson P (1967) Wirkungsmechanismen der Hormone: Springer, Berlin.

Sutherland EW, Rall T (1960) The relation of adenosine-3', 5'-phosphate and phosphorylase to the actions of catecholamines and other hormones. Pharmacol Rev 12:265-299.

Tang WJ, Hurley JH (1998) Catalytic mechanism and regulation of mammalian adenylyl cyclases. Mole Pharmacol 54:231-240.

Tanoue S, Krishnan P, Krishnan B, Dryer SE, Hardin PE (2004) Circadian clocks in antennal neurons are necessary and sufficient for olfaction rhythms in Drosophila. Curr Biol 14:638-649.

Taylor CW (1990) The role of G proteins in transmembrane signalling. Biochem J 272:1.

Thom C, Guerenstein PG, Mechaber WL, Hildebrand JG (2004) Floral CO2 reveals flower profitability to moths. J Chem Ecol 30:1285-1288.

Thurm U, Wessel G (1979) Metabolism-dependent transepithelial potential differences at epidermal receptors of arthropods. J Comp Neurol 134:119-130.

Tomioka K, Abdelsalam S (2004) Circadian organization in hemimetabolous insects. Zool Sci 21:1153-1162.

Tomioka K, Matsumoto A (2010) A comparative view of insect circadian clock systems. Cell Mol Life Sci 67:1397-1406.

Tomioka K, Uryu O, Kamae Y, Umezaki Y, Yoshii T (2012) Peripheral circadian rhythms and their regulatory mechanism in insects and some other arthropods: a review. Journal of comparative physiology B, Biochemical, systemic, and environmental physiology 182:729-740.

Tumlinson JH, Brennan MM, Doolittle RE, Mitchell ER, Brabham A, Mazonmenos B, Baumhover AH, Jackson MD (1989) Identification of a Pheromone Blend Attractive to *Manduca sexta* (*L.*) Males in a Wind Tunnel. Archives of Insect Biochemistry and Physiology 10.

Villet RH (1978) Mechanism of insect sex-pheromone sensory transduction: Role of adenylyl cyclase. Comp Biochem Physiol 61C:389-394.

Vogl A, Noe J, Breer H, Boekhoff I (2000) Cross-talk between olfactory second messenger pathways. Eur J Biochem 267:4529-4535.

von Nickisch-Rosenegk E, Krieger J, Kubick S, Laage R, Strobel J, Strotmann J, Breer H (1996) Cloning of biogenic amine receptors from moths (*Bombyx mori* and *Heliothis virescens*). Insect Biochem Mol Biol 26:817-827.

Wachowiak M (2011) All in a sniff: olfaction as a model for active sensing. Neuron 71:962-973.

Wei H, Stengl M (2011) Light affects the branching pattern of peptidergic circadian pacemaker neurons in the brain of the cockroach *Leucophaea maderae*. J Biol Rhythms 26:507-517.

Wei H, el Jundi B, Homberg U, Stengl M (2010) Implementation of pigment-dispersing factor-immunoreactive neurons in a standardized atlas of the brain of the cockroach Leucophaea maderae. J Comp Neurol 518:4113-4133.

Wei HY, Yasar H, Funk N, Giese M, El Baz S, Stengl M (submitted) Pigment-dispersing factor inhibits potassium and sodium channels in insect circadian pacemaker neurons and signals not exclusively via adenylyl cyclase activation PLoS One.

Wicher D (2007) Metabolic regulation and behavior: how hunger produces arousal - an insect study. Endocr Metab Immune Disord Drug Targets 7:304-310.

Wicher D, Schafer R, Bauernfeind R, Stensmyr MC, Heller R, Heinemann SH, Hansson BS (2008) Drosophila odorant receptors are both ligand-gated and cyclic-nucleotide-activated cation channels. Nature 452:1007-1011.

Wiedenmann G (1980) Two peaks in the activity rhythm of cockroaches controlled by one circadian pacemaker. J Comp Physiol 137:249-254.

Wiedenmann G, Martin W (1980) Running activity patterns of females and last larval instars of the cockroach *Leucophaea maderae*. Zeitschrift für Naturforschung, C 35:816-818.

Willoughby D, Cooper DM (2007) Organization and Ca2+ regulation of adenylyl cyclases in cAMP microdomains. Physiol Rev 87:965-1010.

Yoshii T, Wulbeck C, Sehadova H, Veleri S, Bichler D, Stanewsky R, Helfrich-Forster C (2009) The neuropeptide pigment-dispersing factor adjusts period and phase of Drosophila's clock. J Neurosci 29:2597-2610.

Yoshimura M, Cooper DM (1992) Cloning and expression of a Ca^{2+}-inhibitable adenylyl cyclase from NCB-20 cells. Proc Natl Acad Sci U S A 89:6716-6720.

Zhou X, Yuan C, Guo A (2005) Drosophila olfactory response rhythms require clock genes but not pigment dispersing factor or lateral neurons. J Biol Rhythms 20:237-244.

Zhukovskaya MI, Kapitsky SV (2006) Activity modulation in cockroach sensillum: the role of octopamine. J Insect Physiol 52:76-86.

Ziegelberger G, van den Berg MJ, Kaissling KE, Klumpp S, Schultz JE (1990) Cyclic GMP levels and guanylate cyclase activity in pheromone-sensitive antennae of the silkmoths *Antheraea polyphemus* and *Bombyx mori*. J Neurosci 10:1217-1225.

Acknowledgements

First, I would like to thank Prof. Dr. Monika Stengl, who gave me the opportunity to work in her laboratory on this exciting topic, supported me with her expertise, and trusted in me. I also would like to thank Dr. Christine Nowack for reviewing this doctoral thesis as well as Prof. Dr. Mireille Schäfer and Prof. Dr. Raffael Schaffrath for participation in the examination committee.

Further, I would like to thank all members of the department of animal physiology, especially my colleagues and friends Andreas Arendt and Petra Gawalek for the enjoyment during the work, for numerous *"düds"*, but also for the interesting scientific discussions.

In addition, I would like to thank all staff of the University of Kassel, involved in this doctoral thesis. In particular to all members of the department of biochemistry, whose well plate reader and ice machine I was allowed to use for approximately a half decade (including diploma thesis).

Finally, I would like to thank my family for their support and motivation and my wife for a lot of funny and successful moments in the lab, for support, and for proofreading. You see errors where nobody else sees. I will always remember this beautiful time.